SEISMIC RESPONSE OF INELASTIC CONCRETE STRUCTURES USING THE EQUIVALENT LINEAR METHOD

By

ERNESTO GABRIEL CRUZ GUTIÉRREZ

Thesis submitted as partial fulfillment of the requirements for the degree of

MASTER OF SCIENCE
IN
CIVIL ENGINEERING

UNIVERSITY OF PUERTO RICO
MAYAGÜEZ CAMPUS
MAYAGÜEZ, PUERTO RICO
2016

Approved by:

Luis E. Suárez Colche, Ph.D. President, Graduate Committee	Date
Luis A. Montejo Valencia, Ph.D. Member, Graduate Committee	Date
Ricardo R. López Rodríguez, Ph.D. Member, Graduate Committee	Date
Alberto M. López Venegas, Ph.D. Representative of Graduate School	Date
Ismael Pagán Trinidad, M.S.C.E. Department Chairperson	Date

ABSTRACT

The equivalent linear method is widely used in Geotechnical Earthquake Engineering to calculate the accelerations at the surface of soil deposits subject to earthquakes of moderate intensity. The method approximately takes into account the non-linear behavior of soils by using equivalent shear moduli and damping ratios that are function of effective shear strains. A series of linear analysis are performed each time using equivalent soil properties until their values at two consecutive steps are approximately equal. The effective strain is defined by reducing the peak strain retrieved from the time response. The reduction factor, usually 0.65, accounts for the fact that the peak strain only occurs at a single instant of time. This thesis investigates the application of this technique to calculate the seismic response of reinforced concrete buildings with moderate non-linear behavior. The method is tested using a 3-D finite element model of a building created in the program ANSYS. Non-linear constitutive relations in the form of stress vs. strain are used to calculate the full non-linear response and also to define the equivalent modulus of elasticity and damping ratio by means of the Masing's rule. It was found that a key parameter affecting the accuracy of the results is the reduction factor. Considering a number of seismic records with different frequency contents an optimal reduction factor was defined that is a function of six parameters related to the intensity of the earthquake. The accuracy of the results obtained with the equivalent linear method depends on the response of interest sought (displacement, shear, moment, acceleration) but it proved to be quite acceptable for all the cases considered. The floor response spectra for the building with non-linear behavior were also obtained and they compare very well with those computed with the exact non-linear analysis.

RESUMEN

El método lineal equivalente es altamente utilizado en Ingeniería Sísmica Geotécnica para calcular las aceleraciones en la superficie de depósitos de suelos sometidos a un sismo de intensidad moderada. El método toma en cuenta en forma aproximada el comportamiento no lineal de los suelos mediante el uso de un módulo de corte y razón de amortiguamiento equivalentes. Se realizan una serie de análisis lineales en el tiempo usando en cada etapa propiedades lineales equivalentes obtenidas de curvas que definen estas propiedades en función de la deformación específica. De la respuesta en el tiempo se extrae el valor máximo el cual se reduce por factor de 0.65 para tener en cuenta que el valor pico no se repite en el tiempo. En este trabajo se aplica esta técnica para calcular la respuesta sísmica de edificios de hormigón armado con un comportamiento no lineal moderado. La respuesta exacta del edificio se calcula usando un modelo con elementos finitos tridimensionales en el programa ANSYS. Usando curvas del módulo de elasticidad y de razón de amortiguamiento equivalentes en función de la deformación unitaria se definen modelos lineales equivalentes. Un parámetro clave que afecta la precisión de los resultados es el factor de reducción. Considerando una serie de registros sísmicos con distintos contenidos de frecuencia se obtiene un factor de reducción óptimo que se define en función de seis parámetros relacionados a una medida de intensidad de los sismos. La precisión de los resultados obtenidos con el método lineal equivalente depende de la respuesta de interés (desplazamientos, cortantes, momentos, aceleraciones) pero los errores se mantienen dentro de márgenes aceptables. También se obtuvieron también los espectros de respuesta de piso para el edificio con comportamiento no-linear y se compararon con los calculados con el análisis no linear exacto lo cual dio buenos resultados.

To my God who gave me life.

To my family for being in every step of the way.

To friends for the support provided during these years.

ACKNOWLEDGMENTS

I would like to express my sincere appreciation to my Principal Supervisor, Dr. Luis E. Suárez for his guidance and support, without which this work would not have been possible. I consider myself fortunate to be under his guidance in writing this thesis. I am grateful for the opportunity to take lectures under his personal guidance. Also, for the opportunity to travel with him that help me grow as a professional.

Without the financial support of the U.S. Nuclear Regulatory Commission (NRC) which offered me a fellowship for graduate studies, this work would not have been possible. Special thanks go to Dr. Luis A. Montejo, for granting me that rare opportunity and for the support during this research. Also, specials thanks for been a member of my graduate committee.

I would also like to recognize the help of Dr. Ricardo R. López for his guidance and support during the development of this thesis. Also, my sincere appreciation for been a member of my graduate committee.

I am grateful to all the lectures that took place in the Department of Civil Engineering of the University of Puerto Rico at Mayagüez campus and the professors for their support towards the successful completion of my studies.

Special thanks to my family, Jasiel Y. Ramos and friends for their support and encouragement every step of the way, during my studies.

This work was performed under award NRC-HQ-12-G-38-0018 from the US Nuclear Regulatory Commission. The statements, findings, conclusions, and recommendations are those of the authors and do not necessarily reflect the view of the US Nuclear Regulatory Commission.

CONTENTS

ABSTRACT iii

RESUMEN iv

ACKNOWLEDGMENTS vi

LIST OF FIGURES x

LIST OF TABLES xiii

CHAPTER I – INTRODUCTION 1

1.1 Justification 1

1.2 Seismic response of nonstructural components 3

1.3 Objectives 5

1.4 Methodology 6

1.5 Literature review 10

CHAPTER II – DEVELOPMENT AND CALIBRATION OF THE STRUCTURAL MODEL 19

2.1 Introduction 19

2.2 Development of the structural model 20

2.2.1. Frame model design 20

2.2.2. Material model 25

2.2.3. Pushover calibration 30

2.3 Development of the finite element model 32

2.3.1. Element selection for the structural model 33

2.3.2. Model meshing 34

2.4 Chapter summary and conclusions 35

CHAPTER III – MODAL AND NON-LINEAR DYNAMIC ANALYSIS 37

3.1 Introduction 37

3.2 Modal analysis 39

3.2.1. Comparison with shear building model 41

3.2.2. Damping model calibration 42

3.2.3. Damping validation ………………………………………………………….. 45
3.2.4. Modal analysis results ……………………………………………………… 47
3.3 Selection of acceleration records ………………………….…………………... 48
3.3.1. Ground motion database ………………...……….……………….…….…... 48
3.3.2. Broad-band earthquake record for detailed studies ………………………... 52
3.3.3. Short-band earthquake records for detailed studies ………………………... 53
3.4 Non-linear dynamic analysis …………………...……………………………… 54
3.4.1. Application of gravity loads …………………………………………….... 55
3.4.2. Results of the dynamic analysis with broad-band record …………………... 55
3.4.3. Results of the dynamic analysis with the short-band record …..…………... 62
3.5 Chapter summary and conclusions ……………………………………………. 67

CHAPTER IV – IMPLEMENTATION OF THE EQUIVALENT LINEAR METHOD ………………. 69

4.1 Introduction ……………………………………………………….…………... 69
4.2 The equivalent linear method ……..……………………...……….………….. 70
4.2.1. Masing's rule formulation ……………..……….……………….…….…... 72
4.2.2. Equivalent linear parameters for the beam elements ..……………………... 75
4.2.3. Equivalent linear parameters for the column elements …...………………... 78
4.3 Equivalent linear dynamic analysis ……………………….…………………... 80
4.3.1. Broad-band seismic record ….…………...……….……………….…….…... 81
4.3.2. Short-band seismic record ………………………..………………………... 91
4.4 Chapter summary and conclusions ……………………………………………. 99

CHAPTER V – PROPOSED REDUCTION FACTOR AND FINAL VALIDATION …………………. 101

5.1 Introduction ……………………………………………………….…………... 101
5.2 Linear equivalent method validation ……………………...…………….……….. 102
5.2.1. The peak ground acceleration ……......………………………….…….…... 102
5.2.2. The peak ground velocity ………………………...………………………... 103
5.2.3. The characteristic intensity ….…………………………………………….... 103
5.2.4. The arias intensity ……………………..……………………………………. 104
5.2.5. The cumulative absolute velocity ………………………………………….. 104
5.2.6. Effective design acceleration ………………………………………………. 105
5.2.7. Proposed optimal reduction factor …………………………………………. 105

5.2.8. Validation of the results ………………………………………………………. 106
5.3 Floor response spectrum results ..…………………………….……………………... 107
5.3.1. Floor spectra for the broad-band earthquake …….…………………..……..... 108
5.3.2. Floor spectra for the short-band earthquake ……...………………………... 108
5.4 Chapter summary and conclusions ….…………………………………………… 111
CHAPTER VI – CONCLUSIONS AND RECOMMENDATIONS ………………………………….. 112
6.1 Summary ……………………………………………………………….…………... 112
6.2 Limitations of the equivalent linear method and the study …..…………….……….. 113
6.3 Conclusions ....……………………….…………………………….…………………... 114
6.4 Recommendations for future work ……………………………………………… 115
REFERENCES …………………………………………………………..…………………. 117
APPENDIX A – MATLAB PARAMETERS SOURCE CODE ALGORITHM ………………………. 121
A.1 Main Matlab source code algorithm …..…………………………….………….... 121
A.2 EDA Matlab separate function …………….…………………...………….……….. 123
APPENDIX B – EQUIVALENT LINEAR METHOD FORMULATION …………...……………… 124
B.1 Mathematica beam equation formulation ...…………………………….………….... 124
B.2 Mathematica column equation formulation …………………………………… 127

LIST OF FIGURES

Figure 1.1 Steps to calculate the floor response spectrum via time history analysis ……… 8
Figure 1.2 Typical non-linear stress-strain constitutive relationship ……………………… 9
Figure 1.3 Stress-strain model proposed for monotonic loading of confined and unconfined concrete ………………………………………………………………………... 11
Figure 1.4 Comparison of acceleration spectra between the direct and SRSS methods where the two orthogonal responses were computed independently ………………... 13
Figure 1.5 Generation of design floor response spectra by enveloping procedures using US NRC guidelines ……………………………………………………………………….. 14
Figure 1.6 Comparison of the acceleration amplification at the roof of a building for four levels of ductility ………………………………………………………………………… 15
Figure 1.7 (a) Ground motion spectra for the nearly elastic response of the building; (b) Comparison of components acceleration demand estimates ……………………………….. 16
Figure 1.8 Scaled acceleration response spectra (a) Case of a 6 story. (b) The case of a 12 story ………………………………………………………………………………………… 17
Figure 1.9 Floor acceleration spectra for 5% damping of a 6 story frame with a first period T1=1.1 s …………………………………………………………………………….. 18
Figure 2.1 3D numerical model of the SMART 2008 structure …………………………... 21
Figure 2.2 Geometry of the SMART 2008 structure ……………………………………… 21
Figure 2.3 3D model of the moment resistant frame in ANSYS ….………………………. 22
Figure 2.4 Overall dimensions of the 3-D frame ………………………………………….. 23
Figure 2.5 Column geometry and reinforcement details …………………………………... 23
Figure 2.6 Beam geometry and reinforcement details …………………………………….. 24
Figure 2.7 Stress-strain relationship for the confined concrete in the columns from SE::MC ………………………………………………………………………………….... 26
Figure 2.8 Stress-strain relationships for Rebar #10 used for the columns by SE::MC …... 26

Figure 2.9 Moment-curvature relationship for the column from SE::MC ………….……... 27
Figure 2.10 Stress-strain relationship for the confined concrete in the beams from SE::MC 27
Figure 2.11 Stress-Strain relationships for rebar #8 used for the beams by SE::MC ……... 28
Figure 2.12 Moment-curvature relationship for the beam from SE::MC ……….......…. 28
Figure 2.13 Assumed stress-strain relationship for reinforced concrete …………………... 29
Figure 2.14 Result from the pushover analysis for the column and the input constitutive relation ……………………………………………………………………………... 31
Figure 2.15 SOLID65 3D reinforced concrete solid element from ANSYS ……………… 34
Figure 2.16 Mesh of 3D frame model ……………………………………………………... 35
Figure 3.1 Newton-Raphson method ……………………………………………………… 38
Figure 3.2 Undamped natural frequencies of the 3-D model ……………………………… 39
Figure 3.3 Second mode of vibration shape ……………………………………………….. 40
Figure 3.4 Vibration modes in the X-Z plane ……………………………………………... 41
Figure 3.5 Rayleigh damping curve ……………………………………………………….. 45
Figure 3.6 Displacement of the roof in free vibration ……………………………………... 46
Figure 3.7 Natural frequencies of the structure with damping …………………………….. 47
Figure 3.8 Acceleration time histories of the selected earthquake records ………..……. 50
Figure 3.9 Acceleration response spectra of the selected earthquake records …………….. 51
Figure 3.10 Acceleration time history and response spectrum of the 1940 Imperial Valley earthquake …………………………………………………………………………….. 52
Figure 3.11 Fourier spectrum of the 1940 Imperial Valley earthquake record ……………. 53
Figure 3.12 Acceleration time history and response spectrum of the 1986 San Salvador earthquake …………………………………………………………………………….. 53
Figure 3.13 Fourier spectrum of the 1986 San Salvador earthquake record ………………. 54
Figure 3.14 Beams and column of the building selected to trace the response ……………. 56
Figure 3.15 Stresses and strains time histories due to the unscaled broad-band record …... 57
Figure 3.16 Stress-strain response and constitutive relation for the broad-band unscaled record ………………………………………………………………………………… 57
Figure 3.17 Stresses and strains time histories due to the 3.5x scaled broad-band record. .. 58
Figure 3.18 Comparison of stress vs. strain curves for the broad-band 3.5x scaled record .. 59
Figure 3.19 Floor accelerations due to the broad-band 3.5x scaled record ………………... 60

Figure 3.20 Time variation of selected response quantities due to the broad-band 3.5x scaled record ………………………………………………………………………….. 61
Figure 3.21 Stresses and strains time histories due to the unscaled short-band record ……. 62
Figure 3.22 Comparison of stress vs. strain curves for the short-band unscaled record …... 63
Figure 3.23 Time history stress and strain data of short-band 2x analysis ………………... 64
Figure 3.24 Comparison of stress vs. strain curves for the short-band 2x scaled record ….. 65
Figure 3.25 Time history final results of short-band 2x non-linear analysis ……………… 66
Figure 3.26 Floor accelerations due to the short-band 2x scaled record ……………...…... 67
Figure 4.1 A typical backbone curve …………………………………………………… 71
Figure 4.2 Hysteresis loop and the associated backbone curve …………………………… 71
Figure 4.3 Masing's cyclical curve model ………………………………………………… 72
Figure 4.4 Initial elastic modulus and secant modulus ……………………………………. 74
Figure 4.5 Masing's damping ratio relationship …………………………………………... 75
Figure 4.6 Beam stress-strain polynomial approximation ………………………………… 76
Figure 4.7 Backbone curve and hysteresis cycle for the beam elements …………………. 77
Figure 4.8 Degradation curve for the secant modulus of beams ………………………….. 77
Figure 4.9 Degradation for the Damping Ratio of Beams ………………………………… 78
Figure 4.10 Column stress-strain polynomial approximation ……………………………... 78
Figure 4.11 Column stress-strain cyclical behaviors ……………………………………… 79
Figure 4.12 Degradation curve for the secant modulus of columns ……………………… 79
Figure 4.13 Degradation for the Damping Ratio of columns ……………………………… 80
Figure 4.14 Broad-band Strain factors vs. %Error ………………………………………… 86
Figure 4.15 Time history final results of broad-band 3.5x linear analysis ………………… 89
Figure 4.16 Time history stress and strain data of broad-band 3.5x analysis ……………... 90
Figure 4.17 Individual floor acceleration of broad-band 3.5x linear analysis …………….. 90
Figure 4.18 Short-band Strain factors vs. %Error …………………………………………. 95
Figure 4.19 Time history final results of short-band 2x linear analysis …………………… 97
Figure 4.20 Time history stress and strain data of short-band 2x analysis ………………... 98
Figure 4.21 Individual floor acceleration of short-band 2x linear analysis ……………….. 99
Figure 5.1 Broad-Band event floor response spectra ……………………………………… 109
Figure 5.2 Short-Band event floor response spectra ………………………………………. 110

LIST OF TABLES

Table 2.1 Concrete and steel material properties ……………………………………………….. 25

Table 2.2 Additional static loading …………………………………………………………... 31

Table 3.1 Natural frequencies and periods of the structure ………………………………... 39

Table 3.2 Comparison of natural periods of the two models ……………………………… 42

Table 3.3 Parameters for calculation of the two constants α and β ………………………... 44

Table 3.4 Constants to define the damping matrix ………………………………………… 44

Table 3.5 Parameters for logarithmic decrement calculation ……………………………… 46

Table 3.6 Damping ratio obtained from the free vibration simulation …………………….. 47

Table 3.7 Final dynamic properties of the lower modes of the 3D building model ……….. 47

Table 3.8 Ground motion selection database ……………………………………………… 49

Table 3.9 Peak stresses and strains due to the unscaled broad-band record ……………….. 56

Table 3.10 Peak stresses and strains due to the 3.5x scaled broad-band record …………… 58

Table 3.11 Maximum non-linear response quantities due to the broad-band 3.5x scaled record ……………………………………………………………………………………… 60

Table 3.12 Peak stresses and strains due to the unscaled short-band record ………………. 62

Table 3.13 Peak stresses and strains due to the 2x scaled short-band record ……………… 63

Table 3.14 Maximum non-linear response quantities due to the short-band 2x scaled record ……………………………………………………………………………………… 65

Table 4.1 Broad-band 3.5x analysis non-linear and linear results ………………………… 82

Table 4.2 Broad-band full strain iteration …………………………………………………. 82

Table 4.3 Broad-band full strain non-linear and linear results …………………………….. 83

Table 4.4 Broad-band full strain damping parameters …………………………………….. 84

Table 4.5 Broad-band 65% strain iteration ………………………………………………... 84

Table 4.6 Broad-band 65% strain damping parameters …………………………………… 85

Table 4.7 Broad-band 65% strain non-linear and linear results …………………………… 85

Table 4.8 Broad-band optimum values to minimize error ………………………………… 86

Table 4.9 Broad-band final recommended value ………………………………………….. 86
Table 4.10 Broad-band 10.71% strain iteration …………………………………………… 87
Table 4.11 Broad-band 10.71% strain damping parameters ………………………………. 87
Table 4.12 Broad-band 10.71% strain non-linear and linear results ………………………. 88
Table 4.13 Stress-strain results of broad-band 3.5x analysis ……………………………… 88
Table 4.14 Short-band 2x analysis non-linear and linear results ………………………….. 91
Table 4.15 Short-band full strain iteration ………………………………………………… 92
Table 4.16 Short-band full strain damping parameters ……………………………………. 92
Table 4.17 Short-band full strain non-linear and linear results ……………………………. 93
Table 4.18 Short-band 65% strain iteration ………………………………………………... 93
Table 4.19 Short-band 65% strain damping parameters …………………………………... 94
Table 4.20 Short-band 65% strain non-linear and linear results …………………………... 94
Table 4.21 Short-band optimum values to minimize error ………………………………... 95
Table 4.22 Short-band final recommended value …………………………………………. 95
Table 4.23 Short-band 12.78% strain iteration ……………………………………………. 96
Table 4.24 Short-band 12.78% strain damping parameters ……………………………….. 96
Table 4.25 Short-band 12.78% strain non-linear and linear results ……………………….. 96
Table 4.26 Stress-strain results of short-band 2x analysis ………………………………… 98
Table 5.1 Accuracy of the response predicted by the equivalent linear method with the proposed reduction factor for a collection of seismic records ……………………………... 107

CHAPTER I

INTRODUCTION

1.1 Justification

It is well known that according to the design philosophy those buildings designed with modern codes will undergo inelastic deformations during a strong earthquake. However, if properly designed and constructed, the damage will be limited and no collapse should occur. In any case, the seismic response of the buildings is calculated using linear analysis, with the earthquake loading defined by a code-issued design spectrum. On the other hand, seismic non-linear analysis of buildings is less used in the engineering practice. Because it involves significantly more effort, non-linear analyses are limited to specific cases. Typical instances when non-linear analyses are carried out include (Deierlein et al., 2010): a) to assess and design seismic retrofit solutions for existing structures; b) for the design of new buildings that employ structural materials, protective systems or other novel devices that are not covered in current building codes; c) when the owner has specific performance requirements (e.g. to assess if immediate occupancy performance criteria are met).

Most buildings and other structures that encompass nuclear power plant installations are usually designed to have a linear elastic behavior. However, it is conceivable that under a particularly severe earthquake not accounted in the design criteria used, a building may undergo inelastic deformations, albeit not significantly beyond the elastic limit. This is an example of a situation this thesis intends to address. It is proposed to adapt and calibrate a method that was originally developed to compute the approximate non-linear seismic response of soil deposits to calculate the response of buildings with moderate non-linear behavior. The procedure to be adapted is known as the “equivalent linear method”.

A most important problem in Soil Dynamics and Geotechnical Earthquake Engineering is the so-called "site response analysis" in which the ground acceleration at the free surface of a stratified soil deposit is computed using as data the earthquake-induced motion at the bedrock or at a rock outcrop. Soil materials undergo non-linear deformations even when subjected to earthquakes of moderate intensity and thus it is important to account for their non-linear behavior, even in an approximate way. Although the response of the soil deposit can be calculated via a rigorous non-linear step-by-step dynamic analysis, this is not the approach followed in practical applications, except in research work or for special projects. Most commonly the "equivalent linear method" originally proposed by Seed and Idriss (1970) and later implemented in the well-known program SHAKE (Schnabel et al., 1972) is used to calculate the seismic response of the soil deposit. Basically, the method consists in performing a series of linear analysis of the deposit by changing at each iteration step the material properties (the shear modulus G and the damping ratio ξ of each layer) so that they are consistent with the so-called "degradation curves". These are graphs that depict the variation (i.e., the degradation) of G and ξ with the shear strain for each soil material.

It is known that the equivalent linear method has some limitations but nevertheless, as it was previously mentioned, it is extensively accepted in practical applications. One of the limitations of the method is that the non-linear behavior of the soils must be moderate: it does not provide good results for soils undergoing strongly non-linear deformations. It is reasonable to conclude that the same limitation will also apply to the intended application of this work, namely for building structures.

One of the reasons for using the equivalent linear method to calculate the seismic response of soil deposits is that the damping is accounted for by means of the complex modulus damping model. This damping model permits to assign different damping ratios to each of the soil layers of the deposit. In addition, it permits to model more accurately the real energy dissipation characteristics of soil materials. However, the complex modulus model requires an analysis in the frequency domain which is based on the Principle of Superposition and thus it cannot be applied to non-linear systems. By iteratively replacing the non-linear behaving soil deposit by a linear model with equivalent properties, one can apply a frequency domain analysis at each iteration step. For the application of this thesis the damping model used will be that available in the program ANSYS (2015), namely the Rayleigh damping formulation. In addition, the series of sequential linear analyses required by the equivalent linear method will not be done in the frequency domain but rather in the time domain, to limit the focus of the study.

Although this is beyond the scope of this thesis, one of the potential applications of the proposed methodology is to study the dynamic soil-structure interaction by using a model of the building which includes the soil deposit represented by a finite element model. The one-dimensional model analyzed with the equivalent linear method and programmed in SHAKE can be extended to higher dimensions. For instance, the program QUAD4M (Hudson et al., 1992) has implemented the equivalent linear method to calculate the seismic response of soil deposits modeled as a 2-D in a state of plane strain. Another case where an equivalent linear analysis is fitting (or necessary) is to calculate the seismic response when there is a device in the structure that is frequency dependent (for example, a damper).

1.2 Seismic response of nonstructural components

There are cases where buildings were able to withstand the forces and accelerations caused by a strong earthquake, and yet their non-structural components failed causing an economic impact comparable to the failure of the structure itself. Non-structural elements are those systems and components attached to the floor or wall of a building that do not form part of the force resistant system (Villaverde, 2004). These systems are sometimes referred to as “secondary systems” but it does not mean that they have lesser importance, especially in facilities like hospitals and power plants. Following a corresponding nomenclature, the structure that houses the secondary systems is also known as the “primary system”. The secondary systems are especially relevant in nuclear power plants because of the important function of equipment like the radiation regulators, power generators or even the reactor itself that can suffer damage during an earthquake. In addition to safety issues, the economic impact of the failure of these components is quite significant since they represent around 60-80% of the total structure cost. This is why one the goals of this investigation is to calculate the seismic response of non-structural components housed on a building that experiences inelastic excursions.

The most commonly used method to analyze non-structural components is the “floor response spectrum”, also known as the “in-structure response spectrum”. The concept is similar to the conventional ground response spectrum, i.e. it is the maximum response of a single degree of freedom oscillator as a function of its natural period, but now it is attached to a particular floor. Therefore, the floor response spectra are defined for each of the floors of the building. The floor response spectrum can be obtained in two steps. First, a dynamic analysis of the structure is carried out using as input an accelerogram at the base for which the absolute acceleration at the floor of interest is calculated. Next, this acceleration time history is used as input to obtain the maximum response of oscillators with different periods (Suárez and Singh, 1989). This approach has a limitation: the use of only one seismic accelerogram cannot properly account for the random nature of the earthquake phenomena. For instance, usually a building at a given site can experience earthquakes originated by different seismic faults located near the area of the structure. Therefore, it is necessary to generate floor response spectra for several ground accelerations and consider an envelope of the different curves to define a spectrum that can be used for design.

Based on the type of demand that has a predominant role in their seismic response, the non-structural components can be classified as acceleration-sensitive or displacement-sensitive. In addition, they can be divided into rigid and flexible structural systems. A non-structural system is considered as rigid if it is firmly anchored to the structure and in addition, the non-structural element itself is constructed in a way that its flexibility can be neglected. According to the provisions of Chapter 6 of the Standard ASCE 7-05 (ASCE, 2006), a system can be considered flexible if its fundamental natural frequency is less than 1 Hz, if it is attached to the structure with flexible supports, or if the flexibility cannot be ignored. When analyzing a rigid system, it is only necessary to determine the absolute maximum acceleration of the point or floor where the non-structural component is located. On the other hand, to calculate the response of a flexible system it is usually modeled as a single degree of freedom and its natural frequency and damping ratio need to be determined. In more complicated cases, a model with multiple degrees of freedom might be required.

For the seismic design of non-structural components, the provisions of Chapter 13 of ASCE 7-05 establish minimum design criteria for components that are permanently attached to structures and for their supports and attachments. The provisions provide formulas to determine the horizontal force that would be exerted at the component's center of gravity. These equations are a function of the height of the floor where the component is located, and the weight of the component, among other parameters. However, these provisions do not consider various factors such as the type of building's structural system used to resist lateral loads and they do not take into account the non-linearity of the primary system when subjected to a strong earthquake.

One of the objectives of this thesis is to investigate the feasibility of applying the equivalent linear method to calculate the floor response spectra at different floors of a building with moderate inelastic behavior. The floor response spectra predicted by the proposed approach will be compared with similar curves obtained by means of full non-linear dynamic analysis using the structural analysis program ANSYS.

1.3 Objectives

The primary objective of the thesis is to study if the equivalent linear method can be implemented to calculate the approximate seismic response of a structure composed of reinforced concrete momnonent resistant frames that have moderate non-linear behavior. Special emphasis will be done to the seismic response of nonstructural components.

To implement the proposed methodology and to verify its accuracy, the following tasks will be undertaken:

- Design a three-story reinforced concrete building with a special moment resistant frame as the lateral force resistant system.
- Prepare a three-dimensional finite element model of the building with the computer program ANSYS.
- Obtain the non-linear stress-strain relation for the beams and columns sections to be used by the finite element program.

- Select two acceleration time histories of historic events. One will represent a broad-band event (i.e. a record with a rich frequency content) and another a short-band ground motion (i.e., typical of an event closer to the site, with less frequency content).
- Run the model of the building considering the non-linear behavior of the reinforced concrete elements. This will be done by considering non-linearities in the structural materials using the degradation curves of the reinforced concrete sections.
- Develop a polynomial representation of the normal stress vs strain relationship (the "backbone curve") and using Masing's rule determine the two degradation curves required by the equivalent linear method, i.e. E vs ε and ξ vs ε.
- Run the finite element model of the building using now equivalent properties and linear dynamic analyses.
- Once the method is calibrated and corroborated with the selected broad and short-band accelerograms, calibrate it further and verify it using another set of acceleration time histories.
- Compare the floor accelerations obtained accounting for the non-linear behavior as well as those computed with the equivalent linear approach.
- Carry out a similar comparison as described in the previous step, but now with the floor response spectra computed at each floor.
- Establish conclusions and set forth recommendations based on the results obtained.

1.4 Methodology

The methodology implemented to achieve the previously mentioned objectives is described in more detail in this section. The tasks in the bullets presented in the previous section provide a quick overview of the work done. In addition, in each chapter a more meticulous description is provided.

The first step was the design of the three-story reinforced concrete building that was used to test the proposed methodology. Next, a model of the structure was generated using the selected finite element program. ANSYS (2015), a commercial computer program was chosen to create a detailed 3-D finite element model and to carry out the non-linear and linear analyses. The lateral force resisting system of the building was a special moment resisting frame that was designed in accordance with the provisions of the standard ASCE 7-05 as well as the codes ACI 318-11 and IBC 2015. Given that the main application of the present project is on nuclear power structures, the structure was designed in a way that it would have a linear elastic behavior, as it is commonly done in this field. Therefore it was assumed in this project that an unexpected earthquake with intensity above the original design scenario would strike the structure. This earthquake will induce a non-linear behavior in the structure but not a very severe one. This limited non-linear behavior is in accordance with the limitations of the equivalent linear method, i.e. this technique is not applicable for a structure with substantial non-linearity. To consider the non-linearity in the structural materials by both methods (the full non-linear analysis and the approximate method), a stress-strain curve was used. In the case of the full non-linear analysis, the curve was directly used by ANSYS to create the hysteresis cycle, and perform a step by step integration, etc. In the equivalent linear method, the curve was used to calculate an effective elastic modulus and an equivalent damping ratio as explained later. There are different methods to calculate the stress-strain curves. However, because the objective of this investigation is not to demonstrate how to obtain them, the curves used were generated with the computer program "SE::MC" (StructureExpress, 2015) that can model any kind of section with a specific rebar configuration.

After generating the model in the software ANSYS, the structure was subjected to a specific broad-band ground acceleration time history and then the analysis was repeated with a short-band record. At this stage, the inelastic behavior of the structures was accounted for with the full non-linear dynamic analysis. The output that was retrieved from the program are the time series of the shear force and bending moment at a critical section of a column, the relative displacement at the roof and the absolute acceleration time histories at each floor. For rigid equipment, the peak value from the acceleration records is the parameter of interest. For flexible equipment, the floor accelerograms were used as input to one degree of freedom oscillators with increasing natural periods to compute the response spectrum (i.e. the floor response spectrum). These oscillators had a linear behavior, i.e. the non-linear behavior was limited to the primary structure. The last process is depicted in Figure 1.1, which shows step by step the time history approach to obtain the floor response spectrum.

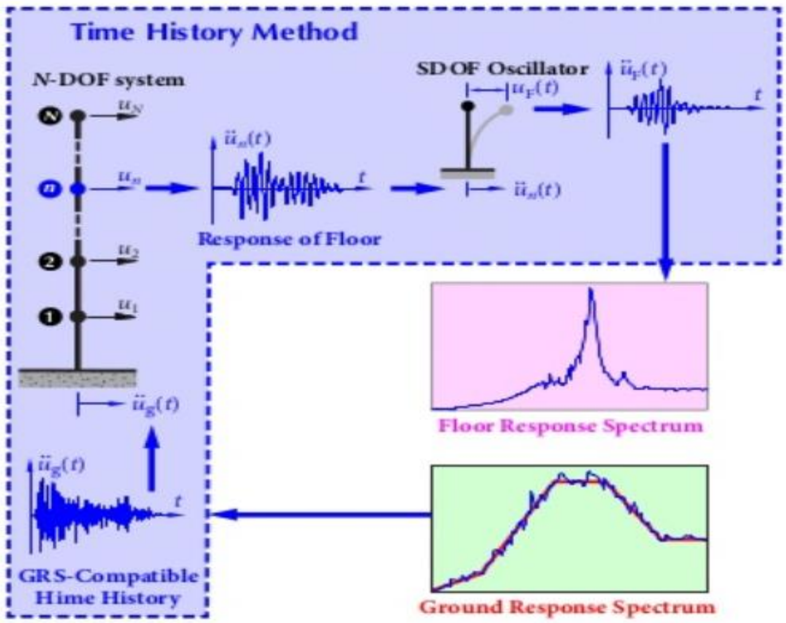

Figure 1.1 *Steps to calculate the floor response spectrum via time history analysis. (Jiang et al., 2015)*

In the second stage, the same building model was subjected to the same two records but the non-linear behavior was approximately accounted for by means of the equivalent linear method. An actual stress-strain curve like that shown in Figure 1.2 was used to model the non-linear behavior of the material. The figure shows a part of the so-called "backbone curve"; however to apply the equivalent linear method the full hysteresis cycle is required. This cycle was defined by means of the Masing rule. Once the full hysteresis cycle was defined, it was used to obtain the two degradation curves. One curve displays the secant elastic modulus for the stress-strain cycle as a function of a deformation parameter. The second curve depicts the variation of the equivalent damping ratio due to the hysteretic behavior as a function of the same deformation parameter. The equivalent linear method is an iterative technique: for the first iteration, an initial deformation was assumed and the effective elastic modulus E and damping ratio ξ was estimated from the corresponding degradation curve. These values were used in the model for the program to carry out a linear dynamic analysis. From the response obtained the maximum deformation (or an effective one, defined by a reduction factor) was recovered and new stiffness and damping values corresponding to this deformation were calculated. They are compared with those from the previous step and if the difference is not small (a preselected tolerance is used for the comparison, which for this thesis was 1%), the process is repeated. This time, the updated stiffness and damping are used to define a new equivalent linear model of the structure. The response is calculated, maximum deformations are retrieved, they are reduced by a factor and new stiffness and damping are computed and compared with the previous ones until convergence is achieved. At the final stage, the floor accelerations are calculated and using them the floor response spectra are defined.

Once the proposed methodology was initially calibrated with the two broad-band and short-band records, other eight accelerograms of historical earthquakes with different characteristics are used to further calibrate the method. The key factor that determines the accuracy of the proposed approach is the reduction factor that is used to define an effective strain by lowering the peak strain. In Soil Dynamics applications, this reduction factor is usually set at 0.65 but it was demonstrated that this value is not applicable to compute the approximate building response. A new factor that accounts for the intensity of the earthquake records was proposed and it was successfully tested.

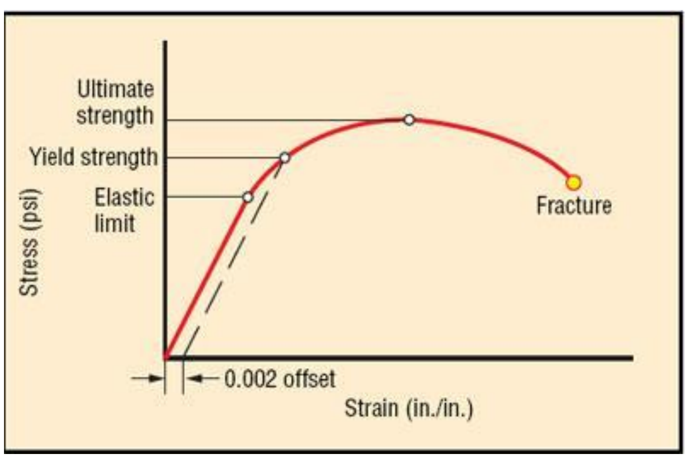

Figure 1.2 *Typical non-linear stress-strain constitutive relationship.*

To assess the accuracy of the approximate method, the accelerations and floor response spectra generated by the full non-linear and the equivalent linear time history analyses were compared. The peak floor accelerations obtained with the two techniques are reasonably similar as long as the non-linear behavior of the structure does not become very strong.

Once the proposed approach is proved to be successful, it can be used to apply the so-called “direct methods” to calculate the floor response spectra in a building with moderate inelastic behavior. The direct methods (Singh, 1975) are those that permit to calculate the floor response spectra using as input the same ground response spectrum used for the analysis and design of the main building (for instance, a design spectrum specified in a code). These methods have the advantage that they eliminate the need to perform time history analyses using spectrum compatible seismic records.

It should be mentioned that the floor response spectra calculated with all the aforementioned methodologies have one common assumption: the dynamic interaction between the primary and secondary structure is neglected. This is a reasonable assumption when the mass of the secondary system is small compared to the mass of the floor where it is attached to the structure, or when the natural frequency of the nonstructural component is not tuned to any of the lower natural frequencies of the building (Suarez and Singh, 1989).

1.5 Literature review

A summary of relevant works dealing with the non-linear response of reinforced concrete structures is presented here. It is followed by a description of works that studied the seismic response of nonstructural components on a supporting structure with inelastic behavior.

The analytical stress-strain models (e.g., Mander et al., 1988) developed for confined concrete define the non-linear properties required to model the behavior of reinforced concrete element subjected to an incremental load. Their formulations stated that if a concrete section contains any general type of confining steel, a single equation can be used to define the stress-strain equation. The model presented by (Mander et al., 1988) allowed for cyclical loading and included the effect of strain rate. Also, their analytical model stipulated the difference in capacity between the concrete inside the steel confinement ("confined concrete") and the concrete outside the reinforcement ("unconfined concrete"). The difference in capacity for the model proposed can be seen in Figure 1.3.

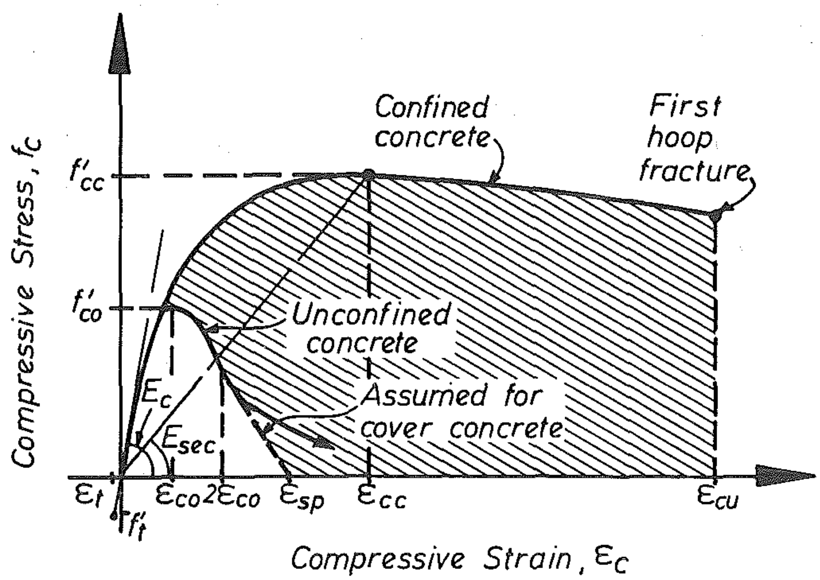

Figure 1.3 *Stress-strain model proposed for monotonic loading of confined and unconfined concrete. (Mander et al., 1988)*

Following a similar idea, Pfrang et al. (1964) presented a method for developing relationships between axial load, moment and curvature for reinforced concrete cross-sections. Like in the case mentioned before, the method was developed in a way that it does not require extensive simplifying assumptions concerning the stress-strain relationship for the concrete and the reinforcement. The formulation proposed will be discussed in more detail in the next chapter.

Researchers from the University of Minas Gerais, Brasil (Barbosa and Ribeiro, 1998) presented a paper that shows the practical application of non-linear models in the analysis of reinforced concrete structures. The analysis was performed using the general purpose finite element code ANSYS, with the goal of investigating the possibilities of performing non-linear finite element analysis of reinforced concrete structures. Their main objective was the prediction of load-deflection curves using models with non-linear behavior. For the implementation of the non-linearity, they incorporated the stress-strain relationship for confined concrete as a material property. This allowed the beam section of the models to reach the ultimate load state and to determine the entire load-deflection diagram. Their results suggested that in spite of the simplifications assumed for the analyzed structure, satisfactory predictions of the response of reinforced concrete structure could be obtained.

Another relevant study was presented by Fragiadakis et al. (2014) for the application of non-linear static procedures for the seismic assessment of regular reinforced concrete moment frame buildings. The research shows the degree to which non-linear static methods can characterize the global and local response demands determined by non-linear dynamic analysis for three reinforced concrete buildings in a moment resistant frame configuration. The parameters measured in the study were peak story displacement, story drifts, story shears and floor overturning moments. The results indicated that the relatively good performance of the single mode methods observed for low-rise buildings rapidly deteriorates as the number of stories increases.

Researchers from Brookhaven National Laboratory (BNL) (Simos and Hofmayer, 2013) conducted a research project called SMART2008 ("Seismic design and best-estimate Methods Assessments for Reinforced concrete buildings subjected to Torsion and non-linear effects") whose main purpose was to develop the best method to analyze the seismic response of a reinforced concrete building using a multi-phase study that part of it was the use of a shaking table experiment. The aim of the project was to compare different methodologies, modeling and numerical approaches to study and predict the non-linear behavior and damage of reinforced concrete structures. For the experiment, they constructed a $1/4^{th}$ scale model of a three story concrete structure using the French code for nuclear structures. One of the observations of the study was that the reinforced concrete appear to undergo stiffness changes due to micro-cracking or adjustment in the concrete-rebar interface under seismic loads much lower than the design earthquake level.

Similar observations were made in another study of the seismic behavior of reinforced concrete but with shear walls (Combescure, 2002). The common observation in the two shaking table experiments were that the natural frequencies of the structure were reduced following seismic loads with intensities as low as 0.1g, a fact attributed to a reduction in the reinforced concrete stiffness. As a result, floor response spectra generated from actual in-structure recordings underwent a shift of their peaks towards the lower frequencies, a feature that may have significant implications for the design of equipment supported on floors.

After processing the data and comparing it with the prediction of the numerical models, it was found that the latter results generally over-predict the in-structure accelerations while under-predicting the displacements. This was primarily attributed to the lack of understanding of the changes in the damping of the RC structure. On the other hand, based on the comparison between the test data with the results from a full non-linear, 3-D analysis of the SMART structure tested by BNL, it was concluded that using the SRSS ("Square Root of the Sum of Squares") method can quite accurately reproduce the response and the damage experienced by the structure even when multi-directional loads are applied on an asymmetric structure. Shown in Figure 1.4 is a verification of the SRSS method using the SMART structure and a bi-directional seismic input with a PGA of 0.2g.

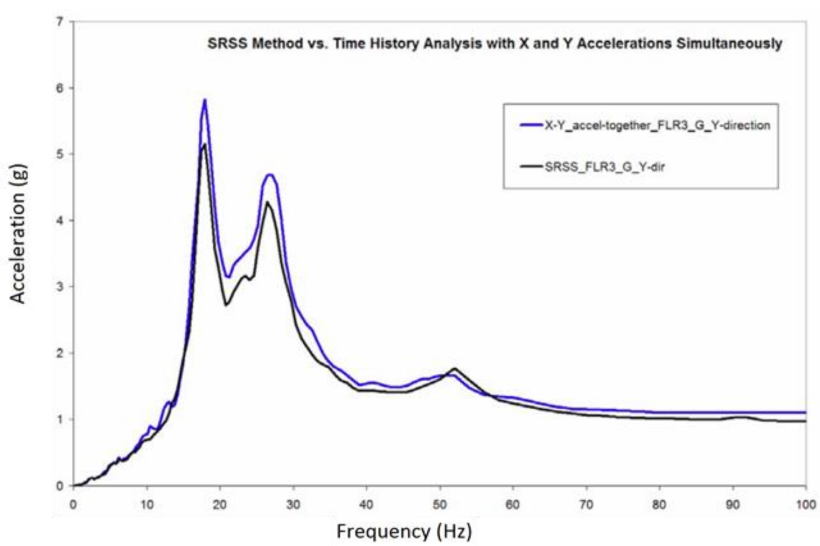

Figure 1.4 *Comparison of acceleration spectra between the direct and SRSS methods where the two orthogonal responses were computed independently. (Simos and Hofmayer, 2013)*

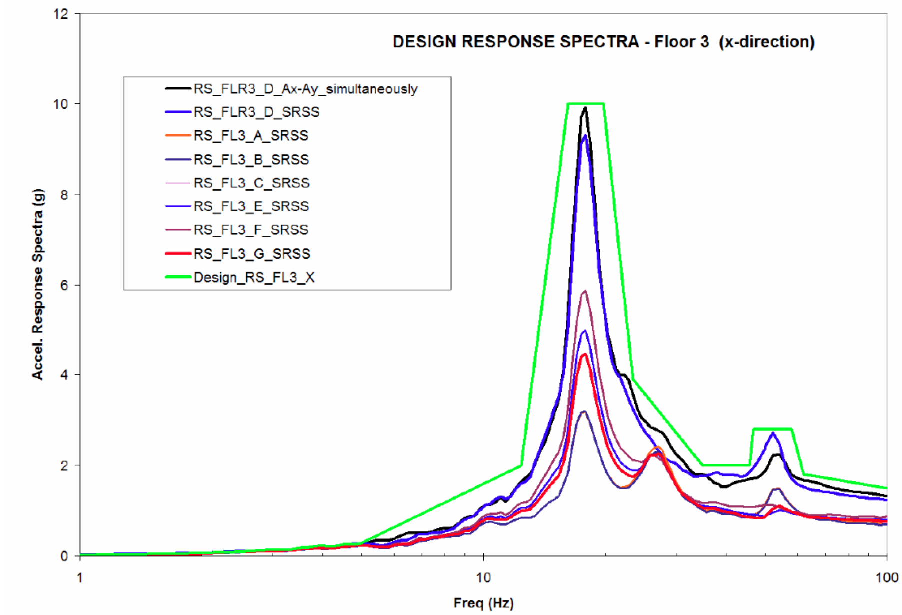

Figure 1.5 *Generation of design floor response spectra by enveloping procedures using US NRC guidelines. (Simos and Hofmayer, 2013)*

They generated the design floor response spectrum shown in Figure 1.5 using the SRSS method, which envelops the floor spectra generated by the simultaneous action of all the two-directional inputs. They established that the generation of design floor spectra can be developed in an adequate manner using as a base the existing guidelines, but for the conditions where the structure exhibits non-linear response. Figure 1.5 shows the “design floor response spectrum” on the 3rd floor of the SMART2008 structure defined using the US NRC guidelines with enveloping procedures and the spectra computed at various floor locations.

Moehle (1992) developed guidelines using a displacement-based design for reinforced concrete structures subjected to earthquake events. Their research shows that rapid dynamic induced structural displacements are the main cause of damage in structures subjected to ground motions. Using simple techniques for estimating structural displacements they developed a design approach based exclusively on expected displacement. The displacement-based approach was used to establish proportions and layouts that can control drift demand, and to determine structural and non-structural details that will allow for proper performance from a design standpoint.

Members of the University of Nevada (Wieser, et al., 2013) conducted a research project whose main purpose was to determine the demand in terms of absolute accelerations on non-structural elements inside moment resisting frame structures. For this study, they created 3-D models of four different buildings with the finite element program OpenSees (PEER, 2010). For the selection of the ground acceleration records, the methodology presented in the ATC-63 project described in the FEMA P-695 (FEMA, 2009) report was implemented, which consisted of 21 earthquakes. An important effect observed was that when the structure reaches the yield level, there is a decrease in floor accelerations. The floor accelerations were then normalized with respect to the ground acceleration to define an "acceleration amplification factor". Also, they proposed some empirical equations to determine the amplification of the accelerations in the structure for each floor, knowing or assuming the yielding point of the structure.

To consider the effects of the ductility of the system, the response levels were divided into three categories: elastic, moderate ductility and high ductility. Figure 1.6 shows the response spectra of a non-structural element placed on the roof of one building under different levels of ductility and its comparison with the code provisions. As seen in Figure 1.7a, the IBC (2006) design spectrum generated with these parameters is comparable to the median ground acceleration spectrum causing near elastic response of the building. Therefore, it is possible to compare the roof acceleration spectrum for nearly elastic response with the component design accelerations developed using the various methods demonstrated in Figure 1.7b.

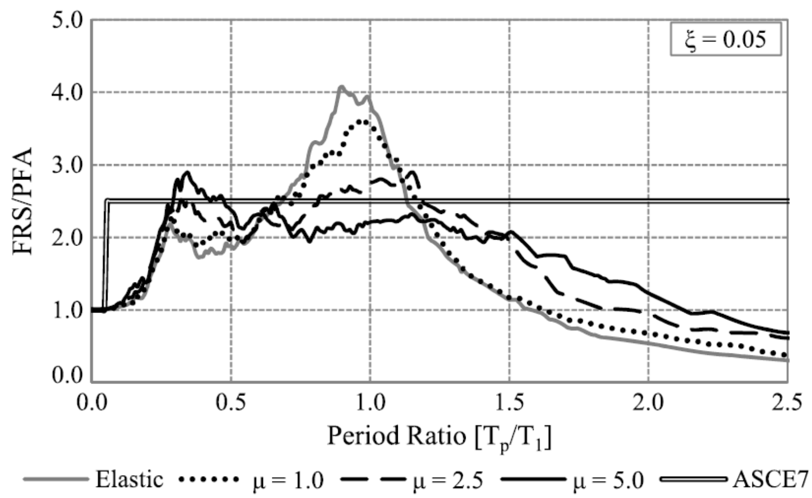

Figure 1.6 *Comparison of the acceleration amplification at the roof of a building for four levels of ductility. (Wieser, et al., 2013)*

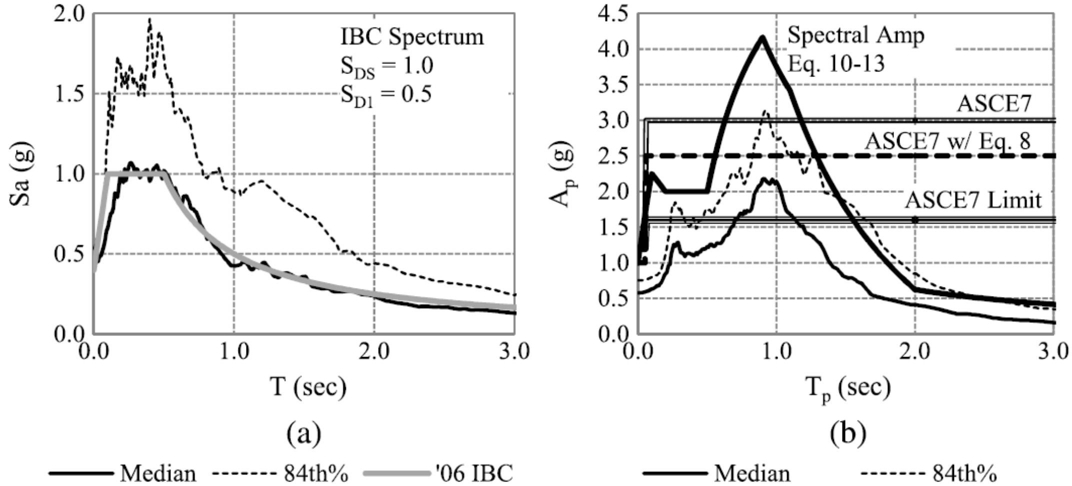

Figure 1.7 *(a) Ground motion spectra for the nearly elastic response of the building; (b) Comparison of components acceleration demand estimates. (Wieser, et al., 2013)*

The seismic floor response spectra (Singh, et al., 2006a; 2006b) are commonly used to define the seismic inputs for non-structural components housed in the main structure. The spectra can be generated using a time history analysis where a ground acceleration record is applied as input at the base of the structure, or by a direct floor response spectrum generation approach where the ground spectrum can be directly used as an input. In either of these approaches, it is assumed that the nonstructural component (represented by a single degree of freedom oscillator) is decoupled from the main structure. This type of analysis is referred to as a "cascade approach": the response of the structure without the secondary system is first computed and it is later used as input to the oscillator. It is reasonable to use this assumption when the mass of the component is negligible since by neglecting the interaction, the computed spectral ordinates are usually on the conservative side. However, this may not be the case if the mass of the component is significant compared to the mass of the floor where it is connected (Suarez and Singh, 1989).

Another relevant study about non-structural components was made at the University of Pennsylvania by Lepage et al. (2012). The purpose of this study was to find a formulation to determine the maximum floor accelerations in a multi-story building subjected to a strong movement. For this purpose, several scale buildings were used and placed on a vibrating table. The aim was to expand the equations provided in the ASCE 7-05 standard (ASCE, 2006) to consider whether the component is flexible or rigid in a general way. The researchers chose a total of 74 ground motion records of ground acceleration measured in buildings in the state of California. The results showed that the variation in the maximum acceleration on the floors varies by type of structure and the resistance of the lateral load. In order to calculate a floor response spectra they first needed an acceleration response spectra that suited the ground motion records used, which were scaled according to the two-step procedure described in the provisions of FEMA (2009). The first step was to scale each record to the same peak ground velocity, and then use a common scale factor that makes the average of the spectral acceleration match the idealized design spectrum at a period T1. The resulting idealized versus average spectra for two cases are shown in Figure 1.8.

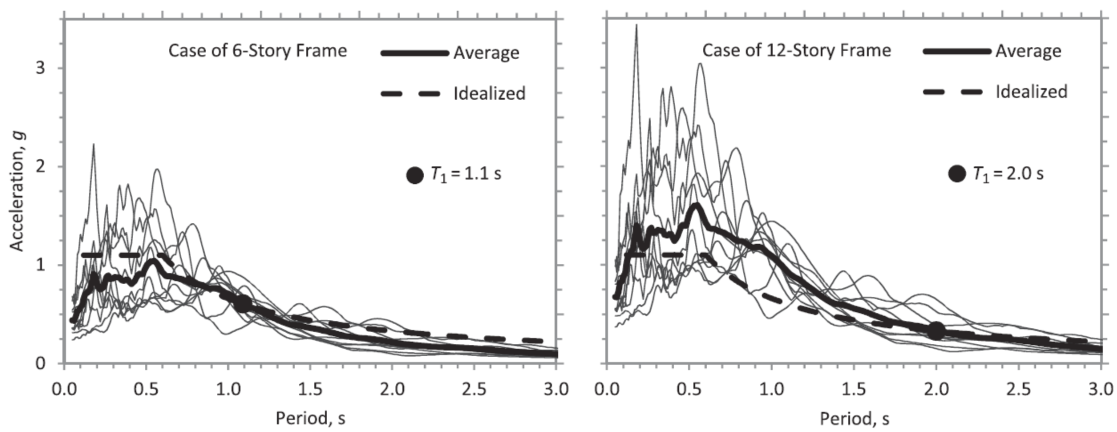

Figure 1.8 *Scaled acceleration response spectra (a)Case of a 6 story.(b) The case of a 12 story.(Lepage et al., 2012)*

Lepage et al. (2012) proposed to use equation (1.1) to estimate the acceleration demand on non-structural components defined in terms of the peak ground acceleration *Ao*. Figure 1.9 shows that the approximation provided by the formula is generally on the safe side, except for a narrow period band of the floor response spectra:

$$Api = Ao\left(1 + \frac{3}{R'}\frac{hi}{hr}\right) ap \tag{1.1}$$

where the following notation is used:

Api = peak component acceleration at level i,

ap = component amplification factor, 1.0 for rigid components and 2.5 for flexible components,

Ao = peak ground acceleration,

hi/hr = ratio of elevation at floor i to the roof elevation,

R' = effective response modification coefficient of the structure: it may be taken as R/Ωo but not less than 1, where:

R = structural response modification coefficient and

Ωo = structural overstrength factor.

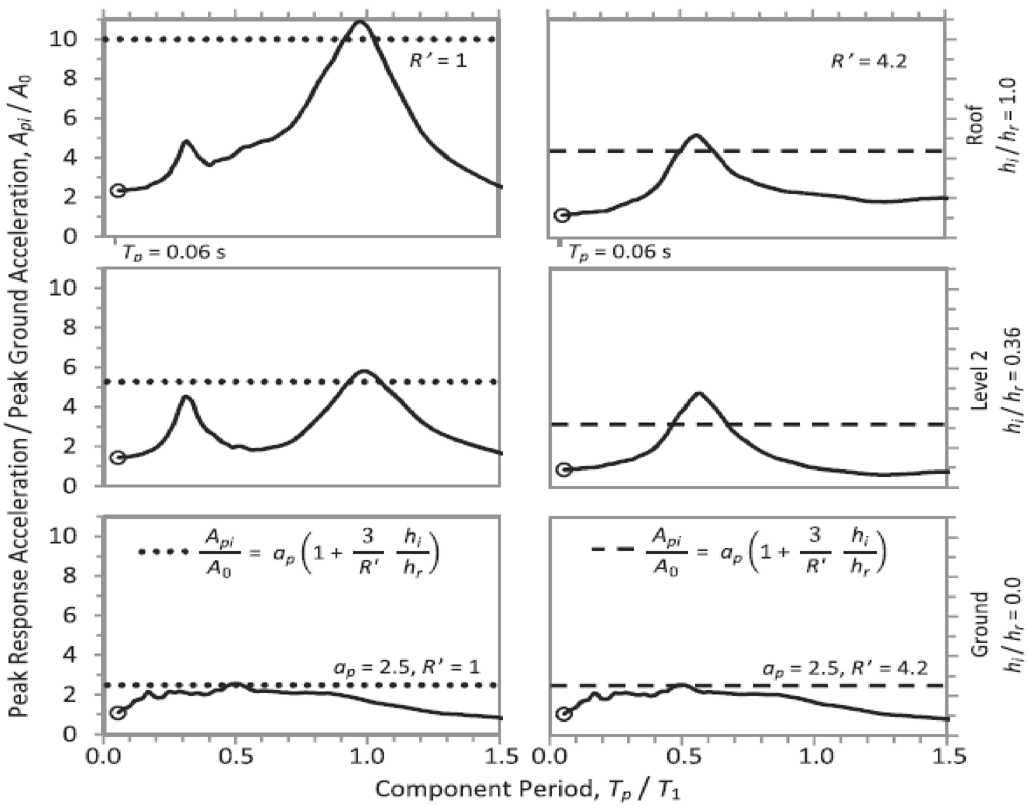

Figure 1.9 *Floor acceleration spectra for 5% damping of a 6 story frame with a first period T_1=1.1 s. (Lepage et al., 2012)*

In summary, there is a lot of research that has been done working on the non-linear response of reinforced concrete structures. Most of which studied the seismic response of structure and non-structural components on a structure that has an inelastic behavior. It is important to mention that even do these theses gives emphasis on the application of nuclear building facilities; it is not exclusive for these types of structure. The methodology mention before will be explained more in details in the following chapters.

CHAPTER II

DEVELOPMENT AND CALIBRATION OF THE STRUCTURAL MODEL

2.1 Introduction

Traditional linear analysis methods remain adequate for the analysis and posterior design of common reinforced concrete structures, special structures such as those in nuclear facilities may require more sophisticated non-linear analysis. The wide dissemination of computers and the development of the powerful finite element codes have provided the means for such analyses using detailed and realistic models. The main obstacle to finite element analysis of reinforced concrete structures is the difficulty in characterizing the material properties since they possess a non-linear behavior when subjected to strong earthquakes and under exceptional loads. Mainly due to the complexity of the nature of the material (i.e. concrete confined with steel rebar), the proper modeling of such structures is a challenging task and requires some assumptions to simplify the analysis, which will be explain in detail in this chapter.

For that purpose, this chapter describes the development of the building model, its characteristics and the calibration processes. A three-dimensional finite element model of the structure was created in the ANSYS (2015) version 16 software. The finite element model will be used in later chapters to perform the equivalent linear analyses and for these tasks it is sufficient to define and use the properties of the concrete. However, it is very important to have a sound and comprehensive model of the building that fully takes into account the non-linear behavior of the reinforced concrete elements because it will be used as an archetype to validate the proposed equivalent linear approach. This chapter explains the generation of the 3-D finite element model, including its geometry, material properties, finite element types, meshes, etc. The information required for the non-linear analysis is also discussed.

2.2 Development of the structural model

The building model that has been used to carry out all the linear and non-linear dynamic analyses is a 3D reinforced concrete frame. The model accounts for the non-linear degrading response of beams and columns using reinforced concrete material data specific for each component. Using the commercial computer program "SE::MC", two non-linear stress-strain curves for the reinforced concrete elements were obtained by subjecting them to uniaxial compressive loading and confining them with transverse reinforcement. This was taken into consideration because tests have shown that the confinement of concrete by suitable arrangement of transverse reinforcement results in a significant increase in both strength and ductility of the compressed concrete (Mander, et al., 1988).

2.2.1. Frame model design

The 3D reinforced concrete structure was designed as a special moment resistant frame following the provisions of ASCE 7-05 (ASCE, 2006), ACI 318-11 (ACI, 2011) and the IBC 2015 (IBC, 2015) specifications. The columns and beams dimensions of the frame were based on a building designed as part of a French research project called SMART 2008 ("**S**eismic design and best-estimate **M**ethods **A**ssessment for **R**einforced concrete buildings subjected to **T**orsion and non-linear effects") (Simos and Hofmayer, 2013). The model that was designed and constructed following the French nuclear design codes is shown in Figure 2.1 and Figure 2.2. It is a simplified representation of a 3 story nuclear electrical building with strong asymmetry. A ¼ scaled model was extensively tested to provide the earthquake engineering community with recommendations and guidelines (Richard et al. 2015; Richard et al, 2016).

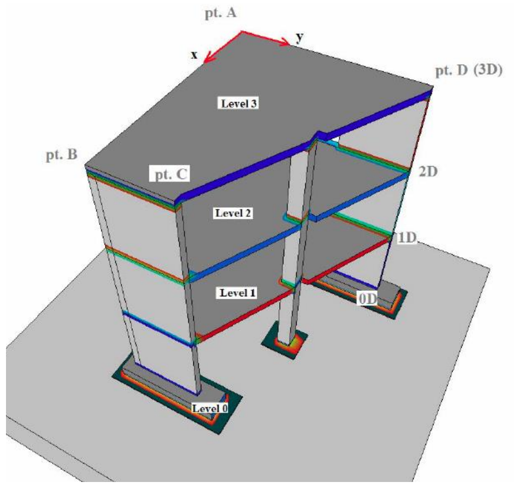

Figure 2.1 *3D numerical model of the SMART 2008 structure. (Simos and Hofmayer, 2013)*

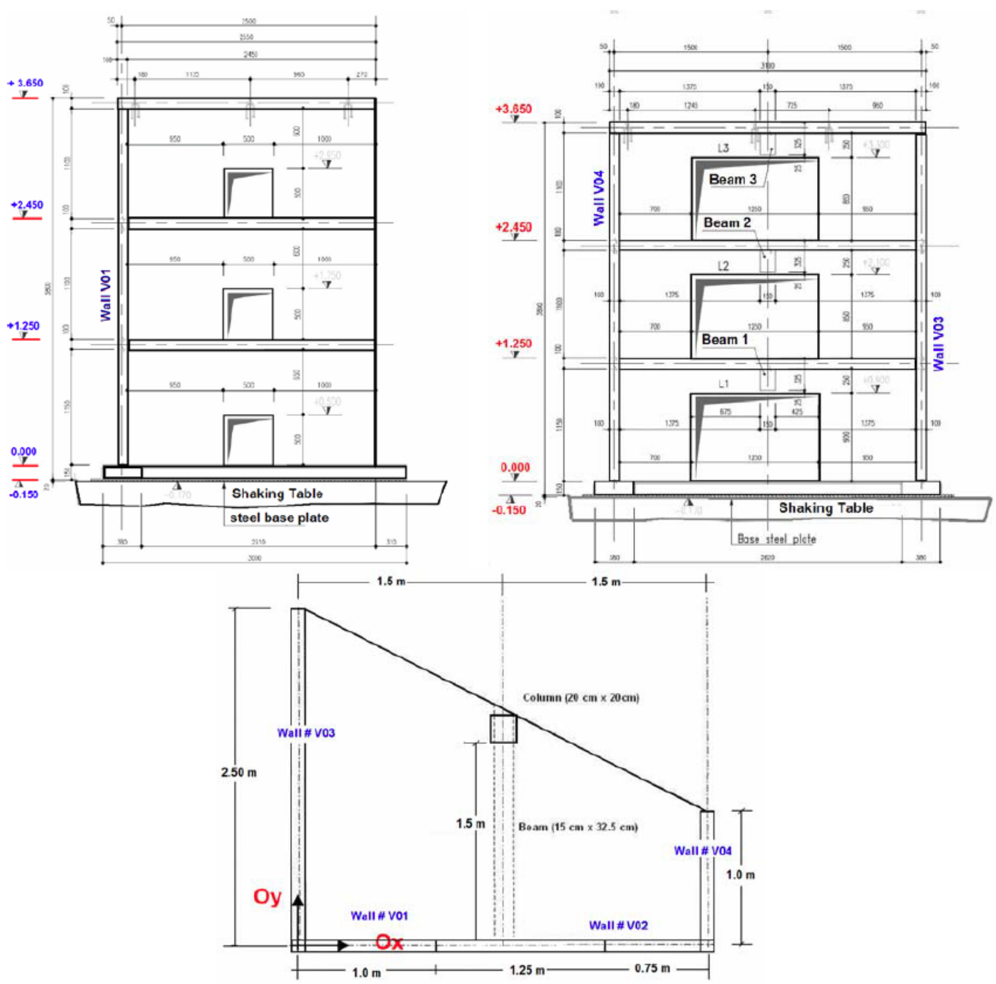

Figure 2.2 *Geometry of the SMART 2008 structure. (Simos and Hofmayer, 2013)*

Contrary to the SMART 2008 project, the building designed for the present study is regular (i.e. the centers of mass and stiffness coincide). The asymmetric character of the building would introduce additional complications in the analysis whose considerations are not part of the objectives of the thesis. The model of three story building created in ANSYS is shown in Figure 2.3. At each level, the building has six columns, seven beams and a uniform slab that covers the entire floor area. To simplify the analysis, special effects such as the soil-structure interaction will be neglected. In addition, the ground acceleration will be applied along the horizontal X axis, i.e. no acceleration will act along the vertical and transverse Z direction.

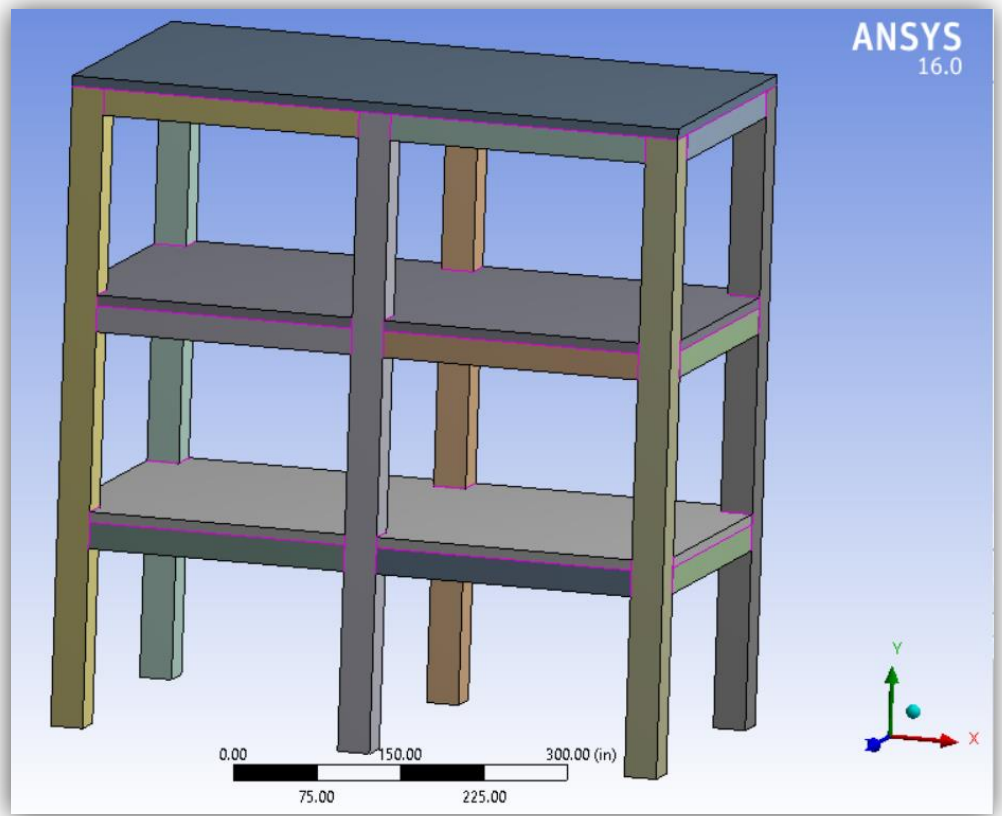

Figure 2.3 *3D model of the moment resistant frame in ANSYS.*

The overall dimensions of the building are provided in Figure 2.4.

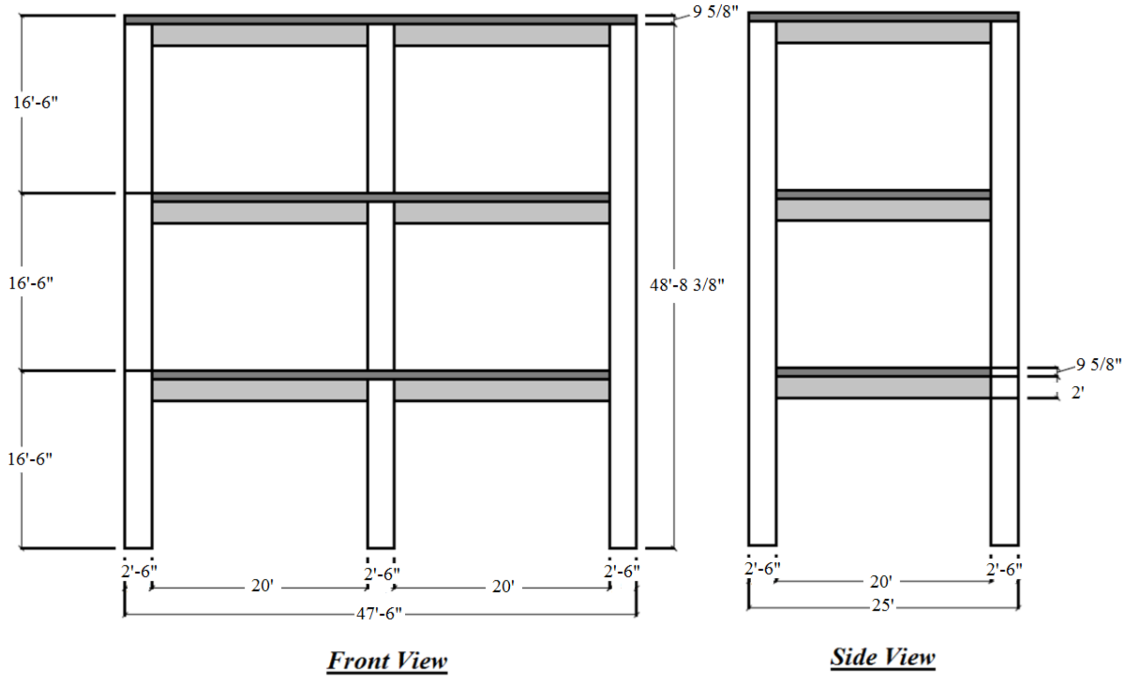

Figure 2.4 *Overall dimensions of the 3-D frame.*

The columns have a 30 x 30 inches cross section with a height of 16.5 ft at each floor level for a total of 49.5 ft. The concrete section has a longitudinal reinforcement steel rebar consisting of twelve #10 (1.27 inches diameter) evenly spaced around the column in a single layer configuration. A volume ratio of transverse reinforcement of 0.015 was used that consisted of single #4 (0.5 inches diameter) rebar hoops. A cover of 2.5 inches was added in all the four faces of the column. The reinforcement layout and the column geometry are shown in Figure 2.5.

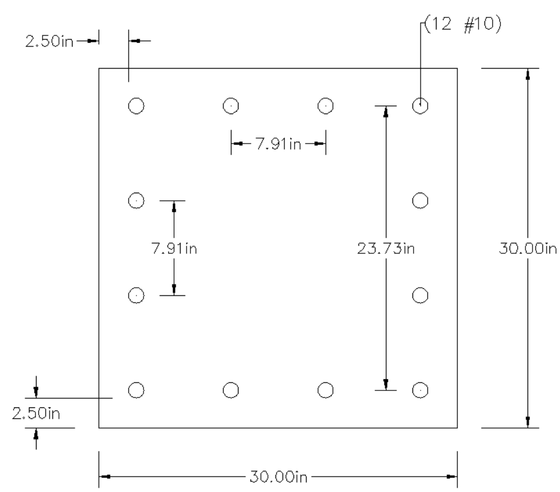

Figure 2.5 *Column geometry and reinforcement details.*

Each beam has a 24 x 12 inches cross section with a total length of 20 ft; the same dimensions were used in all directions. The longitudinal reinforcement steel rebar consists of six #8 (1-inch diameter) with two rebars at the top and four at the bottom in a single layer. A volume ratio of transverse reinforcement of 0.013 was used that consisted of single #4 (0.5 inches diameter) rebar hoops. A cover of 2.5 inches was added at the top and the bottom of the beam. The reinforcement layout and the column geometry are displayed in Figure 2.6.

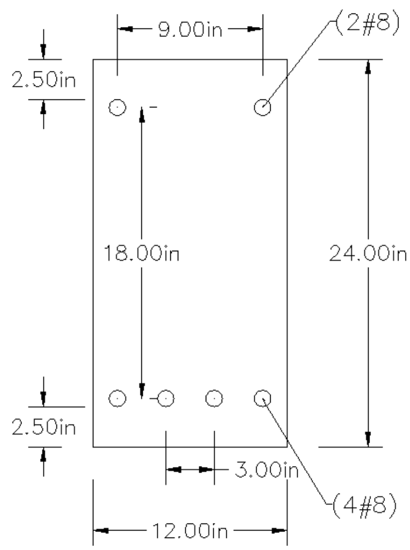

Figure 2.6 *Beam geometry and reinforcement details.*

The slab at each floor was designed with a thickness of 9.6 inches in order to eliminate the need to calculate and check the deflections, in accordance with Table 9.5(a) of the code ACI 318-11. For simplification purposes, a one-way slab was considered in the analysis since the measurements of stress at the slab are irrelevant for the verification of the proposed equivalent linear method. Nevertheless, the slabs weight and their contribution to the stiffness of the structure are all accounted for.

2.2.2. Material model

As it is commonly done for the non-linear analysis of frames, it will be assumed that the beams and column are the elements that can undergo inelastic deformations. The slabs are assumed to have a linear behavior. Because the analysis was done using 3D solid finite elements model (described later in Section 4.3), the usual representation of the non-linear behavior for one-dimensional elements, namely the Moment-Curvature curve, cannot be implemented directly. Rather the stress-strain relationships for the beam and column confined concrete sections were used as an input data. The computer software SE::MC from StructureExpress (2015) was used to determine the stress-strain curve for the columns and beams. SE::MC is a computer program that allows the user to perform moment-curvature type of analysis on structural member sections.

The material properties used for all the reinforced concrete elements are presented in Table 2.1.

Table 2.1 *Concrete and steel material properties.*

Material properties	***Value***
Concrete compressive strength, f'c	4,000 psi
Yield stress of longitudinal reinforcement, fy	60,000 psi
Poisson's ratio	0.2
Specific weight	150 lb/ ft^3

The stress-strain constitutive relation obtained with the program SE::MC for the confined concrete in the columns with the 30 x 30 inches cross-section is shown in Figure 2.7. The result shown takes into consideration the longitudinal rebar #10, the geometry of the section and the confinement rebar.

The curve shows that after the section reached a yield state (close to a strain of 0.01in/in), it started to lose capacity. When this feature was introduced into the finite element model in ANSYS it created serious convergence problems in the dynamic non-linear analysis. Therefore, it was necessary to make some adjustments: the stress capacity after yield was modified and it was assumed constant, as shown in Figure 2.7. It is important to point out that this modification is not crucial for the purposes of the study, i.e. to compare the results of a non-linear dynamic analysis with an approximate equivalent linear one.

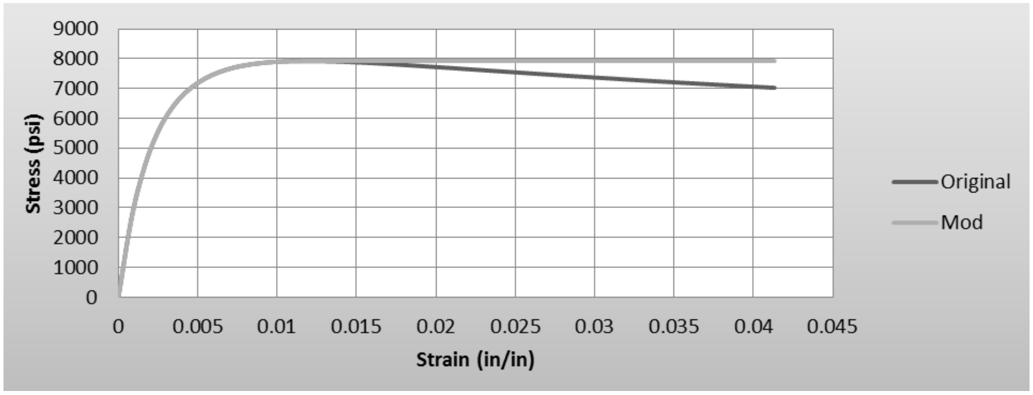

Figure 2.7 *Stress-strain relationship for the confined concrete in the columns from SE::MC.*

The software also provided additional information that was incorporated in the development of the stress-strain degradation curve for the element. For example, the steel rebar has an entirely different material degradation curve than concrete, as shown in Figure 2.8. The program also provided the moment-curvature graph displayed in Figure 2.9. Even though, as mentioned before, this is not the information input to ANSYS, it is shown here because this is the most common representation of the load-deformation behavior of a reinforced concrete section.

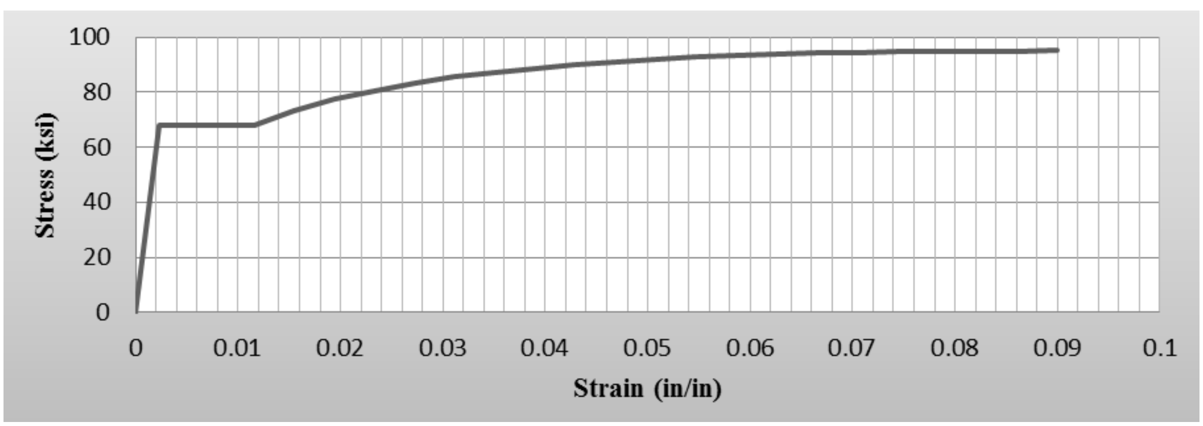

Figure 2.8 *Stress-strain relationships for Rebar #10 used for the columns by SE::MC.*

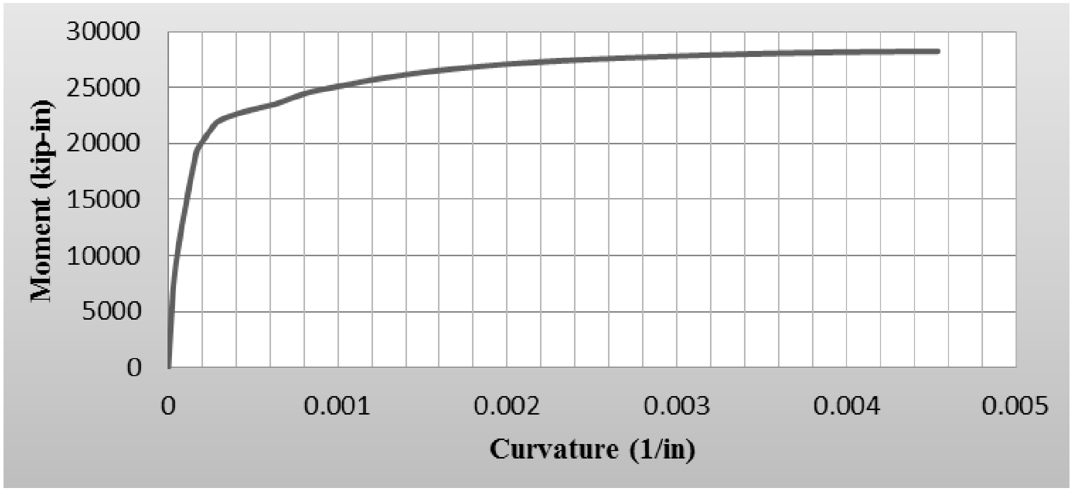

Figure 2.9 *Moment-curvature relationship for the column from SE::MC.*

The Stress-Strain constitutive relation used for the beams with 24 x 12 inches cross section is shown in Figure 2.10. The results shown account for the longitudinal rebar #8, the geometry of the section and the confinement rebar. As it happened in the case of the columns, the same behavior can be seen in the σ-ε curve, i.e. the capacity of the section reduces after reaching the yield state (close to a strain of 0.01). Therefore the same modifications were made, i.e. a constant stress capacity was assumed for simplification purposes.

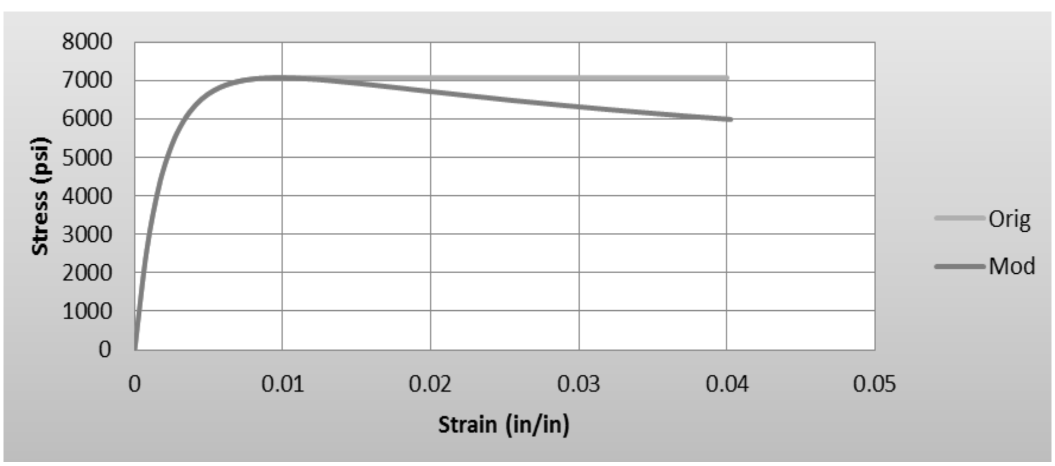

Figure 2.10 *Stress-strain relationship for the confined concrete in the beams from SE::MC.*

For the case of the beams the software SE::MC also provided some key additional information that was incorporated in the development of the stress-strain degradation curve for the element. For example, the stress-strain relation for the rebar has the shape displayed in Figure 2.11. Also, the moment-curvature curve for the beams (not used in ANSYS) can be seen in Figure 2.12.

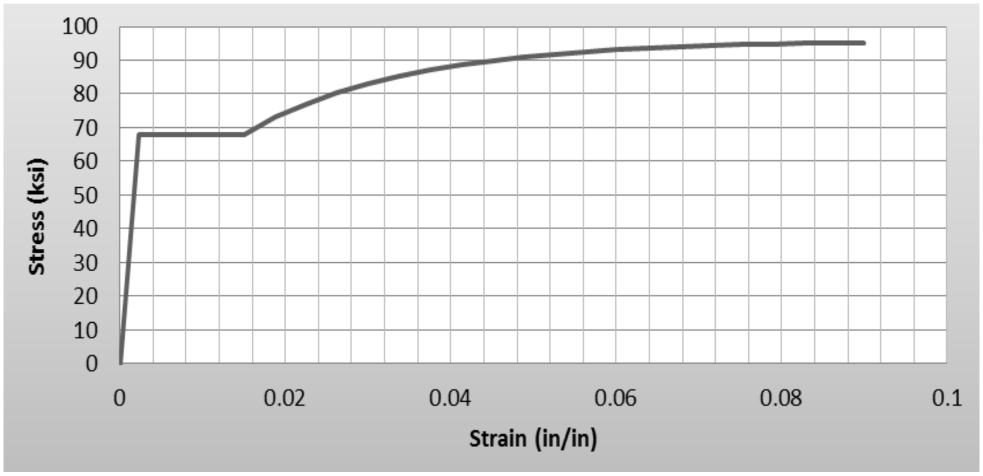

Figure 2.11 *Stress-Strain relationships for rebar #8 used for the beams by SE::MC.*

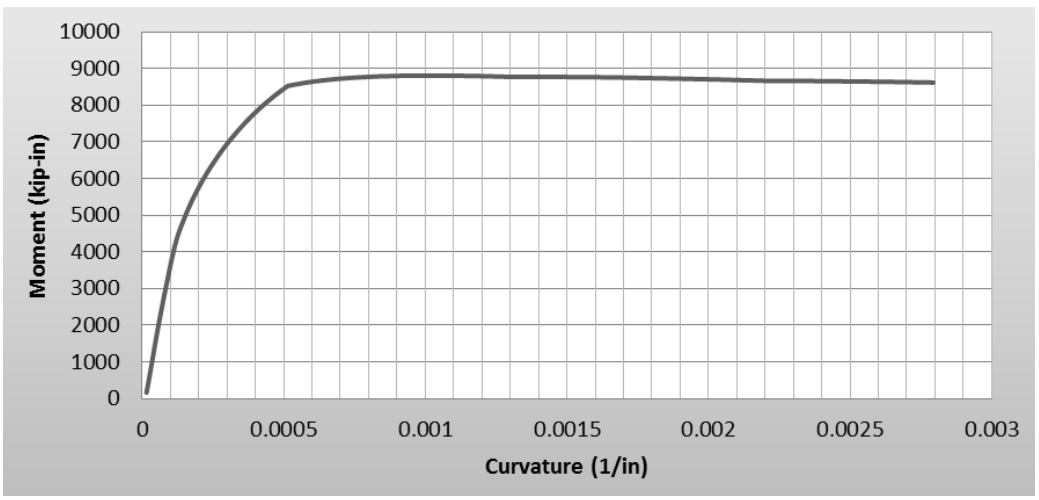

Figure 2.12 *Moment-curvature relationship for the beam from SE::MC.*

It should be mentioned that there are theoretical methods to determine the compressive uniaxial stress-strain relationship for confined reinforced concrete in a practical way. One of these methods (Pfrang, et al.,1964) was derived by Hognestad (1951) from tests on short concrete columns subjected to combined axial load and bending. To simplify the derivation, in this method bending is assumed to occur about only one of the principal axes of the section. In addition, in this formulation the concrete is also assumed to have no tensile strength. The graph of the stress-strain relation and the equations to define it are shown in Figure 2.13.

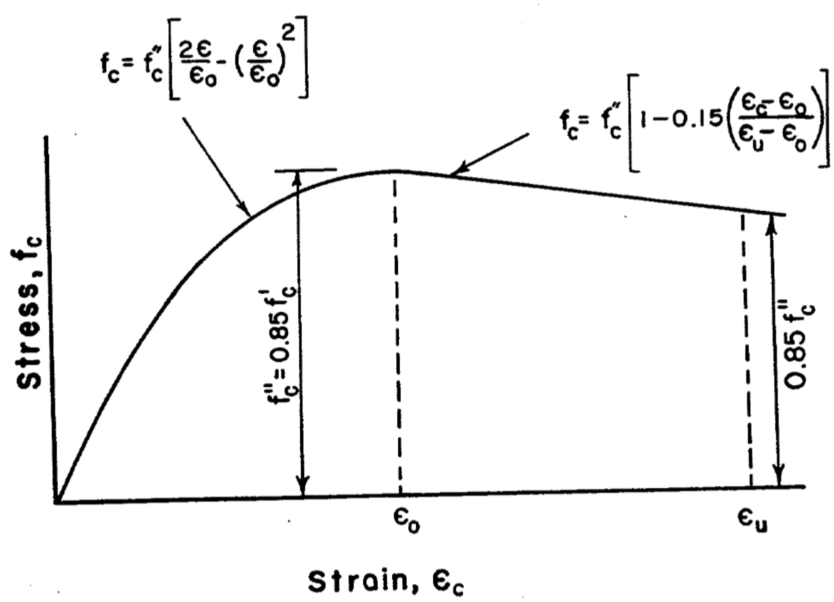

Figure 2.13 *Assumed stress-strain relationship for reinforced concrete. (Pfrang, et al.,1964)*

where the following notation is used:

fc	= *concrete normal stress at any strain,*
f'c	= *compressive strength of concrete determined from 28 days cylinder test,*
f''c	= *compressive strength of concrete in reinforced concrete members,*
ε	= *normal strain,*
ε_o	= *compressive strain in concrete corresponding to maximum stress,*
ε_c	= *compressive strain in concrete, and*
ε_u	= *useful limit of compressive strain in concrete.*

It is important to mention that even though this method was not implemented in this thesis to determine the stress-strain curve that was input to the program, it is shown here because it can be used as an alternative approach. For example, a stress-strain curve for unidirectional monotonic compressive loading similar to the first zone in Figure 2.13 was used by Musmar (2013) to study the effect of openings in the behavior of reinforced concrete shear walls. An ideal elastic-perfectly plastic material model was adopted for the steel reinforcement. This author used the two constitutive relations in the ANSYS program along with the same element Solid65 adopted in the present study.

2.2.3. Pushover calibration

The pushover analysis is a procedure to carry out a static non-linear analysis of a structure, usually a model of a building. The structure is subjected to a lateral load loading pattern, either concentrated or distributed and as the load is slowly increased, the displacement of a selected point is recorded. For buildings, the lateral displacement is usually measured at the roof. As the load increases, the elements of the building pass from an elastic state to an inelastic behavior until an ultimate condition is reached.

Here a pushover analysis was performed on a single column of the building that will be the subject of further studies. The point load was applied at the top end in one direction and then in the opposite direction to complete one cycle of loading. This process was performed in order to understand the loading and unloading behavior of the column. The test was done to determine if the element would follow the strain-stress curve calculated for the column and as such it serves as a mean to calibrate the model. Rather than displaying the traditional force vs displacement curve, only the normal stress and strain at the bottom of the column are reported in Figure 2.14. It can be observed that the stresses and strains in the column section behaved exactly as the predicted non-linear constitutive relationship for the material. Also, the loading and unloading cycle behavior can be seen clearly as the force applied at the top changes direction.

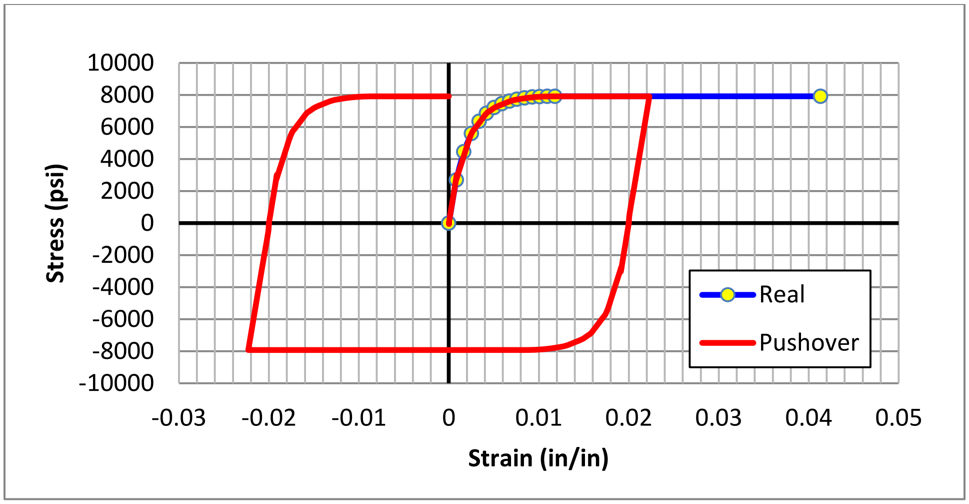

Figure 2.14 *Result from the pushover analysis for the column and the input constitutive relation.*

2.2.4. Additional Loading

Some additional static loading were added to the dynamic loads caused by the earthquake ground motion. These loads must be applied before the earthquake loads and then they act simultaneously with them because due to the non-linear behavior of the structure they cannot be combined afterward. The additional loads represent the weight of the internal and external non-structural walls, ceilings, additional equipment and piping, etcetera, that can be classified as a distributed load. To achieve this purpose, the loads were applied throughout the entire floor and roof slab area; their magnitudes are provided in Table 2.2. These loads are separate from the weight of the concrete structural elements, which are also accounted for.

Table 2.2 *Additional static loading.*

Area Section	***Loading***
First Floor	30 lb/ft^2
Second Floor	30 lb/ft^2
Roof	15 lb/ft^2

2.3 Development of the finite element model

There are several ways to model a structure to carry out dynamic non-linear analysis. The different models differ in the way how the plasticity is distributed along the element. Basically, the modeling approaches can be divided into concentrated plasticity and distributed plasticity models (Deierlein, et al., 2010). The simplest and most widely used models are those where the inelastic deformations are concentrated at the end of beams and columns either by means of a rigid plastic hinges or non-linear spring with hysteretic properties. At the other end of the spectrum are the most sophisticated models, i.e. the finite element models where the continuum along the complete member length is divided into small subdomains. Although the finite element method is nowadays a well-known and widely used technique for static and dynamic analysis, it is still not extensively applied for non-linear analysis of reinforced concrete structures. There are several reasons that impede its widespread application, namely the computational costs, the parameters calibration, the difficulty in interpreting the results in relation to design acceptance criteria that are still based on rotations (Deierlein, et al., 2010), etc. As a consequence, the finite element method for non-linear structural analyses is still mostly limited to research applications.

Notwithstanding the cited limitations, there is a number of powerful commercial finite element software that can be applied for non-linear dynamic analysis of reinforced concrete structures. Among them are ANSYS, Abaqus, and LS-Dyna. As it was mentioned previously on several occasions, for the present work the ANSYS program was chosen. There are a couple of reasons for this choice. First, the author of this thesis became acquainted with the program when he spent a summer as an intern at the Brookhaven National Laboratory in Uptown, New York, as part of the requirements of his Nuclear Regulatory Commission (NRC) fellowship. The second, and perhaps the most important reason, is that ANSYS is one of the structural analysis programs that meets the standards of NRC. The computer programs to be used in the nuclear industry need to be in full compliance and meet the requirements of applicable provisions of the U.S. NRC's 10CFR21 and 10CFR50 Appendix B regulations (Nuclear Regulatory Commission, 2016a; 2016b).

2.3.1. Element selection for the structural model

To carry out an analysis using finite element models it is necessary to select an element type which depends on the degrees of freedom that are desired to be considered to calculate the response. Another important consideration is that each type of element has unique properties that allow to perform specific tasks, like for example analyzing the cracking that appears in the concrete as the load increases. The type of elements also depends on the element and material; for example, concrete beams and columns are defined better using solid elements, whereas standard steel sections that have small wall thickness may be better defined using shell elements.

It was decided to model all the elements of the building using a 3-D solid element since the cross sections of the beams and columns are almost equal in magnitude in both directions (as opposed to a steel W section, where shell elements could be more appropriate). The three-dimensional finite element known as SOLID65, typically used to model 3-D solid bodies in ANSYS, was selected for the model of this thesis. These elements have properties that are specifically oriented for modeling 3D reinforced concrete sections. The SOLID65 element is defined by a total of eight nodes having three degrees of freedom at each of the nodes: translations along the x, y, and z directions, as shown in Figure 2.15.

SOLID65 can be used for modeling concrete solids with or without reinforcing bars. For concrete applications, for example, the solid capability of the element may be used to model the concrete behavior while the rebar capability is available for modeling the reinforcement behavior. Up to three different rebar specifications may be defined. Also one of the most important features of this type of element is its capability for incorporating the non-linear material properties. It is able to model the concrete cracking (in three orthogonal directions), crushing, plastic deformation, and creep. However, it must be pointed out that these capabilities were not used for the present study. For the building model studied here, the elements are homogeneous (without rebars) and the non-linear behavior is accounted for the stress-strain constitutive relation previously presented.

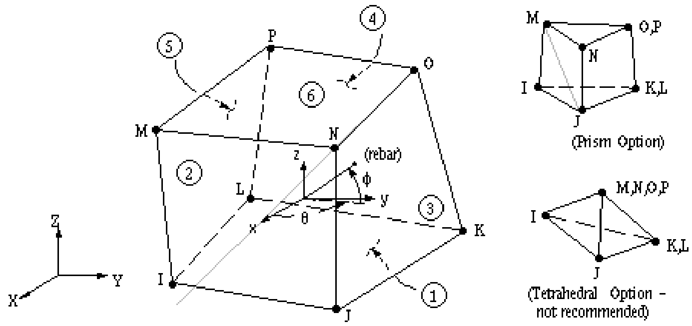

Figure 2.15 *SOLID65 3D reinforced concrete solid element from ANSYS.*

2.3.2. Model meshing

A mesh is the partition of an arbitrary domain into simpler geometrical objects or elements. Those elements are a compound of nodes, edges, faces and the relations between them. In other words, the mesh divides a complex geometry into non-overlapping elements that fill the domain. As in the elements, there are also several types of ways to carry out the meshing and in the case of 3D models, there are three major types: Tetrahedron, Hexahedron and Multi-Zone. In the MultiZone Meshing Method, ANSYS automatically generates a pure hexahedral mesh whenever possible and then it fills the more difficult to capture regions with an unstructured mesh (i.e., one that does not follow a uniform pattern).

In many cases, non-linear simulations can be challenging and the meshing quality can determine the accuracy of the results. Obviously, a very fine mesh can lead to more precise results but the time required to get the final answer also increases, and this is important when many analysis need to be run. To achieve the best results in the beams, columns and at the roof, which are the elements where the response is measured, a mesh with hexahedrons was implemented. The hexahedron is a cube-shaped element that has 8 vertices, 12 edges and it is bounded by 6 quadrilateral faces. After testing models with several mesh sizes, the best accuracy versus time consumption was obtained with elements with a size of 20 inches, which represents the maximum distance allowed between each node. For the floor slabs, a tetrahedron mesh was used since it gives faster results and a high precision was not necessary for these locations. A single tetrahedron has 4 vertices, 6 edges and is bounded by 4 triangular faces. The mesh model is shown in Figure 2.16 for the complete frame structure. The mesh in the roof slab looks different because it was automatically generated by the program and since there were no columns coming out of the surface, it led to a simpler mesh compared to the floor slabs.

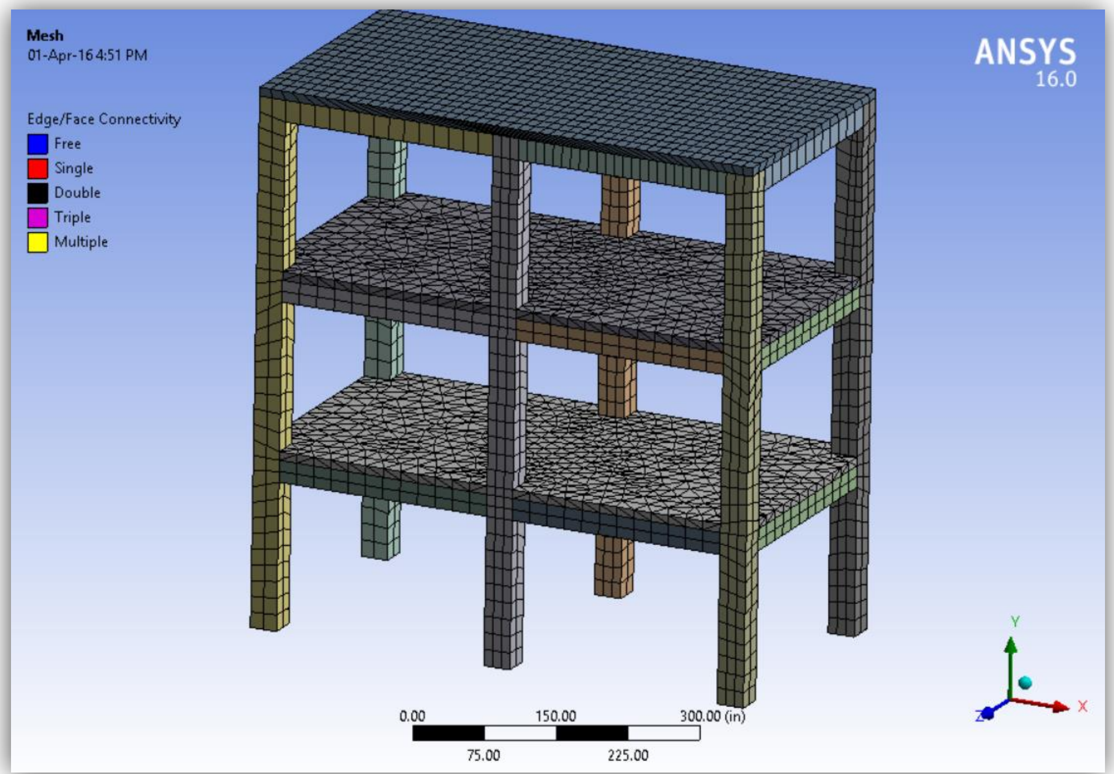

Figure 2.16 *Mesh of 3D frame model.*

2.4 Chapter summary and conclusions

The main objective of this chapter was to give a clear understanding of the model development process and all the parameters that were established. In the following chapter, the described model will be subjected to different linear and non-linear analysis and all of them will be using the same base structure. The structure as mention above consists of a 3D three story building. The structural analysis was assumed as a special moment resistant frame that is fixed at the bottom of the end of each column, and free at the top with no lateral or vertical restrictions in movement. The entire model consists of reinforce concrete material that has been defined with non-linear properties that will capture a more real behavior of the structure.

In order to analyze this structure and combine all the parameters (material properties and dimensional cross section), a finite element analysis was implemented. All results processes were generated using ANSYS v16 computer software. The finite element method was used because of the ability to handle the complex process and make 3D simulations that will allow the predictions of non-linear structural behavior using loads that can change in time in magnitude and direction. For the model, a mesh of 20 *in* hexahedral shape was determine, after several tests that optimize the analysis process giving the most accurate results in the less computational time necessary. Also, the SOLID65 was determined as the element type for the structure because of the ability to better predict the behavior of reinforced concrete in smaller cube shape elements.

CHAPTER III

MODAL AND NON-LINEAR DYNAMIC ANALYSIS

3.1 Introduction

This chapter presents the methodology and examples of application to calculate the non-linear dynamic response of the three-story reinforced concrete building presented in Chapter 2. Non-linear static procedures are becoming more popular to evaluate structures that are subjected to strong earthquake loading and are the methods used for the design of new buildings with the performance-based design philosophy. However, non-linear dynamic analysis (Fragiadakis, et al., 2014) has been proven to be the most rigorous analysis method available. Nevertheless, there are several reasons that are normally cited to explain why they are not more widely used in structural engineering practice. Among them are the computational expense of the method, the need for detailed information about the structure and its material, the scarceness of appropriate and user-friendly structural analysis software, and the need for careful selection of the ground acceleration time histories to be used as seismic input. These drawbacks are slowly being overcome and it is reasonable to foresee that the non-linear analysis methods will become more popular in the near future. In any case, full non-linear dynamic analyses are required for this thesis because the response calculated with this rigorous approach will be used as a benchmark to evaluate the accuracy of the equivalent linear method.

To implement a non-linear time history dynamic analysis, ANSYS v16 uses an iterative process in order to generate results. Each iteration involves solving a linearized equilibrium equation where the mass and stiffness matrices must be calculated for each time step. For this purpose the program uses the Newton-Raphson method (Huei-Huang, 2015), using the difference in displacement, force or even bending moment to determine convergence in the results and move on to the next time step. If the residual force is smaller than a criterion, then the substep converged. Otherwise, another equilibrium iteration equation takes place. The analysis is completed when the convergence criteria are satisfied for all the time steps as shown in Figure 3.1. In general, this method is a root-finding algorithm that uses the first few terms of the Taylor series of a function *f*(*x*) in equation (3.1) in the vicinity of a suspected root.

$$f(x_0+\epsilon)=f(x_0)+f'(x_0)\,\epsilon+\frac{1}{2}f''(x_0)\,\epsilon^2+\ldots. \tag{3.1}$$

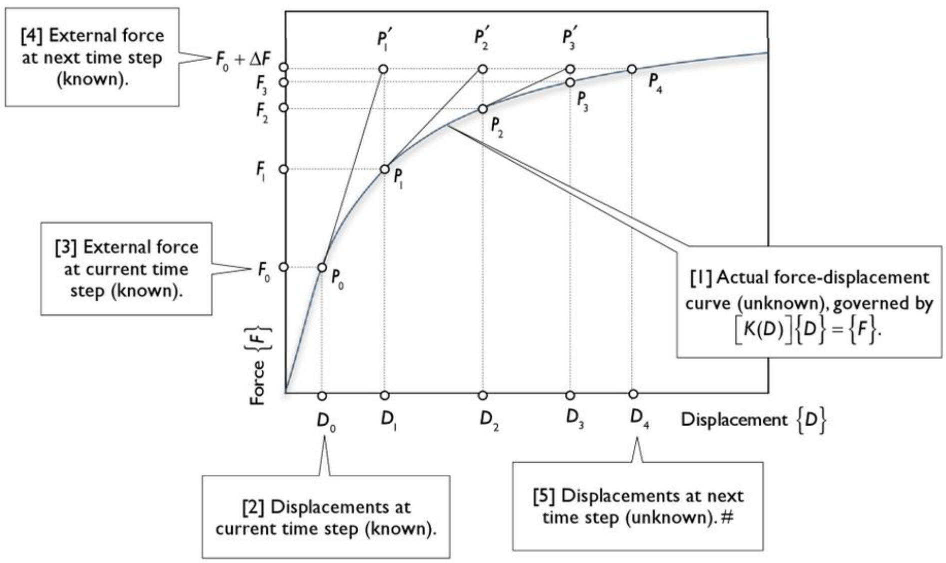

Figure 3.1 *Newton-Raphson method. (ANSYS, 2015)*

This chapter also presents the results of non-linear dynamic analyses performed using a short-band and broad-band earthquake that were applied to the model structure defined in the previous chapter. The purpose of the analysis was to obtain realistic values of the shear force and bending moment at a first floor column base, and the relative displacement at the roof. These quantities are compared with the results from the equivalent linear model in the next chapter. The absolute acceleration of each floor was also recorded to generate floor response spectra that are used for the seismic design of non-structural components and equipment. In the next chapter the acceleration time histories will be used to calculate floor response spectra with two approaches: the full non-linear analyses presented here and the equivalent linear method introduced in Chapter 4.

3.2 Modal analysis

The first step in a dynamic analysis of a structure, whether it is a linear or non-linear one, should be to obtain its dynamic properties, namely the natural frequencies, natural periods and modes of vibrations. Examining the natural periods and associated modal shapes one can detect problems in the model. Moreover, inspecting the natural period's one can select the proper time step for a posterior forced vibration analysis of the structure, and estimate which modes will have more influence in the response, etc. Therefore, a modal analysis was performed in ANSYS and the first six natural frequencies and periods are shown in Table 3.1. Figure 3.2 displays the natural frequencies in a graphical form.

Table 3.1 *Natural frequencies and periods of the structure.*

Mode	***Frequency (Hz)***	***Period (s)***
1	2.6267	0.3807
2	2.7378	0.3653
3	3.4304	0.2915
4	8.5653	0.1168
5	8.7781	0.1139
6	11.1291	0.0899

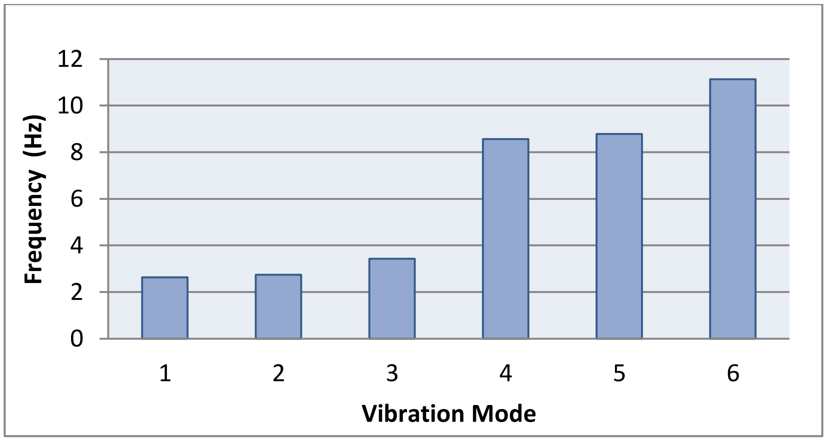

Figure 3.2 *Undamped natural frequencies of the 3-D model.*

Because the model of the building is three-dimensional, a discussion of the frequencies and modes is warranted. The first mode with a period of 0.3807 s corresponds to a deformation in the vertical Y-Z plane. The second mode of the building has a natural period of 0.3653 s and it is associated with a motion in the X-Z plane. Figure 3.3 displays the second vibration mode of the 3D model of the building calculated with ANSYS and the resulting magnitude of deformation in feet of the entire structure.

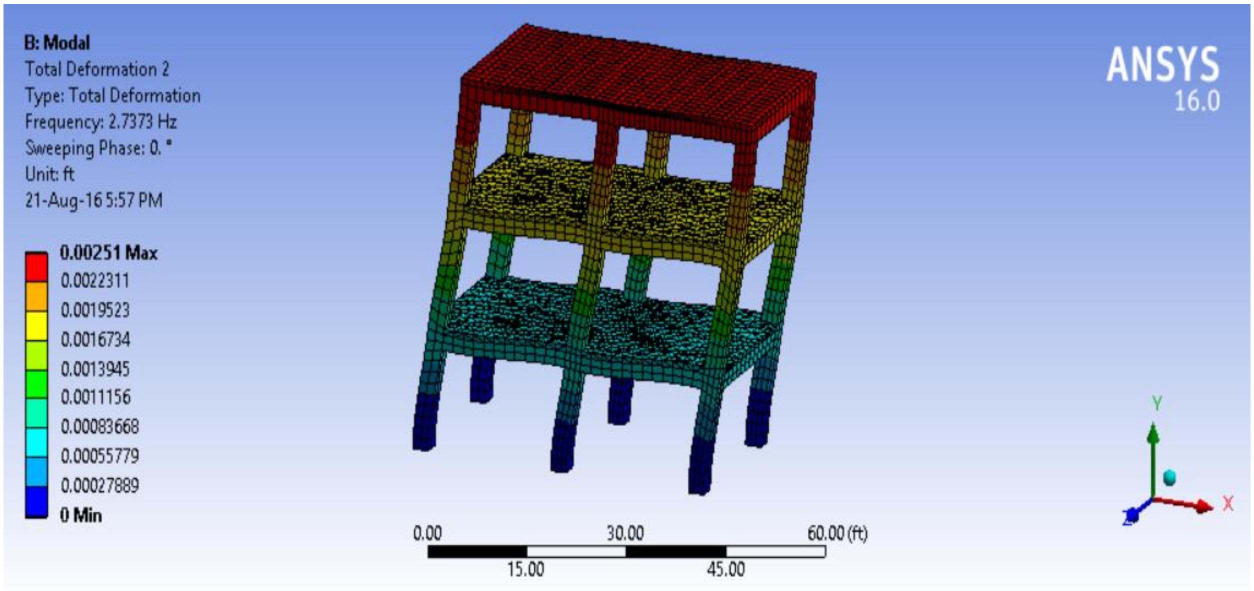

Figure 3.3 *Second mode of vibration shape.*

It is recalled that the building is regular in the sense that the centers of mass and stiffness at each floor coincide and thus the first two modes are uncoupled. The third mode with the natural period of 0.2915 s is a torsional one (around the vertical axis). The fourth mode (with period 0.1167 s) displays a motion of the floor masses in the Y-Z plane: the first and second floor move in opposite direction to the third floor. This modal shape would be associated with the second mode of a 2-D model of the building. In a similar fashion, the shape of the fifth mode (with period 0.1139 s) is confined to the X-Z plane and has the shape of the second mode of a 2D building. The shape of the sixth mode has a complex form and it is a combination of torsion and flexural deformation in the Y-Z plane.

To calculate the seismic response, the ground acceleration will be applied along the horizontal X axis and thus the main modes of interest are those in the X-Z plane, i.e. the second and fifth modes among those presented in Table 3.1. The maximum displacements of the floor slabs for the second and fifth modes were recovered from the ANSYS output and are plotted in Figure 3.4. They clearly reveal that these are the first and second modes of vibration of a plane model of a three-story building, as it was mentioned before.

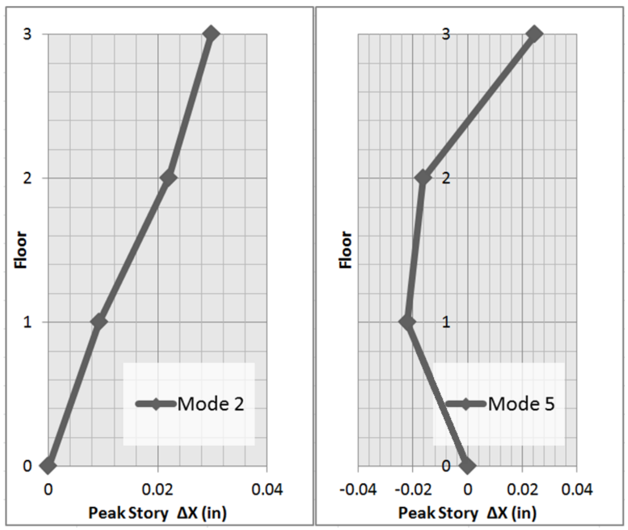

Figure 3.4 *Vibration modes in the X-Z plane.*

3.2.1. Comparison with a shear building model

As a means to corroborate the dynamic properties of the building model created in ANSYS, the simple and well known shear building model was used. Because the shear building model used was 2-D, only the lower frequencies and modes in the X direction can be verified, in particular the second and fifth modes of the ANSYS model. It is recalled that in a shear building model the beams and slabs are assumed to be rigid in-plane and out-of-plane and they are represented by lumped masses; the mass of the columns is also merged with these floor masses. Using the properties of the columns, the following stiffness matrix of the shear building was obtained:

$$[K] = \begin{bmatrix} 4514.1 & -2257.1 & 0 \\ -2257.1 & 4514.1 & -2257.1 \\ 0 & -2257.1 & 2257.1 \end{bmatrix} \text{ in } {}^{kip}\!/_{inches} \tag{3.2}$$

The lumped mass matrix is:

$$[M]=\begin{bmatrix} 1.2215 & 0 & 0 \\ 0 & 1.2215 & 0 \\ 0 & 0 & 0.84705 \end{bmatrix} \quad in\ \frac{kip.\sec^2}{inches} \tag{3.3}$$

Solving the associated eigenvalue problem with these two matrices, the natural periods displayed in Table 3.2 were obtained. They are compared in the same table with the natural periods of the ANSYS model. The differences are reasonable considering that the shear building is a very simplified model with only three degrees of freedom compared with the 3-D finite element model of ANSYS with thousands of degrees of freedom.

Table 3.2 *Comparison of natural periods of the two models.*

Mode	***ANSYS Periods (s)***	***Shear Building Periods (s)***	***Difference***
2	0.36526	0.30049	17.7%
5	0.11392	0.10961	3.8%

3.2.2. Damping model calibration

The estimation of the damping present in the structures poses a very difficult problem for structural dynamics. Unlike the mass and stiffness matrix of a structural system, damping does not relate to a unique physical property but it is rather due to a number of phenomena difficult to identify and quantify.

When the building is vibrating due to an earthquake ground motion, there are two sources of damping present. One is the inherent or natural damping which is always present in the structure, even when it is in free vibration or oscillating with low amplitude vibrations. This dissipation of energy is due to several factors which are very difficult to quantify separately. Usually a linear viscous damping model is used to account for all the different sources in a simple way.

The other source of energy dissipation occurs when the structural elements undergo inelastic excursions and it is sometimes referred to as hysteretic damping. The amount of damping is proportional to the area of the hysteresis cycle form in the elements that deform inelastically. This damping is not calculated with any specific model but rather it is inherently being accounted for when the equations of motion are numerically integrated.

The ANSYS program needs an explicit damping matrix [C] to account for the inherent damping. There are two common ways to define such a damping matrix. One is to use the classical damping assumption, i.e. to presume that the matrix [C] is diagonalizable using the mass normalized eigenvector matrix [Φ]. It can be shown that in this case the damping matrix can be calculated as:

$$\left[C\right]=\left[M\right]\left[\Phi\right]\left[2\xi_j\omega_j\right]\left[\Phi\right]^T\left[M\right] \tag{3.4}$$

where [M] is the mass matrix and ξ_j and ω_j are, respectively, the modal damping ratio and natural frequency of the j^{th} mode. The other approach to define a damping matrix is to use the Rayleigh damping model. In this method the damping matrix [C] is defined as a linear combination of the mass matrix [M] and stiffness matrix [K]:

$$\left[C\right]=\alpha\left[M\right]+\beta\left[K\right] \tag{3.5}$$

where α and β are two constants that need to be determined. This way to define the damping matrix is also known as the proportional damping model since the matrix [C] is proportional to the mass and stiffness matrices. Equation (3.5) is usually implemented for the whole structure but it could be applied to individual elements. To determine the constants α and β, equation (3.5) is pre and post multiplied by the mass normalized matrix of vibration modes [Φ]. Doing so and using the orthogonal properties of the modes with respect to the mass and stiffness matrices, one can write:

$$2\xi_j\omega_j=\alpha+\beta\omega_j^2 \quad ; \quad j=1,\ldots,n \tag{3.6}$$

Because equation (3.6) is an overdetermined system of equations (n equations for 2 unknowns), to solve for α and β from equation (3.5) one needs to select two modes, for example the m^{th} and p^{th} modes:

$$\begin{aligned} \xi_m &= \frac{\alpha}{2\omega_m} + \frac{\beta}{2}\omega_m \\ \xi_p &= \frac{\alpha}{2\omega_p} + \frac{\beta}{2}\omega_p \end{aligned} \tag{3.7}$$

Solving these equations it is straightforward to show that the constants can be obtained in terms of the modal damping ratios ξ_m and ξ_p and natural frequencies ω_m or ω_p of the two selected modes as:

$$\alpha = \frac{2\omega_m\ \omega_p}{\omega_p^2 - \omega_m^2}\left(\omega_p\ \xi_m - \omega_m\ \xi_p\right) \tag{3.8}$$

$$\beta = \frac{2\omega_m\ \omega_p}{\omega_p^2 - \omega_m^2}\left(\frac{\xi_p}{\omega_m} - \frac{\xi_m}{\omega_p}\right) \tag{3.9}$$

To determine the constants α and β with equations (3.8) and (3.9), the natural frequencies of the second and fifth modes of the 3D model were selected as ω_m and ω_p. It is recalled that these modes are equivalent to the first and second modes of a 2D model of the building in the X-direction. This is the direction of interest because the earthquake ground motion is applied along this axis. Table 3.3 displays the frequencies and damping ratios used to define the constants α and β and Table 3.4 shows the values of the two constants.

Table 3.3 *Parameters for calculation of the two constants α and β.*

Mode	***Frequency (Hz)***	***Symbol***	***Frequency (rad/s)***	***Symbol***	***Damping***
2	2.7378	ω_m	17.2021	ξ_m	0.02
5	8.7781	ω_p	55.1544	ξ_p	0.02

Table 3.4 *Constants to define the damping matrix.*

Constant	***Value***
α	0.524498
β	0.000552818

It is important to mention that the Rayleigh damping has some limitations. Since the damping ratio can only be assigned to two modes of vibration, this causes that those modes corresponding to frequencies smaller than ω_m or bigger than ω_p will have larger values. At the same time, the modes with frequencies in between the two frequencies selected, ω_m and ω_p, will have lower damping ratios, as shown in Figure 3.5. This can be easily shown by solving for the damping ratio from equation (3.6) and dropping the subscripts to create a continuous function:

$$\xi = \frac{\alpha}{2}\frac{1}{\omega} + \frac{\beta}{2}\omega \tag{3.10}$$

when equation (3.10) is evaluated at $\omega = \omega_m$ or $\omega = \omega_p$, it yields the correct damping ratios, but the other modes can be overdamped or underdamped.

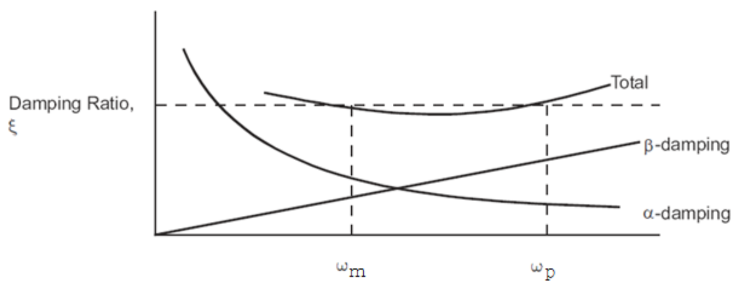

Figure 3.5 *Rayleigh damping curve*

3.2.3. Damping validation

In order to validate the correct implementation of the damping in the model created in ANSYS, a simple test was simulated. It is well known that for a structure to vibrate with the natural frequency of a selected mode, it should be initially deformed with the shaped of this mode and then release it in free vibration. This test was simulated in ANSYS using the maximum displacements of each floor corresponding to the second mode of vibration obtained from the modal analysis. Each floor of the building was slowly pushed from an undisturbed state during one second until it reached the same displacement that the structure experience in the second mode. It should be mentioned that the program allows the user to apply displacements that increase with time in a predefined way. This process was also implemented to apply the gravitational loading on the structure (describe on section 3.4.1). After the selected time was reached, the loads were suddenly removed and the structure was allowed to vibrate freely. The displacement at the roof was measured and it is displayed in Figure 3.6 for the first two seconds of the motion.

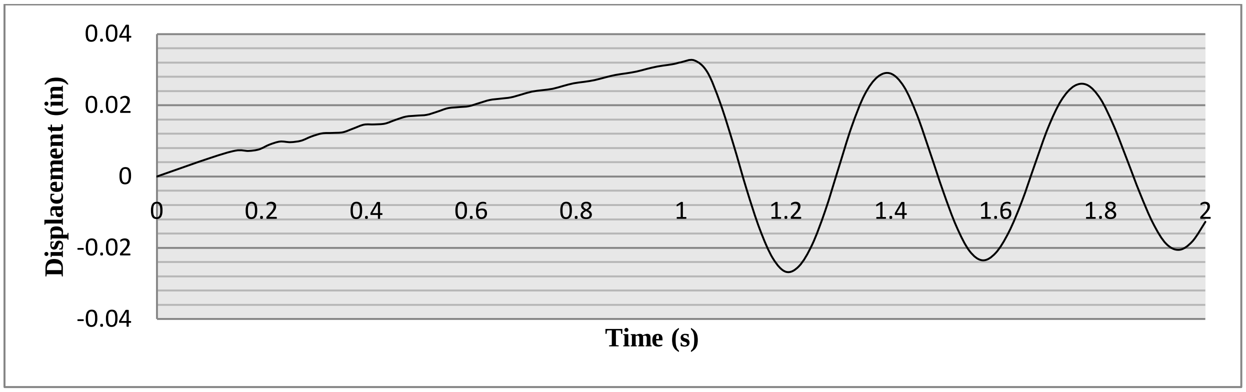

Figure 3.6 *Displacement of the roof in free vibration.*

The damping ratio can be determined by calculating the logarithmic decrement δ. The logarithmic decrement can be computed using the values of the displacements at two peaks (consecutive or not) with the same sign as follows:

$$\delta = \log\left(\frac{u_1}{u_2}\right) \tag{3.11}$$

The damping ratio associated to the vibration mode of the test can be obtained with the following expression, valid for small values of ξ:

$$\xi = \frac{\delta}{2\pi} \tag{3.12}$$

Table 3.5 displays the two instants of time and the corresponding peak displacements used to define the logarithmic decrement and Table 3.6 shows the value of δ and the estimated damping ratio of the second mode. The damping ratio obtained from the simulation of the free vibration test is equal to that selected to define the two constants of the Rayleigh damping model, which validates its implementation in the program ANSYS.

Table 3.5 *Parameters for logarithmic decrement calculation.*

Point	***Time (s)***	***Displacement (in)***
1	1.4	0.02889
2	1.75	0.02163

Table 3.6 *Damping ratio obtained from the free vibration simulation.*

Decrement (δ)	***Damping (ξ)***
0.12569	0.02

3.2.4. Modal analysis results

After the calibration of the model and validation of the damping parameters, the final linear dynamic properties of the 3-D model of the building are displayed in Table 3.7. Also, it is shown the damping that each mode of vibration will experience. Because of the limitations of the Rayleigh model discussed before, only the second and fifth modes have the exact damping ratio of 0.02. The damped natural frequencies in ascending pattern are shown in Figure 3.7: because of the small value of the intrinsic damping, they are very similar to those with no damping.

Table 3.7 *Final dynamic properties of the lower modes of the 3D building model.*

Mode	***Damped frequency (Hz)***	***Period (s)***	***Modal damping ratio***	***Logarithmic decrement***
1	2.6261	0.38079	0.0205	-0.12853
2	2.7373	0.36532	0.0200	-0.12569
3	3.4299	0.29155	0.0181	-0.1139
4	8.5636	0.11677	0.0197	-0.12411
5	8.7763	0.11394	0.0200	-0.12569
6	11.126	0.08988	0.0231	-0.14505

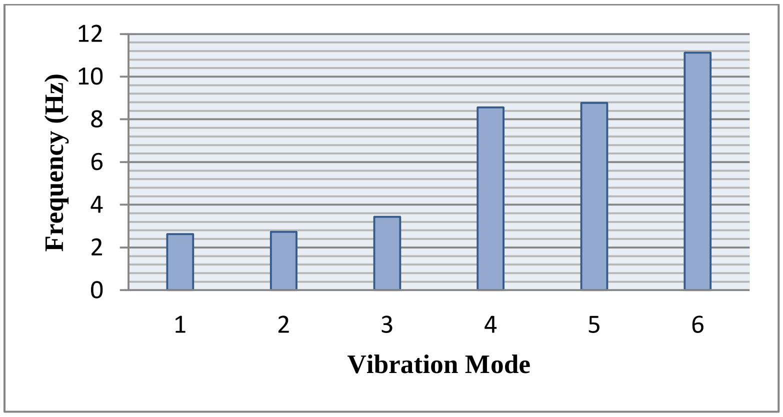

Figure 3.7 *Natural frequencies of the structure with damping.*

3.3 Selection of acceleration records

The selection of an acceleration time history to carry out the linear or non-linear dynamic analysis is always an important issue. Usually a suite of accelerograms are required to represent the randomness of the earthquake phenomenon. They should represent the seismic hazard conditions at a site and thus factors such as the magnitude of the expected earthquake event, the distance to the causative fault, the faulting mechanism and the local site geology are used in the selection process.

The objective of the present study is not to obtain adequate seismic accelerograms for the design or verification of a building, but rather to assess if an approximate method can provide reasonably accurate results compared with a full non-linear dynamic analysis. In fact, the geographical location of the building is not an issue for this study. Therefore, the selection of the accelerograms was not based on parameters such as the magnitude, focal distance, etc. Even though, there are two options that can be used to define the acceleration time series: a) use accelerograms that are compatible to a design spectrum; b) employ real accelerograms from documented earthquakes. It is argued that the first option poses a problem for non-linear dynamic analysis because they have a large number of cycles of strong motion and thus an unrealistic high energy content (Bommer and Acevedo, 2004). Therefore, the second choice was adopted for this thesis.

3.3.1. Ground motion database

Once the decision to select records of documented earthquakes was taken, the next step is choose the specific records. The intensity of the accelerograms was not an issue because they will be scaled so they generate a controlled non-linear response. Therefore, it was decided to select records with different frequency content: for this purpose they are divided into “broad-band” and “short-band” records depending on whether they have a Fourier spectrum that is spread out through the frequency range or the dominant components are clustered in a narrow frequency band. The Pacific Earthquake Engineering Research Center (PEER) ground motion database which has a very large set of ground motions recorded worldwide of shallow crustal earthquakes was used to choose and pick the accelerograms (PEER, 2016). A total of eight recorded acceleration time series were retrieved and they are plotted in Figure 3.8. Some of the parameters of these records are displayed in Table 3.8 where they are classified as short or broad-band events. The pseudo-acceleration response spectrum for each of the selected earthquake records was computed and they are shown in Figure 3.9. The original PGA ("peak ground acceleration") of each accelerogram is shown in Table 3.8 and Figure 3.8. The spectral accelerations corresponding to the two modes that most contribute to the seismic response (modes 2 and 5 of the 3-D model) are listed in the third and fourth columns of Table 3.8 and also shown in Figure 3.9.

Table 3.8 *Ground motion selection database*

Earthquake	***Δt (s)***	***Acc. mode 2 (fracc. of g)***	***Acc. mode 5 (fracc. of g)***	***PGA (fracc. of g)***	***Class***
SanSalvador-GIC1986	0.005	1.4778	1.2851	0.875	Short
ImperialValley1940	0.01	0.68797	0.67866	0.31288	Broad
LomaPrieta-Gilroy1-1989	0.005	1.1629	0.83802	0.41088	Short
Northridge-Sylmar1994	0.02	2.7747	1.1886	0.84331	Short
BorregoMountain1968	0.005	0.021578	0.015177	0.011177	Broad
HectorMine1999	0.01	0.11528	0.048211	0.043514	Broad
Managua1972	0.01	0.82455	0.72063	0.42127	Broad
Parkfield1966	0.01	0.38176	0.42938	0.27264	Short

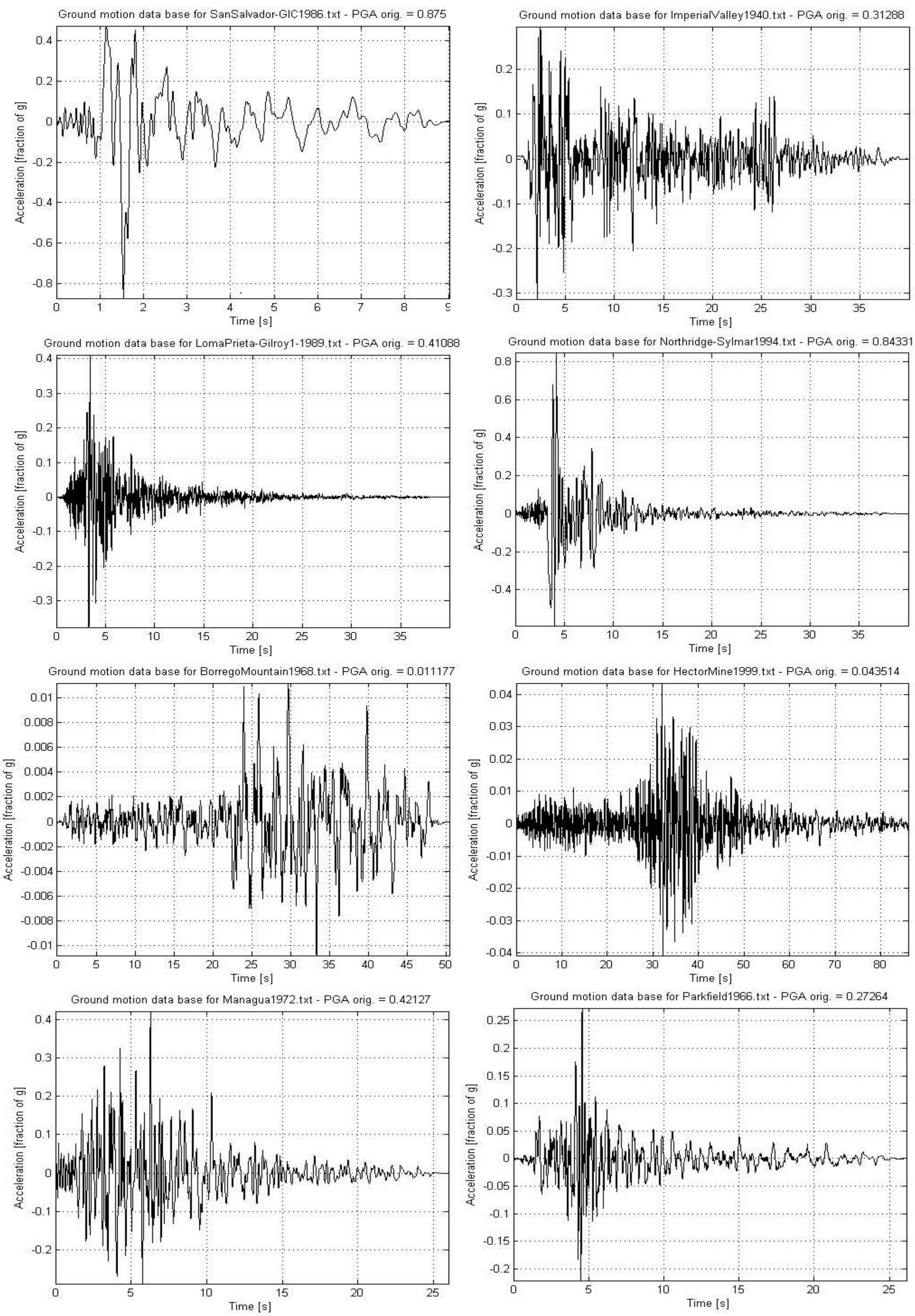

Figure 3.8 *Acceleration time histories of the selected earthquake records.*

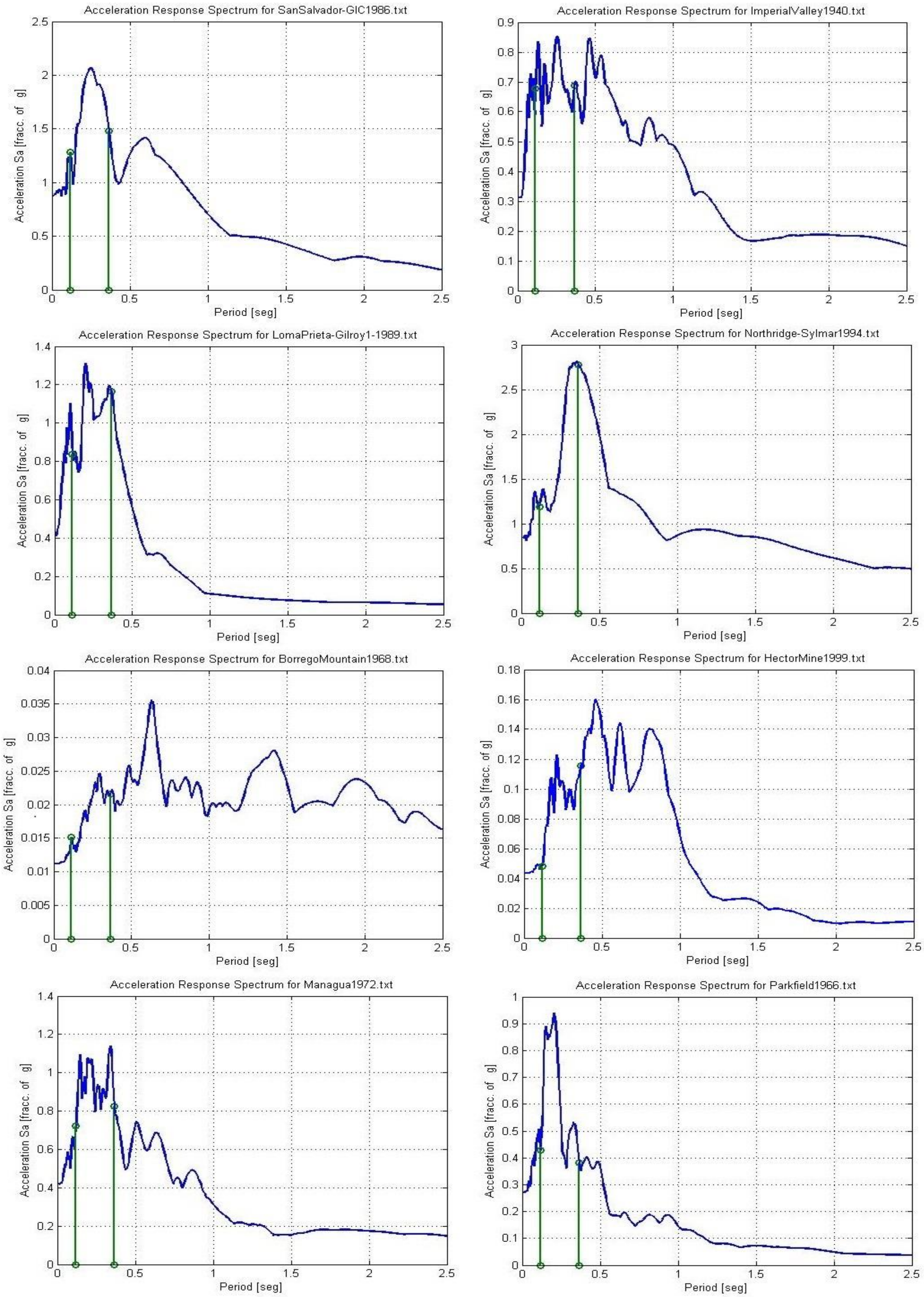

Figure 3.9 *Acceleration response spectra of the selected earthquake records.*

3.3.2. Broad-band earthquake record for detailed studies

The first broad-band seismic record that will be used to examine in more detail the accuracy of the equivalent linear method is the accelerogram of the well-known El Centro earthquake of May 19, 1940. This event is officially known as the 1940 Imperial Valley earthquake and was a 6.9 in magnitude event. It was recorded by the “El Centro Array” number 9 and is associated with station 117 in the USGS database. The acceleration time history with a PGA of 0.313g and the corresponding response spectrum for 5% damping are displayed in Figure 3.10.

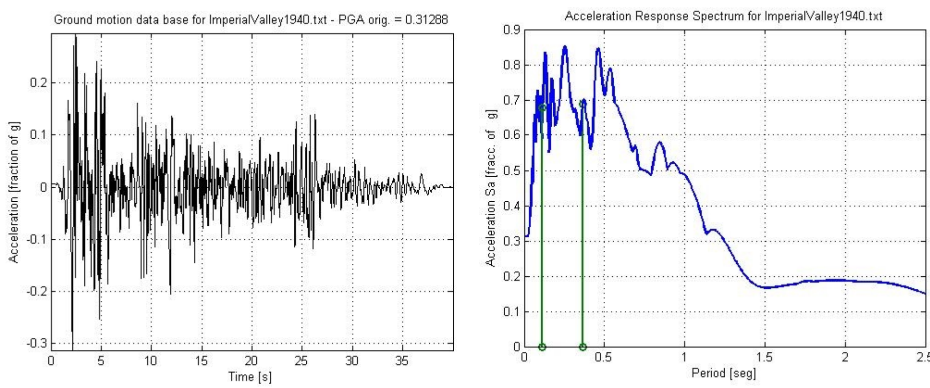

Figure 3.10 *Acceleration time history and response spectrum of the 1940 Imperial Valley earthquake.*

The Fourier spectrum (the absolute value of the Fourier transform) of the Imperial Valley record is shown in Figure 3.11. There are two graphs shown: the first one (with a dotted line) corresponds to the original spectrum and the second one (with the dark, continuous line) was smoothed out by processing the original spectrum using a running average (also known as a rolling or moving average). This is a numerical procedure used to smooth out irregularities (i.e., the numerous peaks and valleys) in a signal or in a plot to help to recognize trends, in our case the dominant frequencies in the spectrum. By comparing the two curves (original and softened) displayed in Figure 3.11, one can appreciate better the most important peaks in the spectrum and the frequencies associated to them.

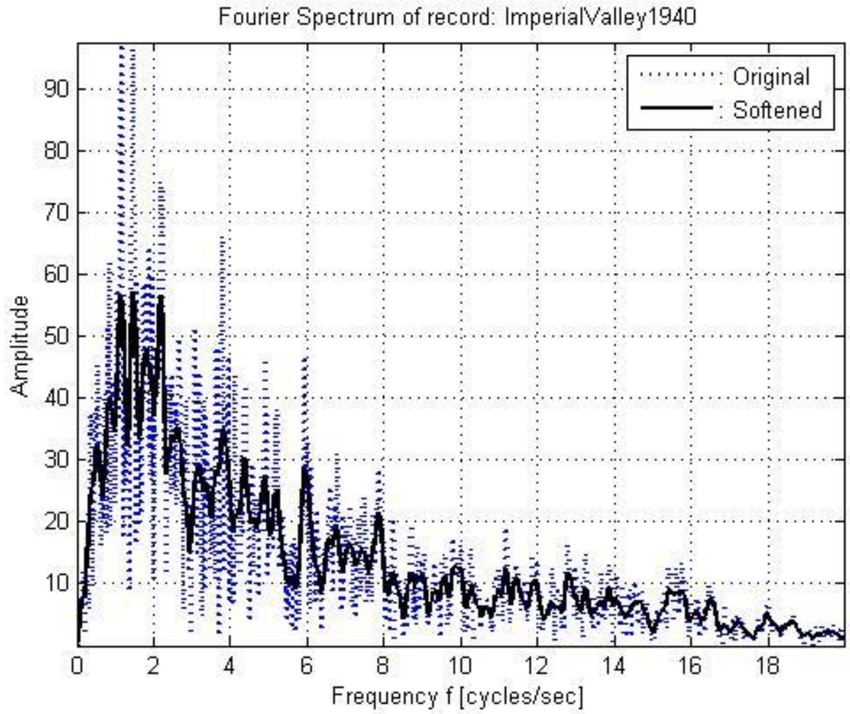

Figure 3.11 *Fourier spectrum of the 1940 Imperial Valley earthquake record.*

3.3.3. Short-band earthquake record for detailed studies

The short-band ground motion record selected for a detailed study of the equivalent linear method was produced by the earthquake that took place on October 10, 1986 in San Salvador, El Salvador. The 1986 San Salvador record selected has a PGA of 0.875 g, it was registered at the "Geotechnical Investigating Center" station 090 and was a 5.7 in magnitude event. The acceleration time history is shown in Figure 3.12 along with its response spectrum.

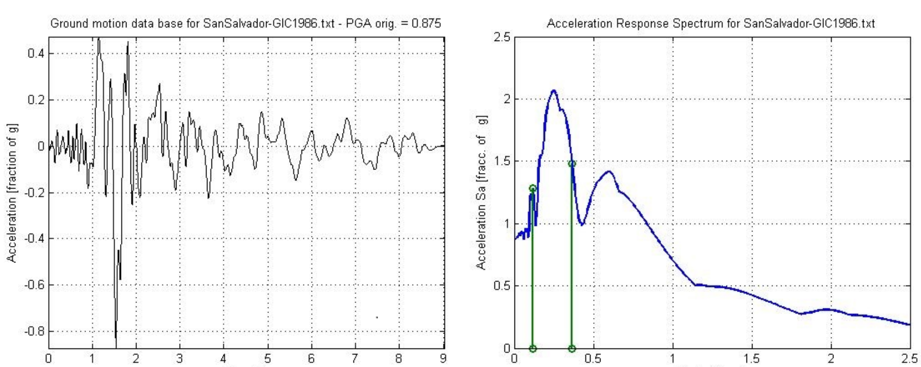

Figure 3.12 *Acceleration time history and response spectrum of the 1986 San Salvador earthquake.*

Figure 3.13 presents the Fourier spectrum of the 1986 San Salvador seismic record. Here again the original spectrum is shown alongside its smoothed version.

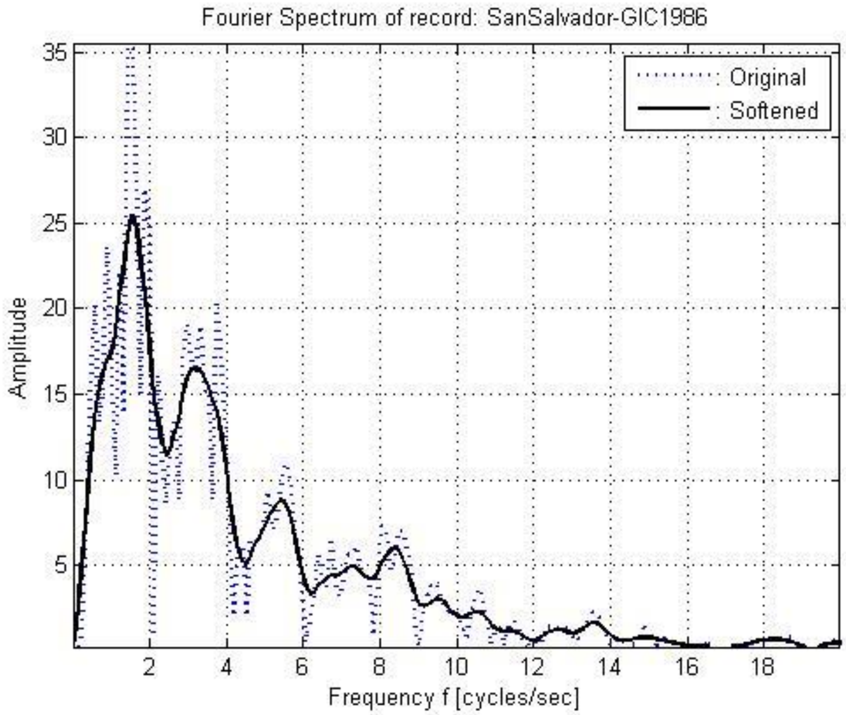

Figure 3.13 *Fourier spectrum of the 1986 San Salvador earthquake record.*

3.4 Non-linear dynamic analysis

The non-linear dynamic procedure, when properly implemented, provides the most accurate prediction of the structural response to a strong ground motion. Since the non-linear dynamic analysis model incorporates inelastic member behavior under cyclic earthquake ground motions, the non-linear dynamic procedure explicitly accounts for the hysteretic energy dissipation in the non-linear range. However, the damping, additional loads and the gravity acceleration load need to be added as parameters in order to be considered as part of the dynamic analysis.

Because a non-linear dynamic analysis involves fewer assumptions than a non-linear static procedure, it is subjected to fewer limitations and in theory at least, it represents better the real response of the structure. However, the accuracy of the results depends on the details of the computer model and how faithfully it captures the significant behavioral effects (Deierlein et al., 2010). Acceptance criteria typically limit the maximum structural component deformations to values where degradation is controlled and the non-linear dynamic analysis models are reliable.

3.4.1. Application of gravity loads

The first step to carry out a non-linear dynamic analysis is to apply the gravitational loads. In a linear analysis the order of the application of the gravitational and earthquake loads is not important because their effects can be later added up. On the contrary, in a non-linear analysis they must be applied simultaneously since the superposition principle does not hold. The specific way how this is done depends on the particular computer program being used. In the case of ANSYS, when a dynamic and static load act simultaneously, the second load must be slowly applied until it reaches its prescribed value. Moreover, in the case of gravitational loads they are applied as an acceleration in the vertical direction (Y-direction) that slowly increases in magnitude until it reaches the acceleration of gravity. For the present study the acceleration of gravity was linearly increased during five seconds. After that it was maintained for an extra second to make sure that any lingering vibratory motion vanishes. Once this time (6 seconds) was reached, the acceleration time-series of the selected earthquake was applied in the X-direction.

3.4.2. Results of the dynamic analysis with the broad-band record

The first non-linear analysis was performed using the selected earthquake ground motion with a broad-band frequency content, i.e. the 1940 Imperial Valley record. The accelerogram was not scaled; it was used as it was originally recorded with a PGA of 0.313g. The purpose was to assess how much this earthquake could push the structure into the non-linear range. It is recalled that the objective of this thesis is to evaluate an approximate method to calculate the seismic response of a structure with moderate non-linear behavior. This means that it seeks that the earthquake provokes an inelastic response of the building but limited in extent.

The next task is to select the types of response to be examined and the structural elements in which they will be calculated. The amount of output information produced by ANSYS for a 3-D finite element model of the building can be overwhelming and thus the response quantities must be cut down to a manageable set: the response in one of the columns of the first floor and one of the beams at the first level. The selected column and beams are identified in Figure 3.14.

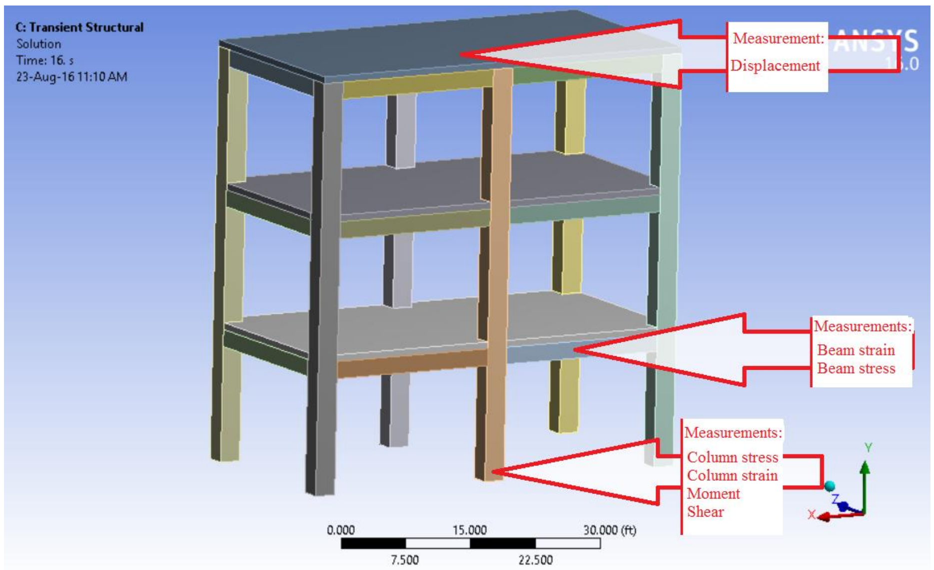

Figure 3.14 *Beams and column of the building selected to trace the response.*

The maximum bending stresses and normal strains in absolute value for the first floor beam and column are shown in Table 3.9. These values were obtained from their respective time histories displayed in Figure 3.15. The four graphs show the absolute values of the time responses during first fourteen seconds once the earthquake acceleration was applied. Note that during the first six seconds of the analysis the response varies slowly while the gravitational loads are applied, as it was explained before.

Table 3.9 *Peak stresses and strains due to the unscaled broad-band record.*

Type of response	***Maximum values***
Beam stress	4.2627 ksi
Beam strain	0.001355 in/in
Column stress	3.405 ksi
Column strain	0.000998 in/in

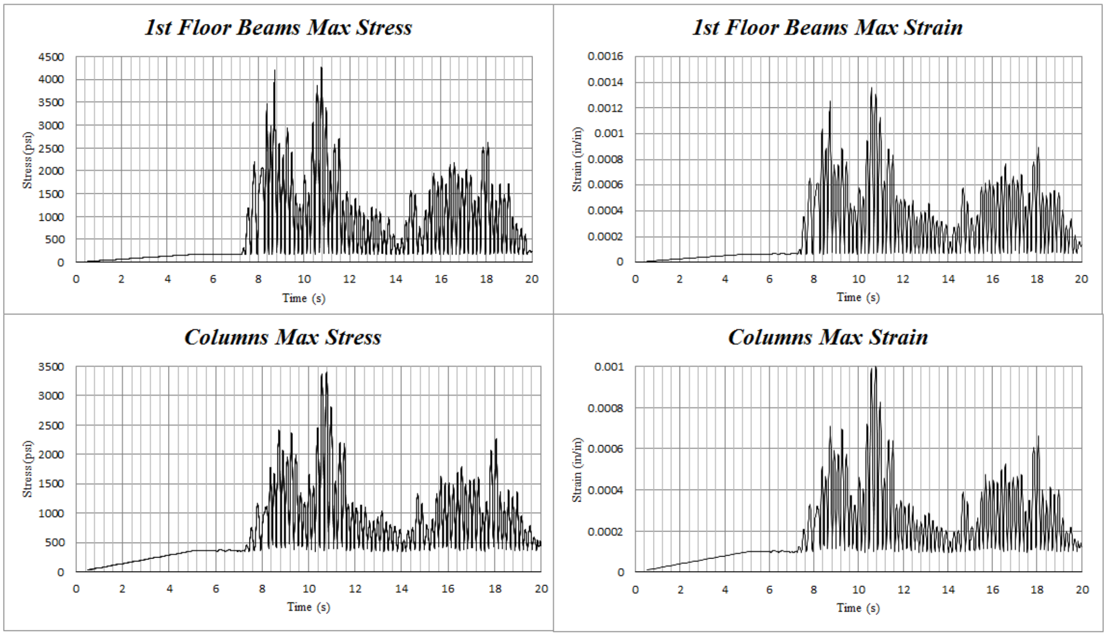

Figure 3.15 *Stresses and strains time histories due to the unscaled broad-band record.*

To assess the level on non-linearity that the structure reached due to the unscaled earthquake, the stress and strain time histories were combined such that the time became a parameter and then they were plotted in an σ-ε plane. The graph was superimposed with the constitutive relationship $\sigma = f(\varepsilon)$ calculated for the beam and column sections. The results are displayed in Figure 3.16. As it can be seen in the two graphs, the earthquake ground motion with its original intensity did not manage to push the structure into the non-linear range. In order to carry out the objective of the study, i.e. to compare the non-linear response calculated with the equivalent linear and exact methods, the record was scaled up so that the structure behaves non-linearly.

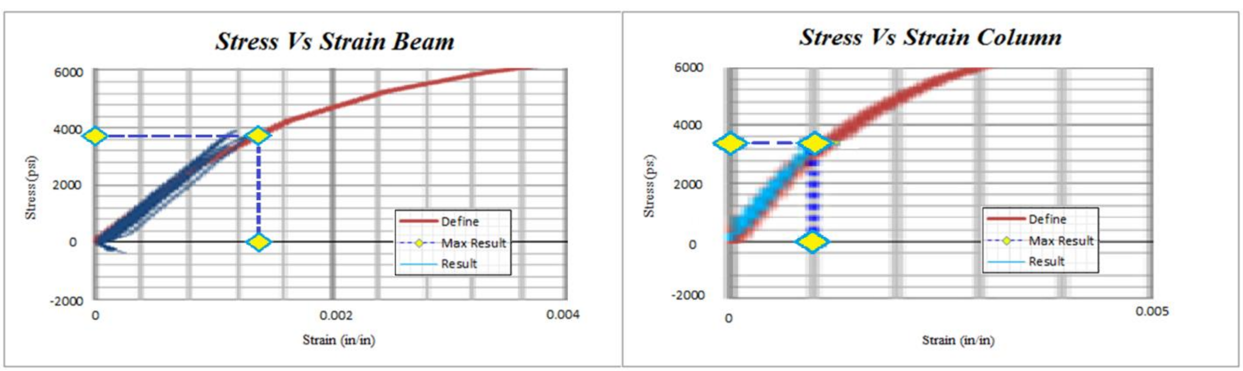

Figure 3.16 *Stress-strain response and constitutive relation for the broad-band unscaled record.*

The acceleration time series of the 1940 Imperial Valley earthquake was scaled by a factor of 3.5, which was selected using a trial and error process to allow the beam and column elements to reach a moderate non-linear behavior. The magnitude of the gravitational loads and all other parameters remained the same in order to capture only the difference in behavior created by the more intense earthquake. The maximum values of the four selected response quantities for the first floor beam and column are shown in Table 3.10. Figure 3.17 shows the time history response data retrieved from ANSYS during the first 14 seconds of the earthquake where the peak acceleration occurs. In addition, the response during first 6 seconds when the gravity loads are applied is included at the beginning of the time histories.

Table 3.10 *Peak stresses and strains due to the 3.5x scaled broad-band record.*

Type of response	***Maximum values***	
Beam stress	7.0684	ksi
Beam strain	0.0084185	in/in
Column stress	7.2121	ksi
Column strain	0.003444	in/in

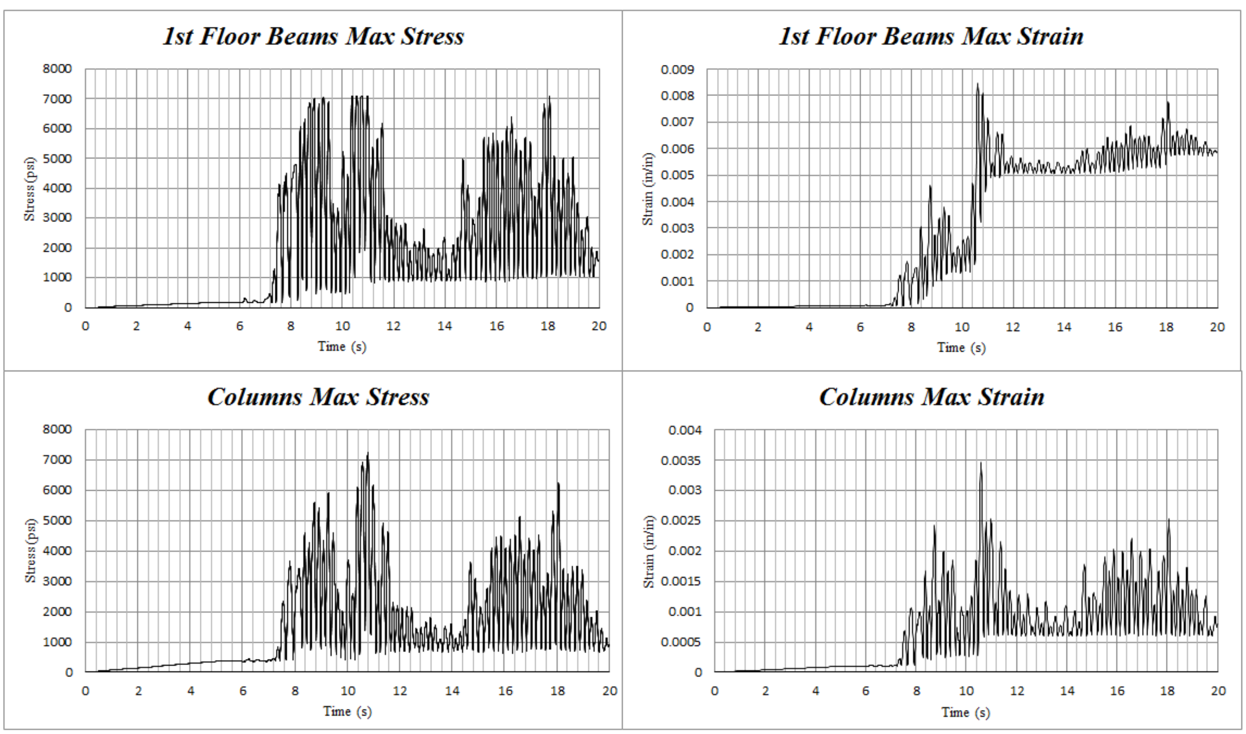

Figure 3.17 *Stresses and strains time histories due to the 3.5x scaled broad-band record.*

To measure the level of non-linear deformations sustained by the structure, the stress and strain time series were used to generate the σ-ε curve and it was then plotted along with the non-linear constitutive relation for the beam and column sections. The results are displayed in Figure 3.18. As it can be seen, now the scaled earthquake pushes the beam elements beyond their elastic range and thus hysteretic cycles are formed.

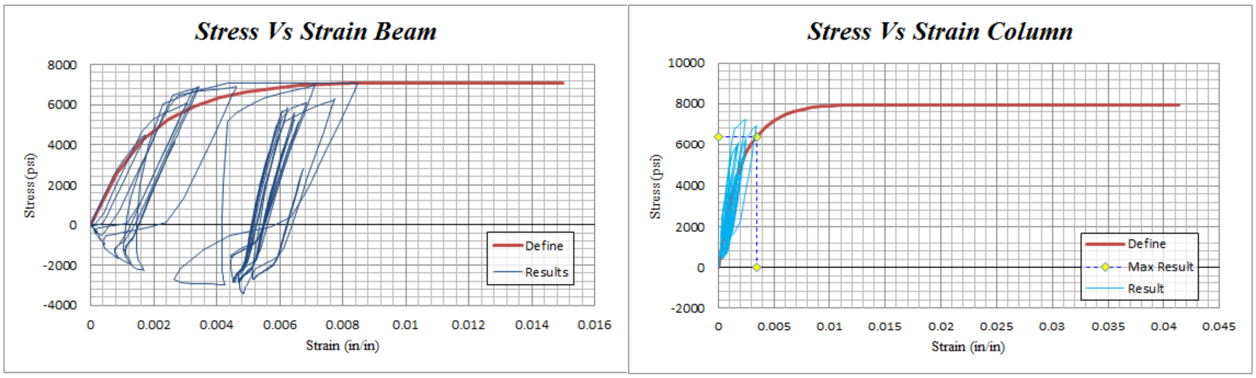

Figure 3.18 *Comparison of stress vs. strain curves for the broad-band 3.5x scaled record*

The columns were designed so that they would undergo much smaller non-linear excursions. In other words, the weak-beam strong-column design approach for RC buildings subjected to earthquake loads was followed. Due to the way that the structure was designed, it is expected that a plastic hinge would form in the beam element very close to the beam-column connection. This explains the fact that even though the earthquake was scaled up, the columns almost remained in the linear regimen, as confirmed by the very small hysteresis cycles in the right graph of Figure 3.18.

Under these increased deformations, it is important to ensure that the structure remains stable without collapsing, i.e., it should not loose vertical load carrying capacity. The ability of a structure to undergo large deformations without collapsing is called ductility. The term is loosely used in earthquake engineering to indicate the degree to which an assembled structure that is damaged can undergo large deformations without collapsing. The measurement of ductility can be defined as the ratio of maximum strain to yield strain of the material. Using this definition applied to the beam elements the ductility for the broad-band event resulted in a value of 3.422. The maximum strain value used in the calculations is shown in Table 3.10 and the yield strain value of 0.00246 in/in obtain from the stress-strain curve.

Once it has been verified that the structure underwent non-linear deformations, additional response quantities were retrieved from the ANSYS output. The relative displacement at a point located at the roof of the building, the shear force and the bending moment at the base of a column at the first floor are three quantities of interest. The time variation of these response quantities are shown in Figure 3.20. The maximum absolute values of the displacement, shear force and bending moment are displayed in Table 3.11. These values are important because they will be used in a following chapter to compare them with similar quantities but obtained with the equivalent linear method.

Another response of interest for the goal of this investigation is the absolute acceleration of the building floors. These acceleration time histories are needed to calculate the floor response spectra for the design of nonstructural components and equipment. The acceleration time histories for the three floors of the building in the X direction are shown in Figure 3.19.

Table 3.11 *Maximum non-linear response quantities due to the broad-band 3.5x scaled record.*

Type of response	***Maximum values***	
Roof displacement	5.3374	in
Bending moment	42442	kip-in
Shear force	407.1	kip

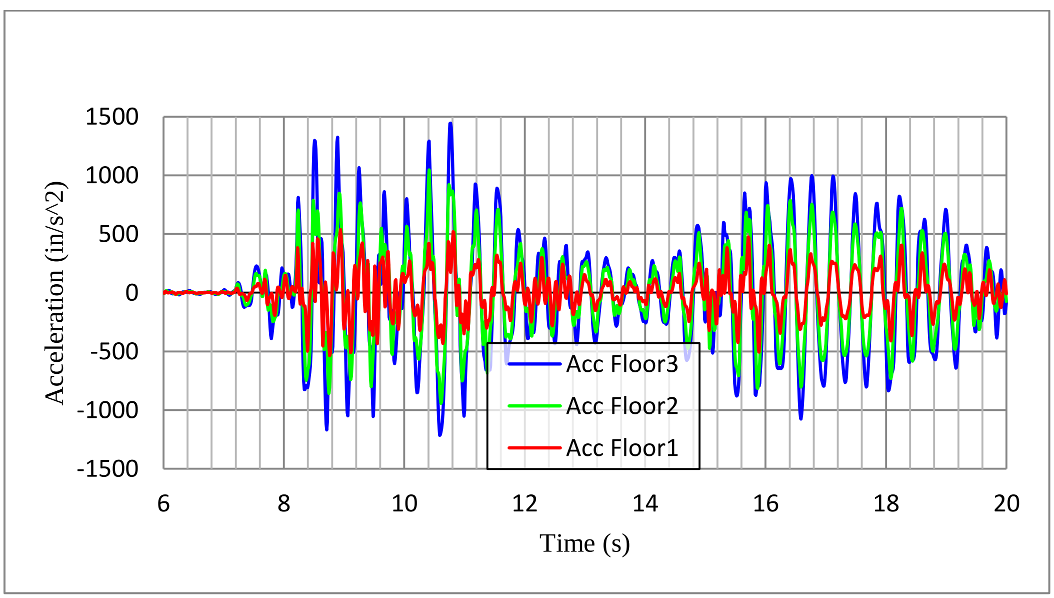

Figure 3.19 *Floor accelerations due to the broad-band 3.5x scaled record.*

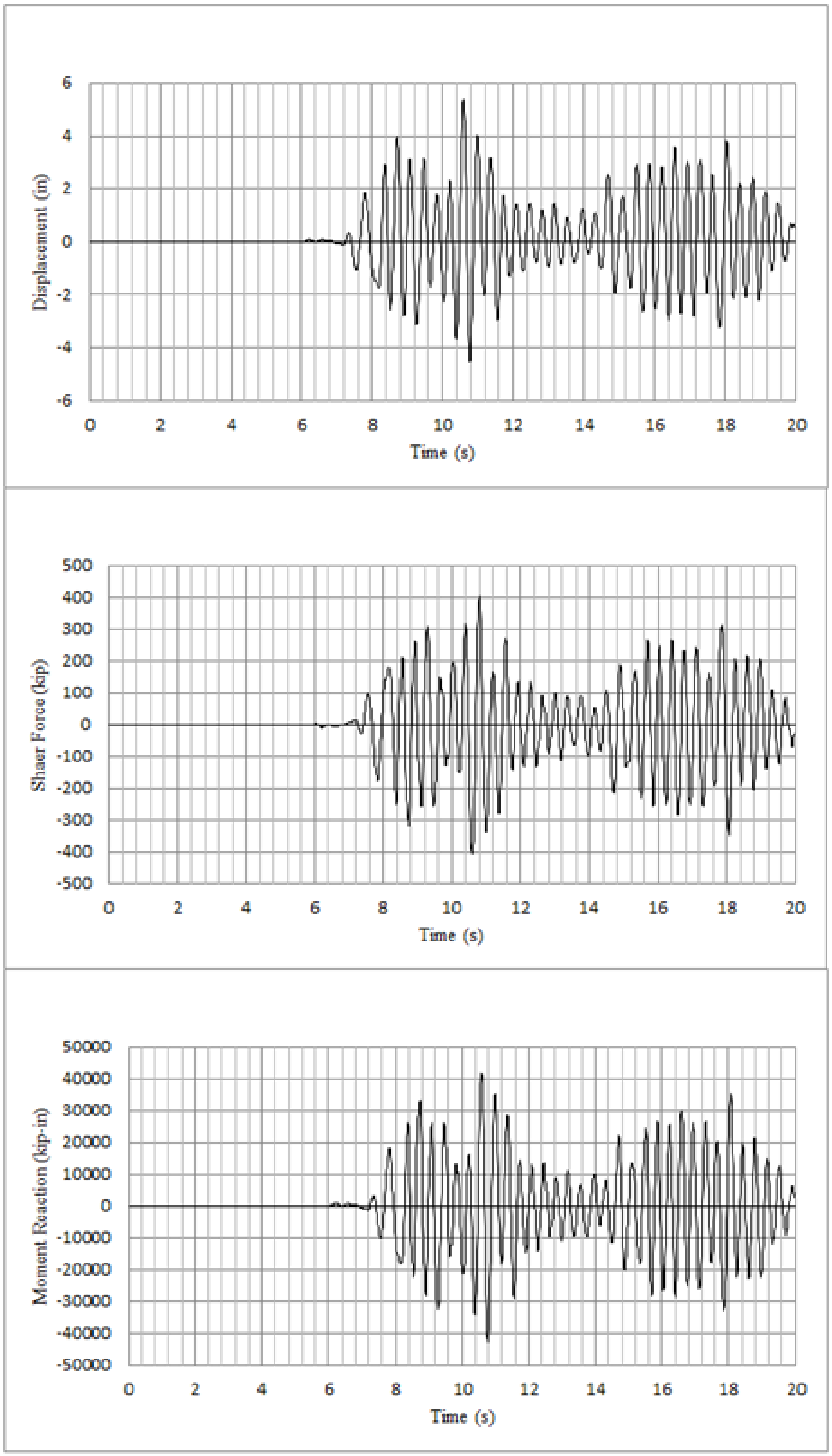

Figure 3.20 *Time variation of selected response quantities due to the broad-band 3.5x scaled record. a) Roof displacement, b) Base column shear force, and c) Base column moment reaction.*

3.4.3. Results of the dynamic analysis with the short-band record

In the third analysis case, the short-band earthquake record, the accelerogram of the 1986 San Salvador event, was applied to the building model with its original intensity. Figure 3.21 shows the time variation of the stress and strain in the critical beam and column during the first ten seconds of the earthquake which corresponds to the strong motion part of the accelerogram. As it was done in previous cases, the first six seconds of the response while the static loads are being applied is also shown in the time histories. The maximum absolute stresses and strains in the first floor beam and column retrieved from the time histories in Figure 3.21 are shown in Table 3.12.

Table 3.12 *Peak stresses and strains due to the unscaled short-band record.*

Type of response	***Maximum values***	
Beam stress	6363.4	psi
Beam strain	0.002730	in/in
Column stress	4509.9	psi
Column strain	0.001469	in/in

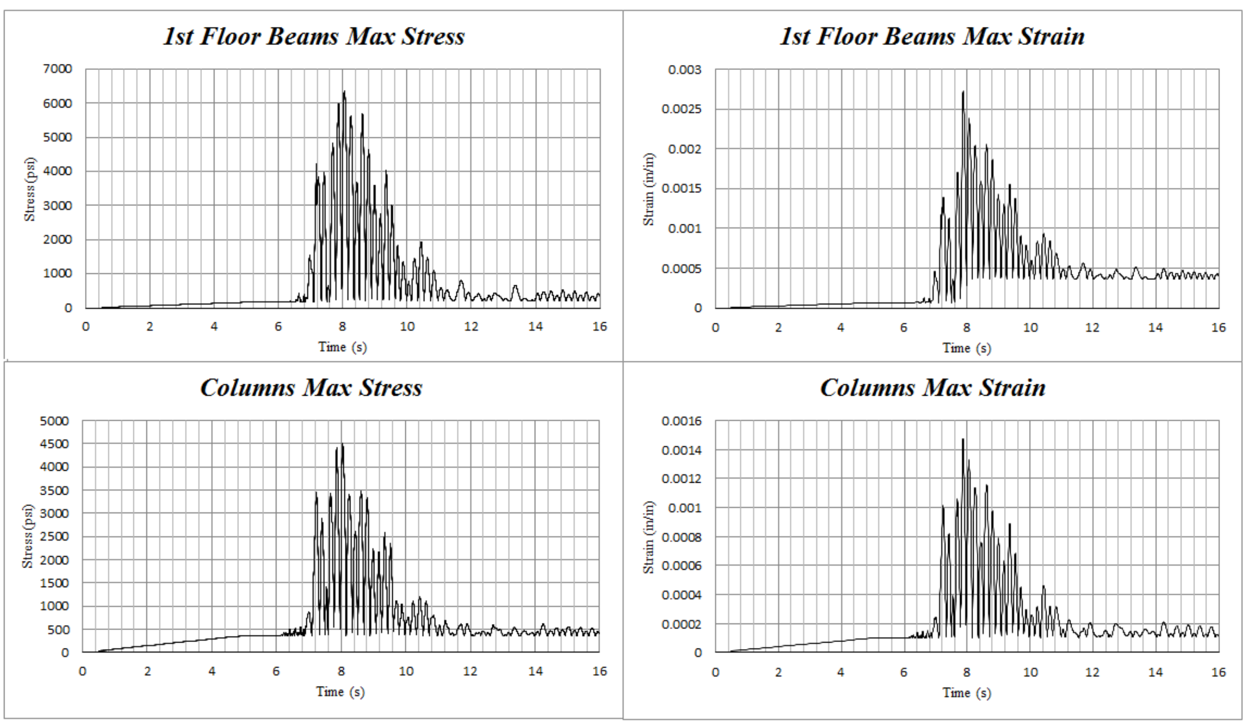

Figure 3.21 *Stresses and strains time histories due to the unscaled short-band record.*

Before proceeding to carry out further analyses, it is important to assess the level on non-linearity that the structure underwent due to the seismic excitation. This is done by combining the bending stress and strain time histories at a point of the beam and columns to obtain the σ - ε curves. They are next plotted in the same graph with the non-linear constitutive relation for the reinforced concrete sections. The results are shown in Figure 3.22 for the beam and column. Examining these graphs it becomes evident that, as it happened with the broad-band record, the earthquake with the original intensity was not able to push the structure into the non-linear region. Therefore, the intensity of the event was scaled up to force the structure to experience a non-linear behavior. Because this is a non-linear problem, it is not possible to predict beforehand by how much the earthquake should be scaled and thus this was done by trial and error.

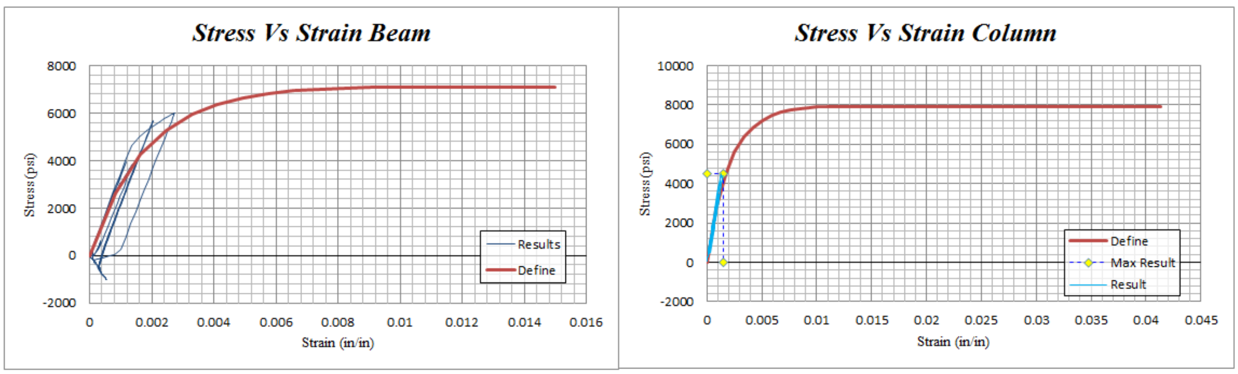

Figure 3.22 *Comparison of stress vs. strain curves for the short-band unscaled record.*

To increase its intensity, the accelerogram of the 1986 San Salvador earthquake was scaled by a factor of 2. As it was previously mentioned, this was value was chosen by trial and error. The first 16 seconds of the stress and strain time histories in the first floor beam and column are presented in Figure 3.23. They include the first 10 seconds of the earthquake were the maximum values of the ground acceleration occur. The peak values were collected from the four time series and they are shown in Table 3.13.

Table 3.13 *Peak stresses and strains due to the 2x scaled short-band record.*

Type of response	***Maximum values***	
Beam stress	7.0683	ksi
Beam strain	0.008134	in/in
Column stress	7.1697	ksi
Column strain	0.003394	in/in

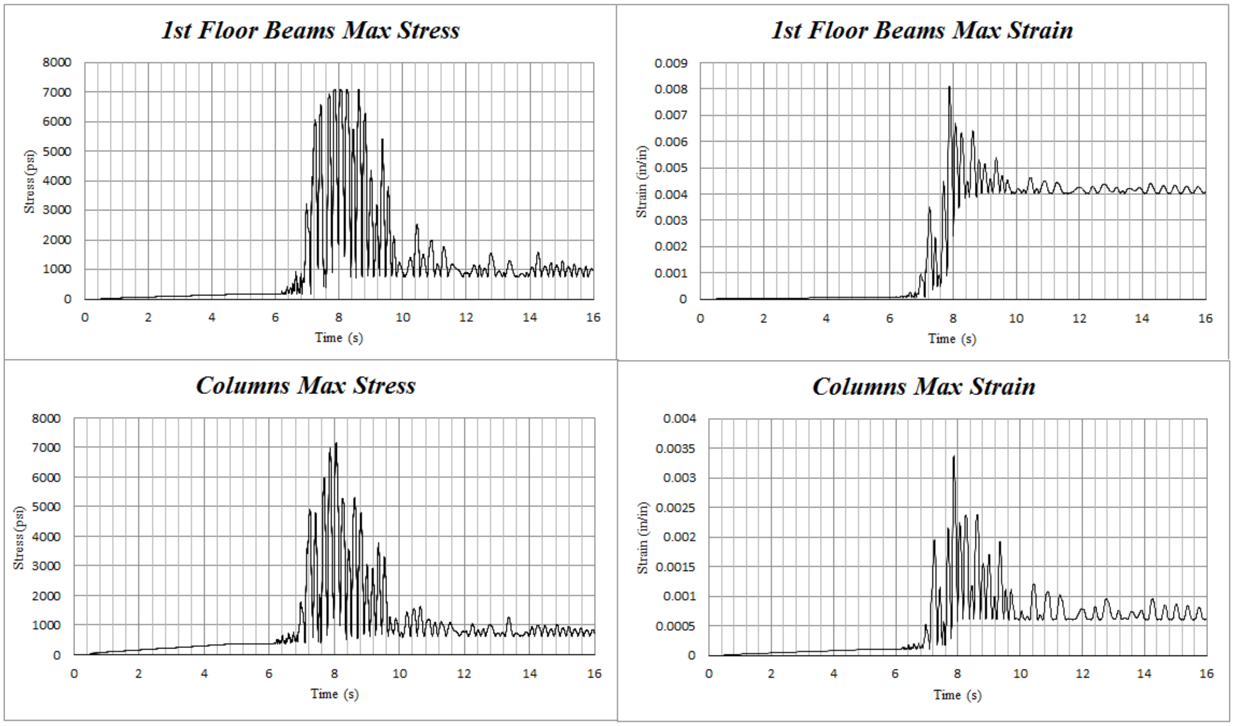

Figure 3.23 *Time history stress and strain data of short-band 2x analysis*

To measure the level on non-linearity that the structure reached, the same process previously explained was implemented. The uniaxial stress-strain relationships for the confined concrete beam and column cross-sections described in Chapter 2 are compared with similar curves derived from the data collected from the numerical simulation. The two sets of curves are presented in Figure 3.24. The scaled earthquake ground motion was now able to push the beam elements to a stress level such that hysteresis loops formed when the load reversed. The results in the beam deviate from the constituve curve, but this might be because of the strong nature of the earthquake that has acceleration in both directions with different magnitudes in short periods of time.

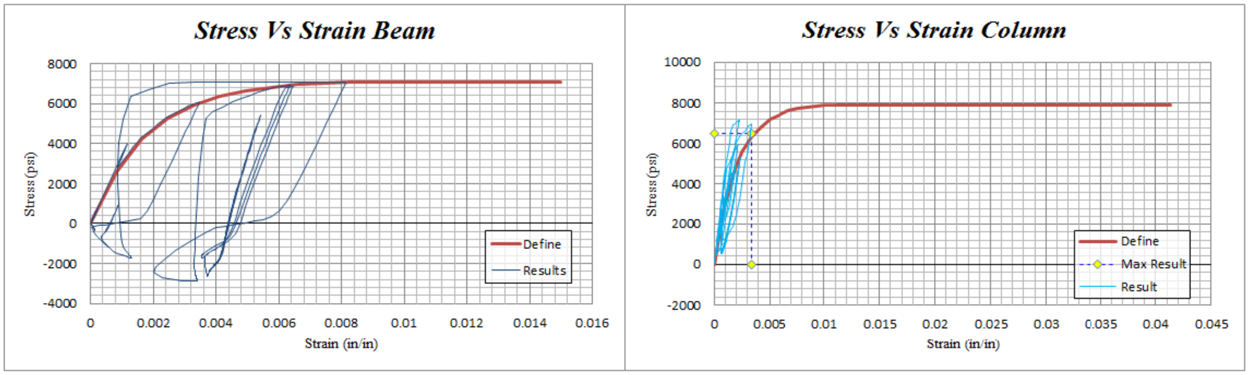

Figure 3.24 *Comparison of stress vs. strain curves for the short-band 2x scaled record.*

It is again pointed out that the columns were designed to have a much lower extent of non-linear behavior since by design the weak elements are the beams. The column sections have a higher stress capacity as it can be seen in the definition of the stress vs. strain curve in the material properties presented in Chapter 2. Also, for this event the ductility is calculated as a reference value. Like before, the same definition describe in the previous case applied to the beam elements the ductility now for the short-band event resulted in a value of 3.3065. The maximum strain value used in the calculations is shown in Table 3.13 and the yield strain value of 0.00246 in/in obtain from the stress-strain curve.

Once it was corroborated that the elements of the structure had moderate inelastic deformations, the selected response quantities that will be used in a following chapter to evaluate the equivalent linear method were collected. They include the relative displacement at the center of the roof, the shear force at the bottom of a first floor column and the bending moment at the same location. Their variation with time is displayed in Figure 3.25. The maximum absolute values for each of these three quantities are presented in Table 3.14.

Table 3.14 *Maximum non-linear response quantities due to the short-band 2x scaled record.*

Type of response	***Maximum value***	
Roof displacement	5.2808	in
Bending moment	42531	kip-in
Shear force	411.43	kip

The final response quantities retrieved from the ANSYS output and stored for later use are the absolute acceleration of the floors in the X direction. The three time series are displayed in Figure 3.26.

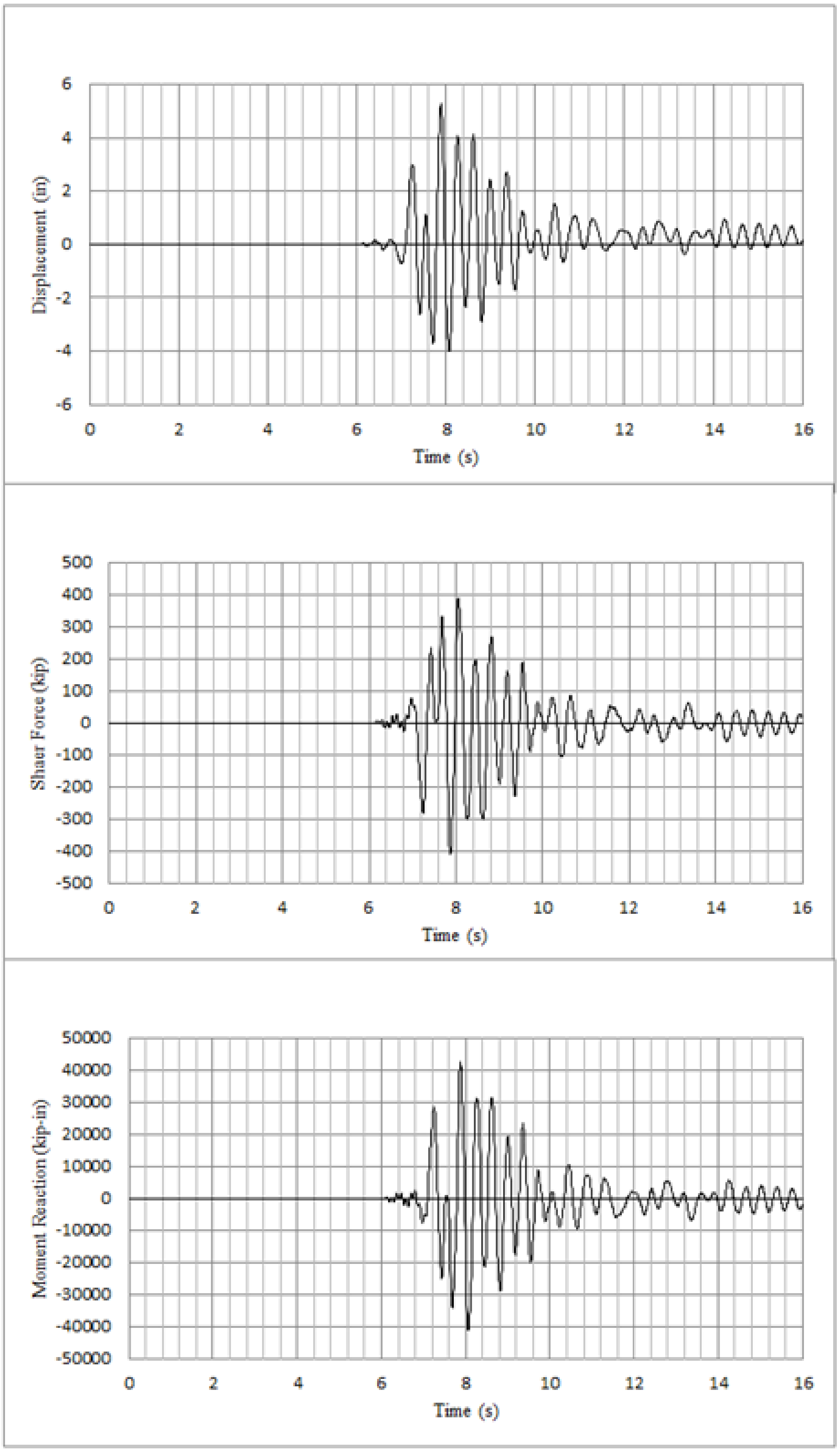

Figure 3.25 *Time history final results of short-band 2x non-linear analysis.*
a) Roof displacement, b) Base column shear force, and c) Base column moment reaction.

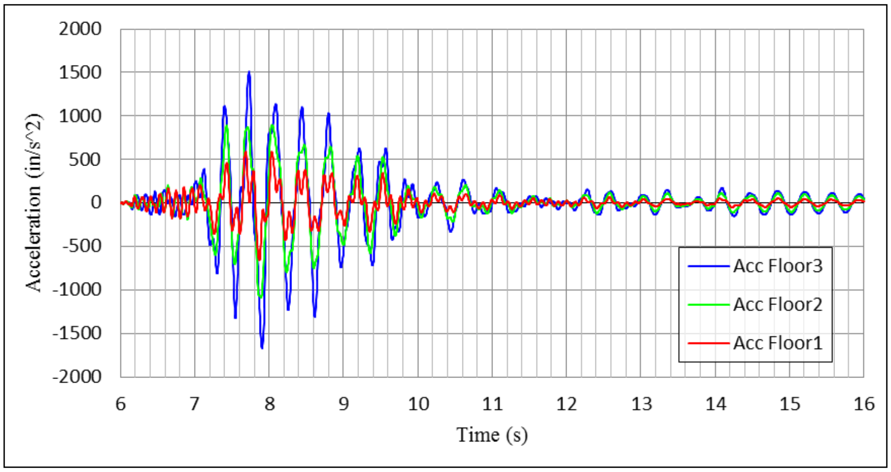

Figure 3.26 *Floor accelerations due to the short-band 2x scaled record*

3.5 Chapter summary and conclusions

The main objective of this chapter was to present the full non-linear dynamic analysis of the three-story RC building subjected to the records of two historical earthquakes with different characteristics. As a first step, and in order to have a better understanding of the dynamic response of the structure, a modal analysis was performed. The natural frequencies and modes of vibration were computed and displayed. The modeling of damping in the program ANSYS, namely the Rayleigh damping model, was discussed. The specific implementation of the Rayleigh formulation for the 3-D finite element model is explained. A damping ratio equal to 0.02 was assigned to the two modes that most contribute to the seismic excitation acting along the horizontal X direction. Next, it was presented a verification that the damping model was correctly implemented in ANSYS; this was done by numerically simulating in the program a free vibration test. Using the displacement time history from the free vibration response and applying the logarithmic decrement method, it was verified that the fundamental mode had the 0.02 damping ratio sought.

The selection of the earthquake ground motions to be used for the non-linear and equivalent linear analyses was presented. First two ground motions with different frequency contents, referred to as a broad-band and short-band event, were selected. They are the records of the well-known 1940 El Centro seismic event and the 1986 San Salvador earthquake. Next six additional seismic records were picked from the PEER database; they are used for the final calibration of the equivalent linear method in Chapter 4.

The broad-band record was used as seismic input for the 3-D model of the building and a step-by-step non-linear dynamic analysis was performed in ANSYS. The accelerogram was used with its original PGA and from the response time history obtained, the stress-strain curves where time is a parameter were plotted. The responses were calculated at two critical points in a beam and column of the first floor of the building. After comparing these curves with the σ vs. ε constitutive relations for the beam and column sections, it was decided to scale up the accelerogram to induce a moderate non-linear response. The dynamic analysis was repeated with the 3.5 times scaled El Centro record and the aforementioned comparison process was replicated. Once the level of the non-linear response was found to be satisfactory, other response time histories and their peak values were retrieved. They are used in the following chapter to verify the accuracy of the proposed equivalent linear method.

The complete process described in the previous paragraph was repeated this time using the short-band record, i.e. the 1986 San Salvador earthquake. Here again, in the first attempt the response of the structure was practically linear. Therefore the accelerogram was scaled by a factor of 2. Now the beam element section reached a plastic state whereas the column almost remained in the linear range. This behavior is consistent with the design approach followed, where the weak part of the structure was designed to be at the ends of the beam, close to the connection with the column. This is because plastic hinges are expected to form in this area which provides the structure with the ductility it needs to absorb the energy of the seismic event.

After it was determined that the structure reached a non-linear state with the scaled San Salvador earthquake, the maximum values of the displacement at the center of the roof, the shear force and the bending moment at the base of the critical column were retrieved. Another results collected for later use were the absolute accelerations at each of the floors. This is important information because it is later employed to calculate the floor response spectra.

CHAPTER IV

IMPLEMENTATION OF THE EQUIVALENT LINER METHOD

4.1 Introduction

This chapter explores the application of the equivalent linear method to calculate the approximate non-linear seismic response of typical reinforced concrete moment resistant frames. The method is widely used in the practice of Geotechnical Earthquake Engineering to calculate the acceleration at the surface of a horizontally stratified soil deposit due to an earthquake acceleration applied at the bedrock or at a rock outcrop. Soil materials undergo non-linear deformations even under earthquakes of moderate intensity and thus it is important to account for their non-linear behavior, even in an approximate way. It is known that the method has some limitations but anyway it is accepted in practical applications. One of the limitations of the method is that the non-linear behavior of the soils must be moderate: it does not provide good results for soils undergoing strongly non-linear deformations. It is reasonable to conclude that the same limitation will also apply to the intended application of this thesis study, namely for building structures.

One of the reasons for using the equivalent linear method to calculate the seismic response of soil deposits is that the damping is accounted for by means of the complex modulus damping model. This damping model permits to assign different damping ratios to each of the soil layers of the deposit. In addition, it permits to model more accurately the real energy dissipation characteristics of soil materials. However, the complex modulus model requires an analysis in the frequency domain which is based on the Principle of Superposition and thus it cannot be applied to non-linear systems. By iteratively replacing the non-linear behaving soil deposit by a linear model with equivalent properties, one can apply a frequency domain analysis at each iteration step.

In the following section a concise description of the equivalent linear method. Because the original method proposed by Seed and Idriss (1970) was intended for soil dynamics applications, it will be adapted for frames undergoing bending deformations. Another difference is that the series of linear analysis required by the method will not be done in the frequency domain but rather in the time domain. In addition, the damping model used will be that available in the program ANSYS, namely the Rayleigh damping formulation.

4.2 The equivalent linear method

The first step in the implementation of the equivalent linear method is to select a non-linear stress-strain relationship. The relationship can be in the form:

$$\varepsilon = f(\sigma) \tag{4.1}$$

which defines the so called “Ramberg-Osgood models” (Suárez, 2008) or in the more common form:

$$\sigma = f(\varepsilon) \tag{4.2}$$

This expression defines the “Davidenkov models”. In many cases both models are interchangeable, i.e. one can solve for one variable in terms of the other. There are, however, models which can only be defined in one of the two ways. In this thesis, the more common Davidenkov models will be adopted.

In Soil Dynamics there are several well-known models, such as the hyperbolic, the exponential, the Ramberg-Osgood model, etc. In this work the stress-strain relationship will be defined using a curve - fitting process as it will be explained in the following section.

The relationships (4.1) or (4.2) define the so called “backbone curve” in the stress vs strain plane. This curve describes the stress generated in an element when it is monotonically deformed in the same direction (positive or negative) and it may be thought as the constitutive equation for a non-linear elastic element. Figure 4.1 displays a typical backbone curve.

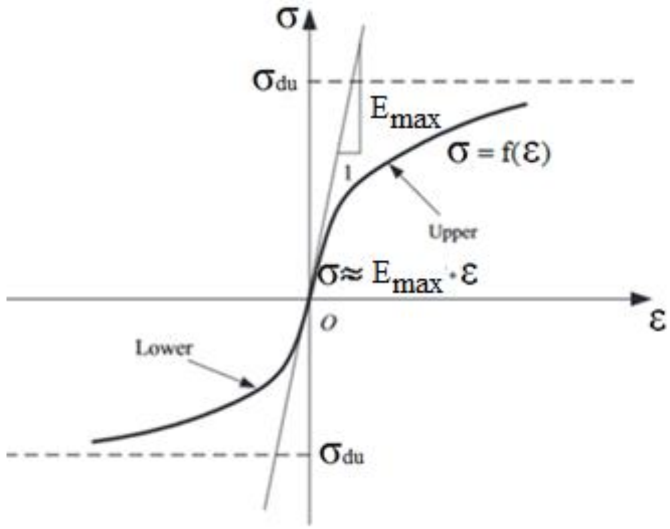

Figure 4.1 *A typical backbone curve. (Suárez, 2008)*

When the load reverses direction, i.e. when the element is subjected to a cyclic loading, the downloading path does not follow the same path as the backbone curve and a hysteresis loop is formed as the process continues. Figure 4.2 displays a typical hysteresis loop. To develop the equivalent linear method we need an explicit expression that defines the upper and lower branches of the hysteresis loop. In Soil Dynamics this is done be means of the so-called "Masing rule" explained in the following section.

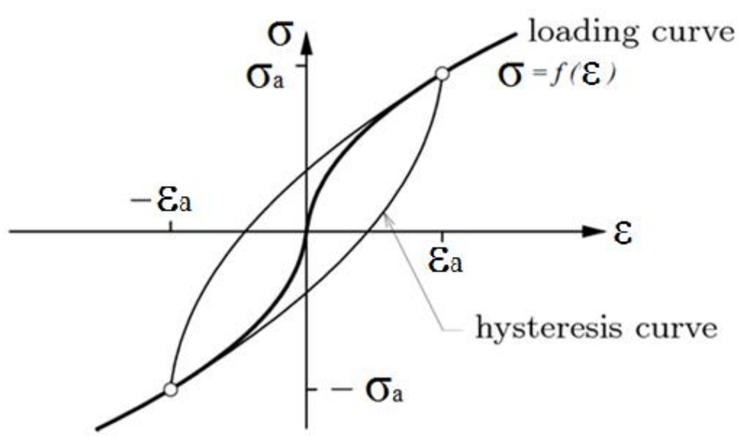

Figure 4.2 *Hysteresis loop and the associated backbone curve. (Suárez, 2008)*

4.2.1. Masing's rule formulation

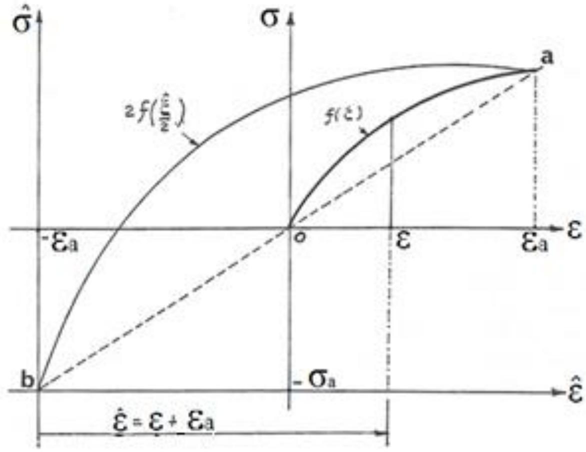

Figure 4.3 *Masing's cyclical curve model. (Suárez, 2008)*

To define the complete hysteresis loop by means of the Masing rule the following variables will be used:

σ = *stress at a given point,*

σ_a = *maximum value of the stress* (*at point of cycle reverse*),

ε = *strain at a given point,and*

ε_a = *maximum value of strain* (*at point of cycle reverse*).

Starting with defining the upper branch of the hysteresis loop. In addition, the curve will be defined in terms of two auxiliary variables $\hat{\sigma}$ and $\hat{\varepsilon}$, as shown in Figure 4.3. The relation between the two set of variables is:

$$\begin{aligned} \hat{\sigma} &= \sigma + \sigma_a \\ \hat{\varepsilon} &= \varepsilon + \varepsilon_a \end{aligned} \tag{4.3}$$

The amplitude of the upper branch in the $\hat{\sigma}$ - $\hat{\varepsilon}$ plane is obtained by amplifying the original backbone curve by a factor of 2. To "stretch" the curve, i.e. to augment its range, the argument of the function $f(\varepsilon)$ is divided by a factor of 2.

$$\hat{\sigma} = 2f\left(\frac{\hat{\varepsilon}}{2}\right) \tag{4.4}$$

In order to obtain the equation in terms of the original variables, one simply needs to replace them from equation (4.3):

$$\sigma = 2f\left(\frac{\varepsilon + \varepsilon_a}{2}\right) - \sigma_a \tag{4.5}$$

Proceeding in a similar fashion it is straightforward to show that the lower branch of the hysteresis loop is defined by the following equation:

$$\sigma = 2f\left(\frac{\varepsilon - \varepsilon_a}{2}\right) + \sigma_a \tag{4.6}$$

The equations that define the backbone curve and the hysteresis cycle are not used directly in the equivalent linear method. Rather they are the basis to determine two essential parameters: the equivalent modulus of elasticity and the damping ratio.

Because the idea behind the method is to specify an equivalent linear system, the physical parameters that define this system are needed. For a homogeneous, isotropic and elastic material only two parameters are needed to uniquely define its constitutive equation. Commonly they are the pairs formed by the modulus of elasticity (or Young's modulus) E and the Poisson's ratio μ, or E and the shear modulus G, or another pair combination of these three. It can be is assumed that the Poisson's ratio is constant regardless of whether the structural system behaves in an elastic or inelastic fashion. Thus, the only parameter that needs to be defined is E or G. In Soil Dynamics the parameter selected is the shear modulus G of the soil because the shear deformation dominates the behavior of the material. For our purposes, it is more relevant to use the modulus of elastic and when it is needed the shear modulus can be calculated using the well-known relationship:

$$G = \frac{E}{2(1+\mu)} \tag{4.7}$$

When the material is subjected to dynamic loads it is important to account for the energy dissipation, especially in the case of long duration excitations such as earthquakes. In this case, the typical constitutive relationship (Hooke's law) is usually replaced by the Kelvin-Voight model. To define this model, in which the damping stresses are proportional to the time derivative of the strains, an additional parameter is required. In the Theory of Viscoelasticity the loss factor η is used to define the model, but in engineering applications, the damping ratio ξ is more commonly used.

In conclusion, we need to determine two material parameters: an equivalent modulus of elasticity and an equivalent damping ratio. The equivalent modulus of elasticity is the secant modulus E_{sec}. This modulus is the slope from the point of origin to the maximum point on the backbone curve, as shown in Figure 4.4.

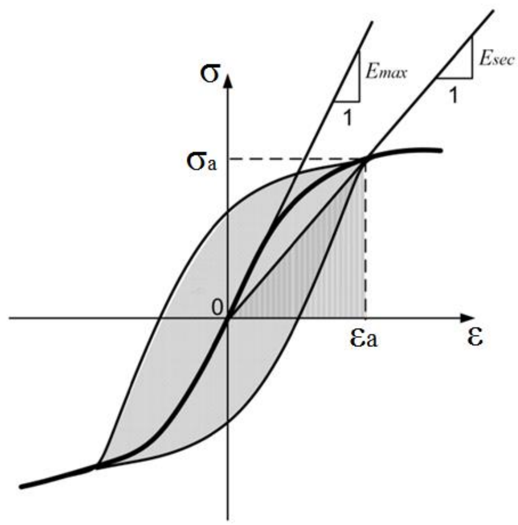

Figure 4.4 *Initial elastic modulus and secant modulus. (Suárez, 2008)*

The secant modulus of elasticity is defined as:

$$E_{\sec} = \frac{\sigma_a}{\varepsilon_a} = \frac{f(\varepsilon_a)}{\varepsilon_a} \tag{4.8}$$

The next parameter that needs to be defined is the equivalent damping ratio. The area enclosed by the hysteresis loop is a measure of the energy dissipated per cycle of motion. This area is identified as ΔW and is the dotted area in Figure 4.5. To make this quantity independent of the maximum deformation the area is normalized by the corresponding elastic energy stored up to the maximum deformation. This is the area identified by the vertical lines in Figure 4.5 and is denoted as W. To complete the definition of ξ, the ratio between the two areas is normalized by 4π:

$$\xi = \frac{1}{4\pi} \frac{\Delta W}{W} \tag{4.9}$$

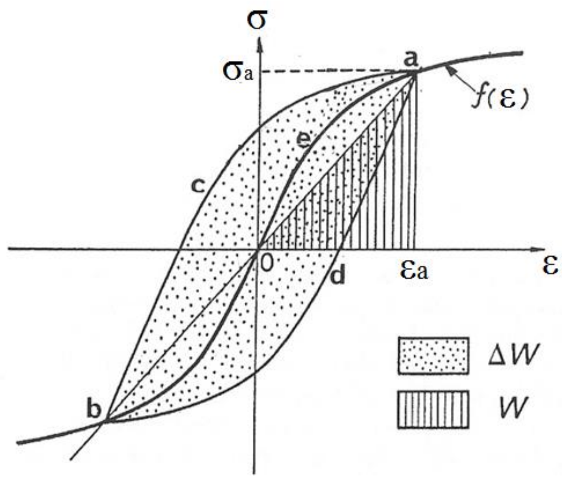

Figure 4.5 *Masing's damping ratio relationship. (Suárez, 2008)*

The area of the elastic energy stored W is simply the area of the triangle in Figure 4.5 and the energy of the hysteris loop ΔW is 8 times the area of the segment o-e-a in the same figure. It is straightforward to demonstrate that they can be calculated as follows:

$$W = \frac{1}{2}\sigma_a \varepsilon_a = \frac{1}{2} f(\varepsilon_a)\varepsilon_a \tag{4.10}$$

$$\Delta W = 8\int_0^{\varepsilon_a} f(\varepsilon)d\varepsilon - 4f(\varepsilon_a)\varepsilon_a \tag{4.11}$$

Substituting ΔW and W in equation (4.9) the equivalent damping ratio becomes:

$$\xi = \frac{2}{\pi}\left(\frac{2\int_0^{\varepsilon_a} f(\varepsilon)d\varepsilon}{\varepsilon_a f(\varepsilon_a)} - 1 \right) \tag{4.12}$$

4.2.2. Equivalent linear parameters for the beam elements

The first step necessary to apply the equivalent linear method to the building is to define the backbone curve. Because the section properties are different for the columns and the beams, two curves $\sigma = f(\varepsilon)$ are needed. The non-linear stress-strain for the beams was described and shown in Chapter 2; it is again displayed here in Figure 4.6. Because we need an analytical expression to define the secant modulus and to calculate the damping ratio, a polynomial equation was fitted to the actual stress-strain curve. The resulting polynomial equation is:

$$f(\varepsilon) = -1.43894\times10^{12}\varepsilon^4 + 5.05688\times10^{10}\varepsilon^3 - 6.31157\times10^8\varepsilon^2 + 3416520.0\varepsilon \qquad (4.13)$$

Figure 4.6 displays the polynomial approximation superimposed on the actual curve.

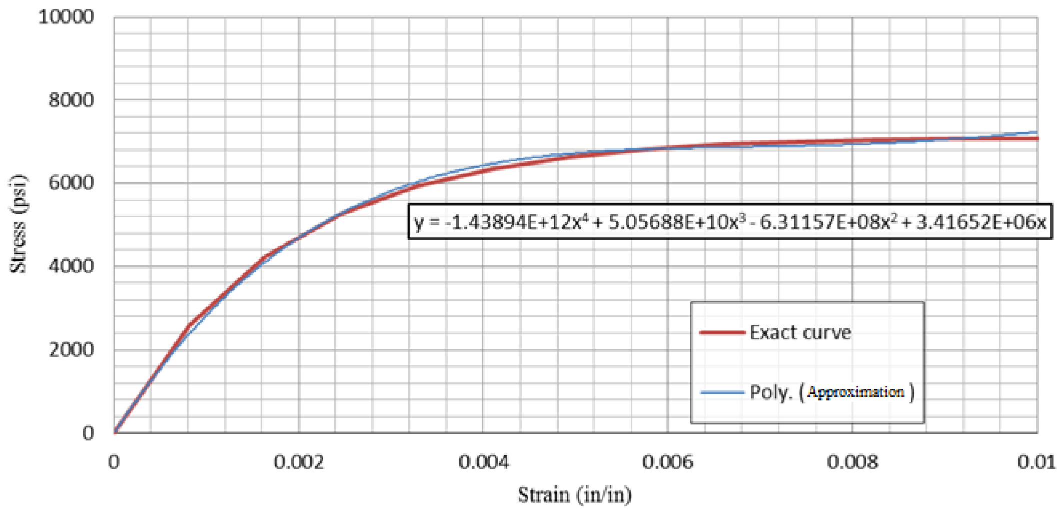

Figure 4.6 *Beam stress-strain polynomial approximation*

Equation (4.13) can only be used to define the positive side of the curve; another equation is needed for the negative quadrant. To complete the definition of the backbone curve for negative values of the stresses and strain, the sign of the terms with even powers of ε needs to be switched. Therefore, the new equation is:

$$f(\varepsilon) = 1.43894\times10^{12}\varepsilon^4 + 5.05688\times10^{10}\varepsilon^3 + 6.31157\times10^8\varepsilon^2 + 3416520.0\varepsilon \qquad (4.14)$$

Now that the information required to define the full backbone curve is available, the complete hysteresis loop can be drawn by combining equations (4.13) and (4.14) with those that define the upper and lower branches of the cycle, equations (4.5) and (4.6). The result is presented in Figure 4.7. Note that this was done only for illustrative purposes because neither the backbone curve nor the hysteresis loop is directly needed to implement the equivalent linear method.

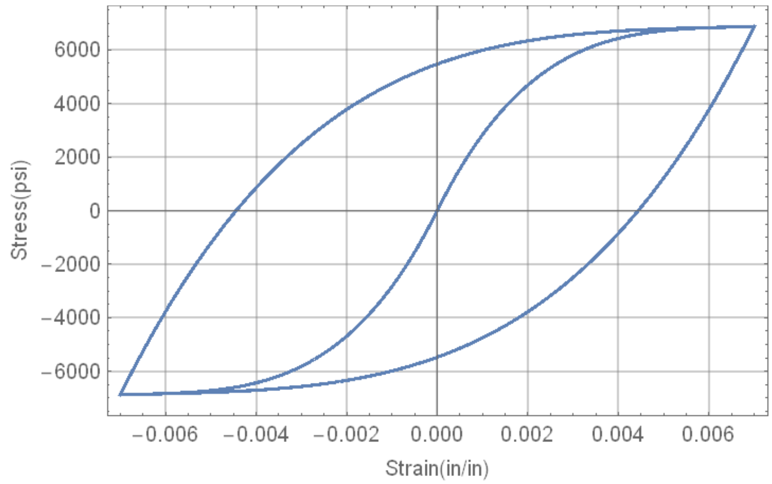

Figure 4.7 *Backbone curve and hysteresis cycle for the beam elements*

The secant modulus E_{sec} is defined using equation (4.8):

$$E_{sec} = -1.43894\times10^{12}\varepsilon^{3} + 5.05688\times10^{10}\varepsilon^{2} - 6.31157\times10^{8}\varepsilon + 3416520.0 \qquad (4.15)$$

To simplify the notation, the maximum strain from now on is denoted as ε instead of ε_a. Figure 4.8 displays the secant modulus for the beam elements.

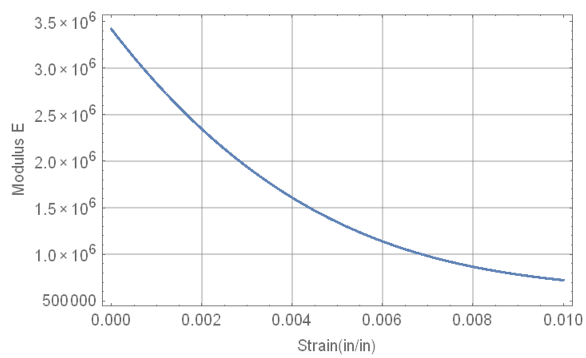

Figure 4.8 *Degradation curve for the secant modulus of beams*

In a similar way, a closed form expression for the equivalent damping ratio can be obtained by substituting equation (4.13) in (4.12). The following equation was obtained with the symbolic manipulation computer software Mathematica v10 (Mathematica, 2014).

$$\xi = \frac{2}{\pi}\left(\frac{3416520\varepsilon^{2} - 4.208\times10^{8}\varepsilon^{3} + 2.528\times10^{10}\varepsilon^{4} - 5.776\times10^{11}\varepsilon^{5}}{3416520\varepsilon^{2} - 6.312\times10^{8}\varepsilon^{3} + 5.057\times10^{10}\varepsilon^{4} - 1.439\times10^{12}\varepsilon^{5}} - 1\right) \qquad (4.16)$$

Figure 4.9 display the degradation curve for the damping ratio applicable to all the beam elements of the building model.

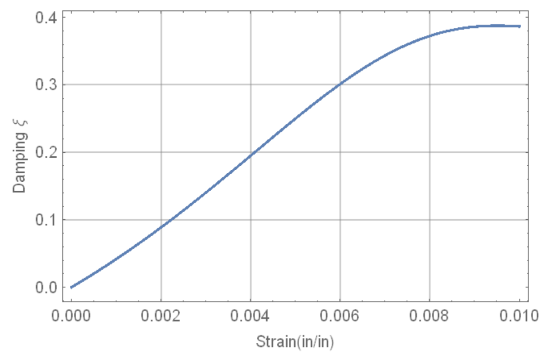

Figure 4.9 *Degradation for the Damping Ratio of Beams*

4.2.3. Equivalent linear parameters for the column elements

Because the non-linear stress-strain relationship is different for the columns than for the beam elements, the process in the previous section must be repeated. We begin by adjusting a polynomial function so that it best fits the σ vs. ε curve shown in Figure 4.10. Following the case of the beam elements, a fourth order polynomial was used. The resulting equation is:

$$f(\varepsilon) = -3.6886\times10^{11}\varepsilon^4 + 2.41744\times10^{10}\varepsilon^3 - 4.40088\times10^{8}\varepsilon^2 + 3124310.0\varepsilon \qquad (4.17)$$

Figure 4.10 displays the polynomial equation (4.17) and the physical non-linear constitutive equation for the column elements.

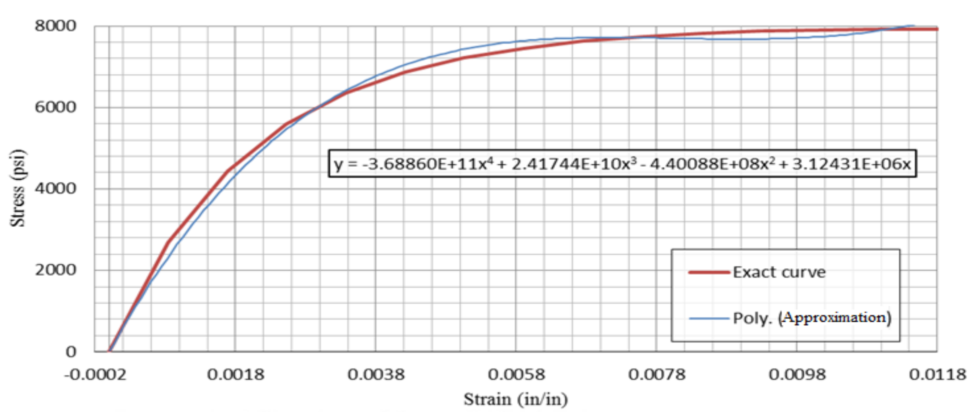

Figure 4.10 *Column stress-strain polynomial approximation*

Equation (4.17) can only be used to define the backbone curve for the positive quadrant. To define it in the negative quadrant the sign of the coefficients of the two even powers of ε is swapped:

$$f(\varepsilon) = 3.6886\times10^{11}\varepsilon^4 + 2.41744\times10^{10}\varepsilon^3 + 4.40088\times10^8\varepsilon^2 + 3124310.0\varepsilon \qquad (4.18)$$

Using equations (4.17), (4.18), (4.5) and (4.6) the backbone curve along with the hysteresis cycle for the column elements can be defined. Both are displayed in Figure 4.11.

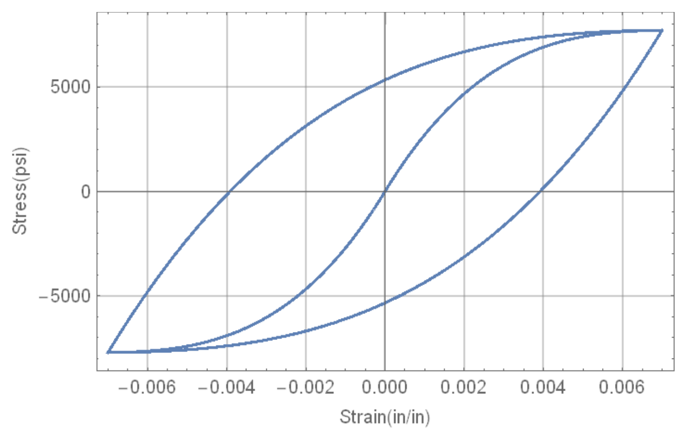

Figure 4.11 *Column stress-strain cyclical behaviors*

The next step is to obtain closed form expressions for the secant modulus and the damping ratio. First, the modulus of elasticity is obtained with equations (4.8) and (4.17):

$$E_{sec} = -3.6886\times10^{11}\varepsilon^3 + 2.41744\times10^{10}\varepsilon^2 - 4.40088\times10^8\varepsilon + 3124310.0 \qquad (4.19)$$

Figure 4.12 displays the secant modulus for the column elements.

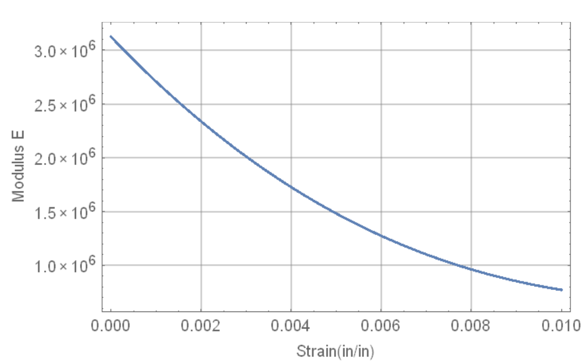

Figure 4.12 *Degradation curve for the secant modulus of columns*

Next replacing $f(\varepsilon)$ from equation (4.17) in (4.12) and solving the integral, etc. with the help of the program *Mathematica*, the following expression is obtained for the equivalent damping ratio:

$$\xi = \frac{2}{\pi}\left(\frac{3124310\varepsilon^2 - 2.934\times10^8\varepsilon^3 + 12.088\times10^9\varepsilon^4 - 14.754\times10^{10}\varepsilon^5}{3124310\varepsilon^2 - 4.401\times10^8\varepsilon^3 + 2.417\times10^{10}\varepsilon^4 - 3.689\times10^{11}\varepsilon^5} - 1\right) \tag{4.20}$$

The equivalent damping ratio for the columns is plotted in Figure 4.13.

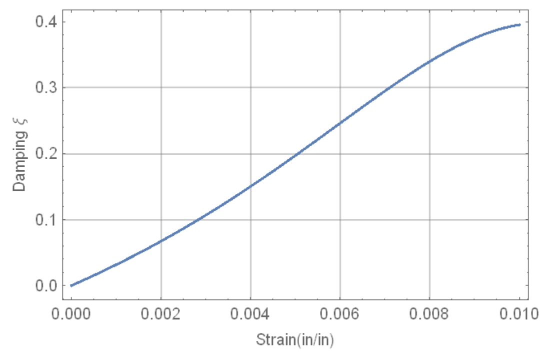

***Figure 4.13** Degradation for the Damping Ratio of columns*

For more details on all formulation development and curves, please make reference to appendix B.

4.3 Equivalent linear dynamic analysis

The building will be subjected to two types of loading: static forces due to the structure's self-weight and a dynamic excitation due to the earthquake ground acceleration. The equations of motion that will be solved at every iteration step are:

$$[M]\{\ddot{u}(t)\} + [C]\{\dot{u}\}(t) + [K]\{u(t)\} = \{W\} - [M]\{r_x\}a_x(t) \tag{4.21}$$

where:

[K] = stiffness matrix,

$[C]$ = damping matrix,

$[M]$ = mass matrix,

$\{u(t)\}$ = relative displacement vector,

$\{\dot{u}(t)\}$ = relative velocity vector,

$\{\ddot{u}(t)\}$ = relative acceleration vector,

$\{W\}$ = static loads due to the structures and components weight,

$\{r_x\}$ = influence coefficient vector in the horizontal X direction, and

$a_x(t)$ = ground acceleration in the horizontal X direction.

Because all the analysis in this chapter is linear, it is possible to calculate the response to the static and earthquake loadings separately and combine them afterward. However, to carry out the analysis in the ANSYS program it is more expedient to apply the two types of load simultaneously. The gravitational load was applied slowing increasing its magnitude for five seconds and then keeping it constant. The earthquake acceleration was applied one second after the gravitational load reached its final magnitude, i.e. at six seconds. This process was repeated for every linear analysis carried out in this chapter.

4.3.1. Broad-band seismic record

The first study is a comparison of the response obtained with a non-linear and a linear analysis of the structure. The building model created in ANSYS was subjected to a typical broad-band event, namely the 1940 Imperial Valley record. This record is typical of a ground motion with a broad-band frequency content. The record was scaled by a factor of 3.5. Four response quantities were calculated, namely the relative displacement (with respect to the base) of a point at the roof, the shear force and bending moment at a column at the base of the building and the absolute acceleration. The maximum response quantities were retrieved from the time histories and are shown in Table 4.1. It is evident that the linear analysis over predicts the true response.

Table 4.1 *Broad-band 3.5x analysis non-linear and linear results*

Displacement (in)		
Non-linear result	***Linear result***	***%Diff***
5.3374	5.9308	11.12%
Shear force (kip)		
Non-linear result	***Linear result***	***%Diff***
407.1	484.0	18.93%
Bending moment (kip-in)		
Non-linear result	***Linear result***	***%Diff***
42442	50700	19.53%
Acceleration (in/s^2)		
Non-linear result	***Linear result***	***%Diff***
1436.8	1899.7	32.22%

Next, the response will be calculated with the equivalent linear method. As it was mentioned previously the method needs an initial estimate of the secant modulus and damping ratio due to the non-linear behavior. An initial value of the normal strain ε equal to 0.001 is used to calculate the secant modulus E_{sec} and equivalent damping ratio ξ. Equations (4.15) and (4.16) are used for the beam elements and equations (4.19) and (4.20) for the columns. These four quantities are used as input to the ANSYS program and the dynamic response to the Imperial Valley record is calculated. The values of E_{sec} and ξ for the beams and columns need to be updated using the newly calculated response. Here the maximum absolute values of the normal strain time histories in a selected beam and column are used. Table 4.2 displays the intermediate and final results obtained during the iteration process.

Table 4.2 *Broad-band full strain iteration*

Equivalent linear beam /maximum strain					
Iteration	***Assume (ε)***	***Damping (ξ)***	***Modulus (E -psi)***	***Result (ε)***	***%Diff***
1	0.001	0.0617672	2834490	0.0054803	448.03%
2	0.0054803	0.295136	1239520	0.0061969	13.08%
3	0.0061969	0.330147	1104800	0.0062896	1.50%
4	0.0062896	0.334345	1089230	0.0062759	0.22%
Equivalent linear column /maximum strain					
Iteration	***Assume (ε)***	***Damping (ξ)***	***Modulus (E -psi)***	***Result (ε)***	***%Diff***
1	0.001	0.0516967	2708030	0.0030056	200.56%
2	0.0030056	0.12697	2009950	0.0028699	4.51%
3	0.0028699	0.121366	2051690	0.0027923	2.70%
4	0.0027923	0.118194	2075910	0.0027648	0.98%

Once the convergence criterion was reached, the maximum response was retrieved at the same points where it as calculated in the previous analysis. Table 4.3 displays the maximum relative displacement and absolute acceleration, and the maximum shear force and bending moment at the base. As it can be seen, in this case the equivalent linear method underestimates the true response (i.e. that obtained with a full non-linear analysis). This means that the equivalent linear method produces a too stiff equivalent structural system. Actually, by comparing Tables 4.1 and 4.3 it is evident that the simple linear analysis yields better results than the equivalent linear method. The most likely reason is that the iteration process was implemented using the maximum normal strains from the time histories. For a nonstationary excitation like an earthquake acceleration this peak value only occurs at a single instant of time and thus it is not reasonable to use the maximum values of the strains. In the following examples, an effective (reduced) strain will be used.

Table 4.3 *Broad-band full strain non-linear and linear results*

Displacement (in)		
Non-linear result	***Linear result***	***%Diff***
5.3374	3.2412	39.27%
Shear Force (kip)		
Non-linear result	***Linear result***	***%Diff***
407.1	241.43	40.70%
Moment Reaction (kip-in)		
Non-linear result	***Linear result***	***%Diff***
42442	25655	39.55%
Acceleration (in/s^2)		
Non-linear result	***Linear result***	***%Diff***
1436.8	877.22	38.95%

Before continuing with the application of the equivalent linear method, it is pertinent to discuss how the equivalent damping ratios obtained at each iteration steps are used in the ANSYS building model. First, it is noticed that at each iteration step two equivalent damping ratios are used, one for the beams and another for the column elements. However, ANSYS (and most structural analysis programs) cannot assign different damping properties to specific parts of a structure. Rather, the damping is usually introduced as modal damping ratios, i.e. each vibration mode is assigned a specific value. Moreover, in ANSYS there is an additional restriction: because the program uses the Rayleigh damping model, only two modes can be assigned a specific value. To implement the equivalent linear method in ANSYS, the mean value of the two equivalent damping ratios obtained at each iteration step from the degradation curves was calculated. This value was assigned to two modes of the building through the damping matrix of the Rayleigh model. The damping ratio (along with the natural frequencies) were used to calculate the parameters α and β as it was explained in the previous chapter. Table 4.4 shows how the parameters α and β change at each iteration step.

Table 4.4 *Broad-band full strain damping parameters*

Iteration	***Damping (ξ)***	***Factor (α)***	***Factor (β)***
1	0.05673195	1.39694	0.00167495
2	0.211053	4.26717	0.00754021
3	0.2257565	4.51673	0.00812654
4	0.2262695	4.5325	0.00812956

When the equivalent linear method is applied for site response analysis, i.e. to calculate the acceleration at the surface of a layered soil deposit, usually an effective shear strain γ_{efec} equal to 65% of the maximum absolute value γ_{max} is used in the process. Therefore to asses if this approach is viable to compute the seismic response of the building, the previous iterative process was repeated using ε_{efec} = 0.65 ε_{max}. The partial results obtained with the iteration process are presented in Table 4.5. Since this was only a trial, the convergence criterion was set equal to 2%. The parameters α y β at each iteration step used to define the damping matrix with the Rayleigh model are displayed in Table 4.6.

Table 4.5 *Broad-band 65% strain iteration*

Equivalent linear beam / 65% of strain						
Iteration	***Assume (ε)***	***Damping (ξ)***	***Modulus (E -psi)***	***Result (ε)***	***0.65 Red (ε)***	***%Diff***
1	0.001	0.0617672	2834490	0.0054803	0.003562195	256.22%
2	0.0035622	0.190614	1744850	0.0053088	0.00345072	3.13%
3	0.00345072	0.18451	1781600	0.005238	0.0034047	1.33%
Equivalent linear column / 65% of strain						
Iteration	***Assume (ε)***	***Damping (ξ)***	***Modulus (E -psi)***	***Result (ε)***	***0.65 Red (ε)***	***%Diff***
1	0.001	0.0516967	2708030	0.0030056	0.00195364	95.36%
2	0.00195364	0.0854747	2354050	0.0025624	0.00166556	14.75%
3	0.00166556	0.0748915	2456670	0.0025094	0.00163111	2.07%

Table 4.6 *Broad-band 65% strain damping parameters*

Iteration	Damping (ξ)	Factor (α)	Factor (β)
1	0.05673195	1.39694	0.00167495
2	0.13804435	3.0618	0.00450334
3	0.12970075	2.92063	0.00416364

Once convergence was achieved with the 0.65 ε_{max} effective strain, the same four maximum response quantities previously used were obtained from the time histories. They are shown in Table 4.7. Although there is a slight improvement in the accuracy of the results compared to the previous case (i.e. using the maximum normal strain ε_{max}), the values of the four response quantities calculated are not satisfactory. The equivalent linear method continues to underestimate the true response. It is then preliminarily concluded that the typical approach to define the effective strain in Soil Dynamics is not applicable for calculating the seismic response of buildings.

Table 4.7 *Broad-band 65% strain non-linear and linear results*

Displacement (in)		
Non-linear result	***Linear result***	***%Diff***
5.3374	3.7013	30.65%
Shear Force (kip)		
Non-linear result	***Linear result***	***%Diff***
407.1	262.93	35.41%
Moment Reaction (kip-in)		
Non-linear result	***Linear result***	***%Diff***
42442	27509	35.18%
Acceleration (in/s^2)		
Non-linear result	***Linear result***	***%Diff***
1436.8	891.69	37.94%

Therefore, since there are no other guidelines to select a reduction factor, it was decided to vary this parameter beginning with 100% (i.e., no reduction) and decreasing it to zero. The building response was calculated by applying the equivalent linear method using each of the reduction factors to define the effective normal strain. The errors in the relative displacement, absolute acceleration, shear force and bending moments at the same selected points as before were calculated and are plotted in Figure 4.14. It is evident that there are optimal reduction factors but their values vary depending on the type of response.

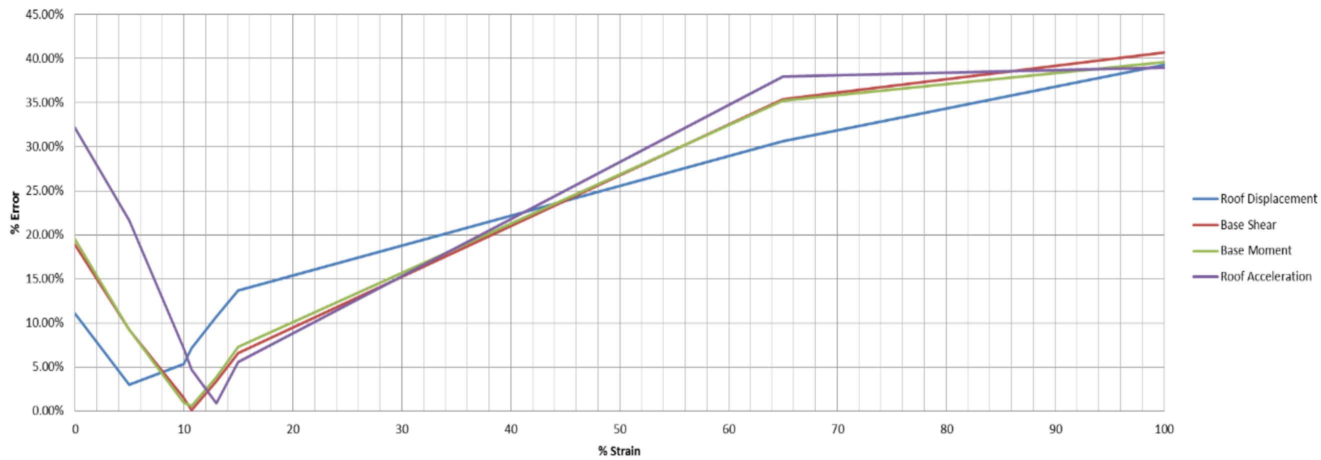

Figure 4.14 *Broad-band Strain factors vs. %Error*

The optimum values for each of the four response quantities are summarized in Table 4.8. The reduction factor varies from 6.8% for the displacement to 12.6% for the acceleration. Clearly, these values are much smaller than the 65% used in the Soil Dynamics applications.

Table 4.8 *Broad-band optimum values to minimize error*

error	***Strain %***
Displacement	6.796
Shear	10.756
Moment	10.432
Acceleration	12.641

For practical applications, it is not convenient to select different reduction factors depending on the response sought. A single value would be preferred, even though the error may be slightly higher for some of the response quantities. In this study, it is recommended to use a weighted average value calculated by given more weight to the shear force and bending moment which are essential quantities for structural design. The final recommended reduction factor is presented in Table 4.9. Obviously, the optimal reduction factors in Tables 4.8 and 4.9 are for the specific seismic record used (Imperial Valley) amplified 3.5 times and for the particular building analyzed.

Table 4.9 *Broad-band final recommended value*

Earthquake	**Scale Factor**	**Class**	**Factor**
Imperial	x3.5	Broad	0.10711

To evaluate the effectiveness of the proposed reduction factor for a broad-band ground motion, the building is again subjected to the acceleration record of the 1940 Imperial Valley earthquake. The details of the iteration process are presented in Table 4.10 and the damping ratio and the coefficients of the Rayleigh damping model are shown in Table 4.11. This time, the tolerance to check the convergence was set 1% in order to get more precise results.

Table 4.10 *Broad-band 10.71% strain iteration*

Equivalent linear beam / 10.71% of strain						
Iteration	***Assume (ε)***	***Damping (ξ)***	***Modulus (E -psi)***	***Result (ε)***	***0.1071 Red (ε)***	***%Diff***
1	0.001	0.0617672	2834490	0.0054803	0.000586984	41.30%
2	0.000586984	0.0438913	3063173	0.0062432	0.000668697	13.92%
3	0.000668697	0.0473579	3016649	0.0061259	0.000656133	1.88%
4	0.000656133	0.0468226	3023761	0.0061465	0.000658339	0.34%
Equivalent linear column / 10.71% of strain						
Iteration	***Assume (ε)***	***Damping (ξ)***	***Modulus (E -psi)***	***Result (ε)***	***0.1071 Red (ε)***	***%Diff***
1	0.001	0.0516967	2708030	0.0030056	0.000321924	67.81%
2	0.000321924	0.0298058	2985128	0.0032868	0.000352043	9.36%
3	0.000352043	0.0307422	2972360	0.0032294	0.000345895	1.75%
4	0.000345895	0.0305508	2974963	0.003239	0.000346923	0.30%

Table 4.11 *Broad-band 10.71% strain damping parameters*

Iteration	***Damping (ξ)***	***Factor (α)***	***Factor (β)***
1	0.056732	1.39694	0.00167495
2	0.036849	0.943299	0.00104489
3	0.03905	0.996468	0.0011107
4	0.038687	0.987747	0.00109976

Table 4.12 compares the exact response with that predicted by the equivalent linear method once convergence was achieved. It can be seen that the results for the internal forces and moments are excellent; the errors for the displacement and acceleration are higher but still quite reasonable. The difference in the errors for these two types of quantities was because, as explained before, the shear force and moment were given priority over the deformations quantities to define the optimal reduction factor for the strains.

Table 4.12 *Broad-band 10.71% strain non-linear and linear results*

Displacement (in)		
Non-linear result	***Linear result***	***%Diff***
5.3374	4.9858	6.59%
Shear Force (kip)		
Non-linear result	***Linear result***	***%Diff***
407.1	408.96	0.46%
Moment Reaction (kip-in)		
Non-linear result	***Linear result***	***%Diff***
42442	42377	0.15%
Acceleration (in/s^2)		
Non-linear result	***Linear result***	***%Diff***
1436.8	1508.7	5.00%

The time series from which the maximum displacement, shear force and bending moments were acquired are shown in Figure 4.15. The absolute acceleration is shown later in another figure. Note that the response begins after six seconds: it is recalled that the gravity loads were first slowly applied to the building during the first five seconds and an extra second was added before subjecting the structure to the ground acceleration.

Other results that were recovered from the equivalent linear analysis are the maximum normal stresses and strains in a beam and column of the first floor. These peak response quantities will be used for comparison in the following chapter. The values of the stresses and strains were obtained from the time histories shown in Figure 4.16 and are displayed in Table 4.13. The time variation of the stresses and strains are shown in absolute values and for the first 14 seconds of the ground motion which is where the peak values take place.

Table 4.13 *Stress-strain results of broad-band 3.5x analysis*

Measure	***Maximum***	
Beam Stress	19.630	ksi
Beam Strain	0.0061465	in/in
Column Stress	10.300	ksi
Column Strain	0.003239	in/in

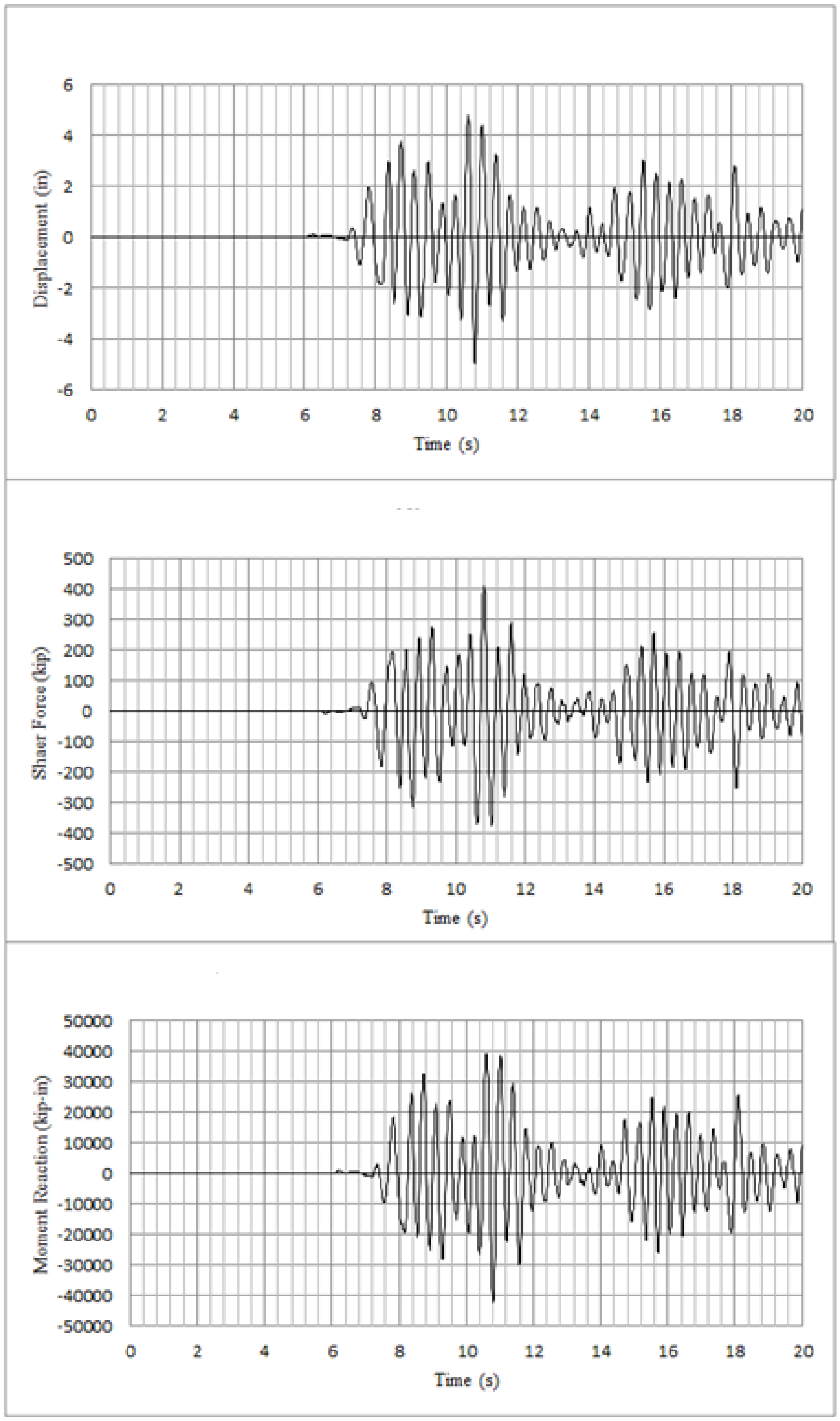

Figure 4.15 *Time history final results of broad-band 3.5x linear analysis*
a) Roof displacement, b) Base column shear force, and c) Base column moment reaction.

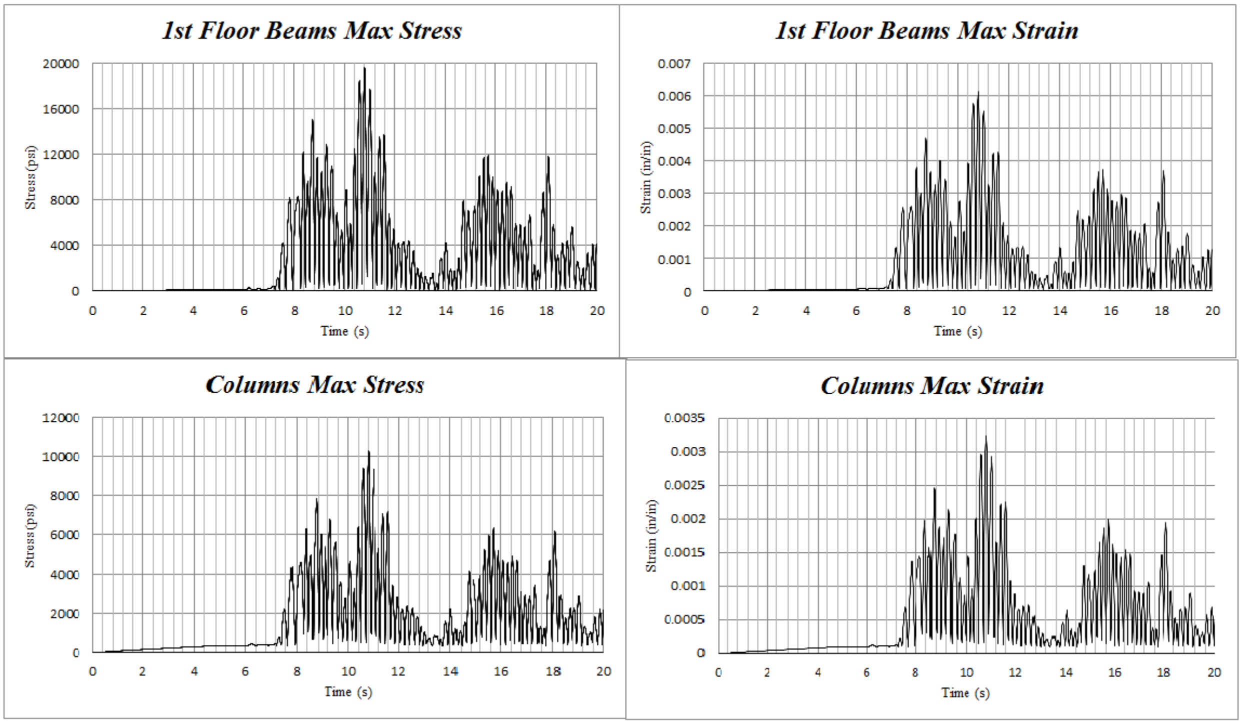

Figure 4.16 *Time history stress and strain data of broad-band 3.5x analysis*

The last results displayed are the absolute acceleration time histories at each of the three building floors in the X direction. They were calculated at the center of masses of the floor slabs and are shown in Figure 4.17. These accelerations will be used to calculate the floor response spectra in the following chapter.

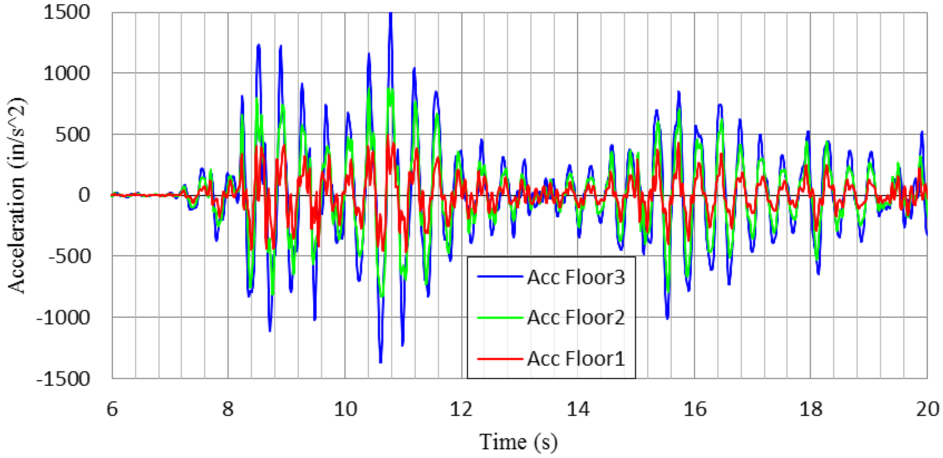

Figure 4.17 *Individual floor acceleration of broad-band 3.5x linear analysis*

4.3.2. Short-band seismic record

The results reported in the previous sections were for two samples of a broad-band earthquake ground motion. Here the study is repeated but using an earthquake ground motion with a typical short-band frequency content, namely the 1986 San Salvador record registered at the CIG station. The first task is to calculate the linear response of the building and compare it with the results of a full non-linear analysis. In order to force a non-linear behavior, the earthquake record is scaled by a factor of 2.

The differences in the maximum values of four response quantities between the non-linear and linear analysis are shown in Table 4.14. As in the previous cases, the responses selected for comparison are the relative displacement and absolute acceleration at the top of the building and the shear force and bending moment at a column at the base of the structure. It can be seen that similarly to the case of the broad-band event, the linear analysis overestimates the four response quantities compared.

Table 4.14 *Short-band 2x analysis non-linear and linear results*

Displacement (in)		
Non-linear result	***Linear result***	***%Diff***
5.2808	5.7681	9.23%
Shear Force (kip)		
Non-linear result	***Linear result***	***%Diff***
411.43	495.00	20.28%
Moment Reaction (kip-in)		
Non-linear result	***Linear result***	***%Diff***
42531	51600	21.40%
Acceleration (in/s^2)		
Non-linear result	***Linear result***	***%Diff***
1676.6	2202.2	31.35%

The building response will now be obtained with the equivalent linear method. Following a similar pattern than for the broad-band case, in a first attempt the secant modulus and equivalent damping ratio will be obtained by entering the degradation curves with the maximum normal strain. The partial results of the application of the equivalent linear method are shown in Table 4.15. To begin the iteration process, an initial value of the normal strain ε equal to 0.001

was assumed to calculate the modulus of elasticity and the damping ratio. The criterion for convergence is that the difference between the maximum normal strains at two consecutive iteration steps should be less than 1%. It can be noticed that the process converges rapidly: only four iterations were required to satisfy this tolerance.

Table 4.15 *Short-band full strain iteration*

Equivalent linear beam /maximum strain					
Iteration	***Assume (ε)***	***Damping (ξ)***	***Modulus (E -psi)***	***Result (ε)***	***%Diff***
1	0.001	0.0617672	2834490	0.0058474	484.74%
2	0.0058474	0.313589	1167250	0.0066929	14.46%
3	0.0066929	0.351517	1026070	0.006944	3.75%
4	0.006944	0.361219	990344	0.0070118	0.98%
Equivalent linear column /maximum strain					
Iteration	***Assume (ε)***	***Damping (ξ)***	***Modulus (E -psi)***	***Result (ε)***	***%Diff***
1	0.001	0.0516967	2708030	0.0031288	212.88%
2	0.0031288	0.132121	1972720	0.0030485	2.57%
3	0.0030485	0.128757	1996910	0.0030311	0.57%
4	0.0030311	0.128031	2002190	0.003027	0.14%

At each iteration step, the values of the damping ratios for the beam and column were averaged and the result was used to obtain the mass and stiffness coefficients α and β of the Rayleigh damping model. They are shown in Table 4.16 for each iteration step.

Table 4.16 *Short-band full strain damping parameters*

Iteration	***Damping (ξ)***	***Factor (α)***	***Factor (β)***
1	0.05673195	1.39694	0.00167495
2	0.222855	4.44432	0.00806716
3	0.240137	4.71804	0.0087972
4	0.244625	4.78515	0.0089937

Once the iteration process has converged, the maximum values of the four selected response quantities are recovered to compare them with the exact results (from the non-linear analysis). The values of the maximum response quantities are displayed in Table 4.17 where the errors are also presented. Examining the table it is apparent that the equivalent linear method overestimates all the responses and in fact, it leads to higher differences than a simple linear analysis. Although this was expected because the excitation is not perfectly cyclic and thus neither is the response (the peak strain only occurs at an unrepeated instant of time), it was considered important to verify it and assess the error in using the maximum strain.

Table 4.17 *Short-band full strain non-linear and linear results*

Displacement (in)		
Non-linear result	***Linear result***	***%Diff***
5.2808	4.7233	10.56%
Shear Force (kip)		
Non-linear result	***Linear result***	***%Diff***
411.43	252.75	38.57%
Moment Reaction (kip-in)		
Non-linear result	***Linear result***	***%Diff***
42531	27154	36.15%
Acceleration (in/s^2)		
Non-linear result	***Linear result***	***%Diff***
1676.6	950.93	43.28%

The equivalent linear method will now be implemented using an effective normal strain ε_{efec} smaller than the peak value. First ε_{efec} will be defined as the 65% of the maximum value, which is the practice recommended for geotechnical earthquake engineering applications. Even though this approach did not work well for the broad-band earthquake record, it is desired to examine the differences between its predictions and the full non-linear response. The iteration process is reported in Table 4.18 and the information to define the damping matrix is presented in Table 4.19. To speed up the process and since this is only a trial, the tolerance was increased to 2%.

Table 4.18 *Short-band 65% strain iteration*

Equivalent linear beam / 65% of strain						
Iteration	***Assume (ε)***	***Damping (ξ)***	***Modulus (E -psi)***	***Result (ε)***	***0.65 Red (ε)***	***%Diff***
1	0.001	0.0617672	2834490	0.0058474	0.00380081	280.08%
2	0.00380081	0.203754	1669130	0.0059238	0.00385047	1.31%
3	0.00385047	0.206499	1653860	0.0058855	0.003825575	0.65%
Equivalent linear column / 65% of strain						
Iteration	***Assume (ε)***	***Damping (ξ)***	***Modulus (E -psi)***	***Result (ε)***	***0.65 Red (ε)***	***%Diff***
1	0.001	0.0516967	2708030	0.0031288	0.00203372	103.37%
2	0.00203372	0.0884758	2326180	0.0027572	0.00179218	11.88%
3	0.00179218	0.0795021	2411120	0.0027029	0.001756885	1.97%

Table 4.19 *Short-band 65% strain damping parameters*

Iteration	***Damping (ξ)***	***Factor (α)***	***Factor (β)***
1	0.05673195	1.39694	0.00167495
2	0.1461149	3.21014	0.0048098
3	0.14300055	3.17019	0.00465886

The results obtained by using ε_{efec} = $0.65\varepsilon_{max}$ are displayed in Table 4.20. There is a slight improvement in the results compared to using maximum normal strains, but clearly the 0.65 reduction factor does not work for the earthquake record with a short-band frequency content.

Table 4.20 *Short-band 65% strain non-linear and linear results*

Displacement (in)		
Non-linear result	***Linear result***	***%Diff***
5.2808	4.7553	9.95%
Shear Force (kip)		
Non-linear result	***Linear result***	***%Diff***
411.43	270.69	34.21%
Moment Reaction (kip-in)		
Non-linear result	***Linear result***	***%Diff***
42531	29029	31.75%
Acceleration (in/s^2)		
Non-linear result	***Linear result***	***%Diff***
1676.6	1071.4	36.10%

Therefore, a more appropriate reduction factor will have to be obtained by varying its value, calculating the responses and comparing them with the exact results. The reduction factor was varied from 0% to 100%: the zero value corresponds to a linear analysis and the 100% value is the first case considered in this section. The errors in percent for the four different response quantities as a function of the reduction factor are presented in Figure 4.18. It is evident from the figure that there is no single optimum reduction factor that is applicable to the four responses.

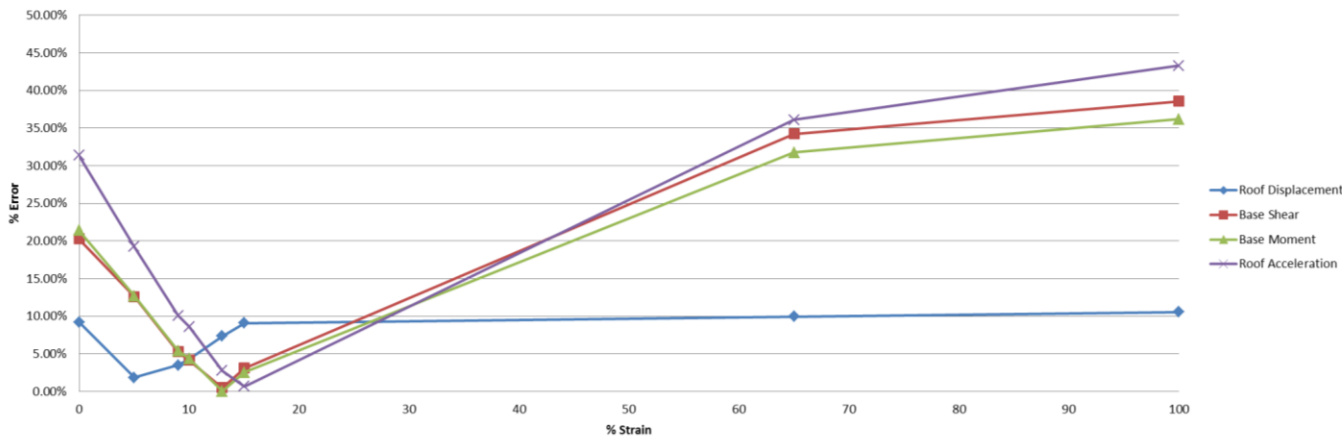

Figure 4.18 *Short-band Strain factors vs. %Error*

The optimum values for each response quantity are summarized in Table 4.21. The range of optimal values goes from 6.5% for the relative displacement to 14.6% for the absolute acceleration.

Table 4.21 *Short-band optimum values to minimize error*

Error	***Strain %***
Displacement	6.494
Shear	12.674
Moment	13.002
Acceleration	14.601

However, like before for practical applications a single reduction factor that can be used for all the responses is desired. In order to obtain this, a weighted average value was calculated where the shear force and bending moment parameters contribute more than the deformation quantities. The final factor recommended is shown in Table 4.22.

Table 4.22 *Short-band final recommended value*

Earthquake	**Scale Factor**	**Class**	**Factor**
Salvador	x2	Short	0.12785

Using this factor to calculate the effective strain, the response of the building to the 1986 SanSalvador earthquake was calculated again with the equivalent linear method. The normal strains, secant moduli and damping ratios at each iteration steps are provided in Table 4.23 and the damping parameters are shown in Table 4.24. Because these are final calculations, the convergence tolerance criterion was set equal to 1% in order to get more precise results.

***Table 4.23** Short-band 12.78% strain iteration*

Equivalent linear beam / 12.78% of strain						
Iteration	***Assume (ε)***	***Damping (ξ)***	***Modulus (E -psi)***	***Result (ε)***	***0.1278 Red (ε)***	***%Diff***
1	0.001	0.0617672	2834490	0.0058474	0.000747561	25.24%
2	0.000748	0.0507363	2972351	0.0063028	0.000805781	7.79%
3	0.000806	0.0532511	2940026	0.0062604	0.000800361	0.67%
Equivalent linear column / 12.78% of strain						
Iteration	***Assume (ε)***	***Damping (ξ)***	***Modulus (E -psi)***	***Result (ε)***	***0.1278 Red (ε)***	***%Diff***
1	0.001	0.0516967	2708030	0.0031288	0.000400001	60.00%
2	0.0004	0.0322399	2952119	0.0033253	0.000425123	6.28%
3	0.000425	0.0330278	2941559	0.0032936	0.00042107	0.95%

***Table 4.24** Short-band 12.78% strain damping parameters*

Iteration	***Damping (ξ)***	***Factor (α)***	***Factor (β)***
1	0.056732	1.39694	0.00167495
2	0.041488	1.05458	0.00118456
3	0.043139	1.09387	0.00123462

The final maximum relative displacement, absolute acceleration, shear force and bending moment obtained with the equivalent linear method and $\varepsilon_{efec} = 0.128\varepsilon_{max}$ are shown in Table 4.25 along with the exact responses and the relative errors. It is evident that the results are excellent for the internal forces and although the differences are higher for the deformation quantities, their accuracy is still very reasonable.

***Table 4.25** Short-band 12.78% strain non-linear and linear results*

Displacement (in)		
Non-linear result	***Linear result***	***%Diff***
5.2808	4.9037	7.14%
Shear Force (kip)		
Non-linear result	***Linear result***	***%Diff***
411.43	410.61	0.20%
Moment Reaction (kip-in)		
Non-linear result	***Linear result***	***%Diff***
42531	42653	0.29%
Acceleration (in/s^2)		
Non-linear result	***Linear result***	***%Diff***
1676.6	1729.1	3.13%

The time variation of the relative displacement at the roof, the shear force and the bending moment at a column of the first floor are shown in Figure 4.19. From these graphs the maximum values presented in Table 4.25 were obtained. It is recalled that the dynamic responses start after six seconds because first the dead loads were slowly applied during this time.

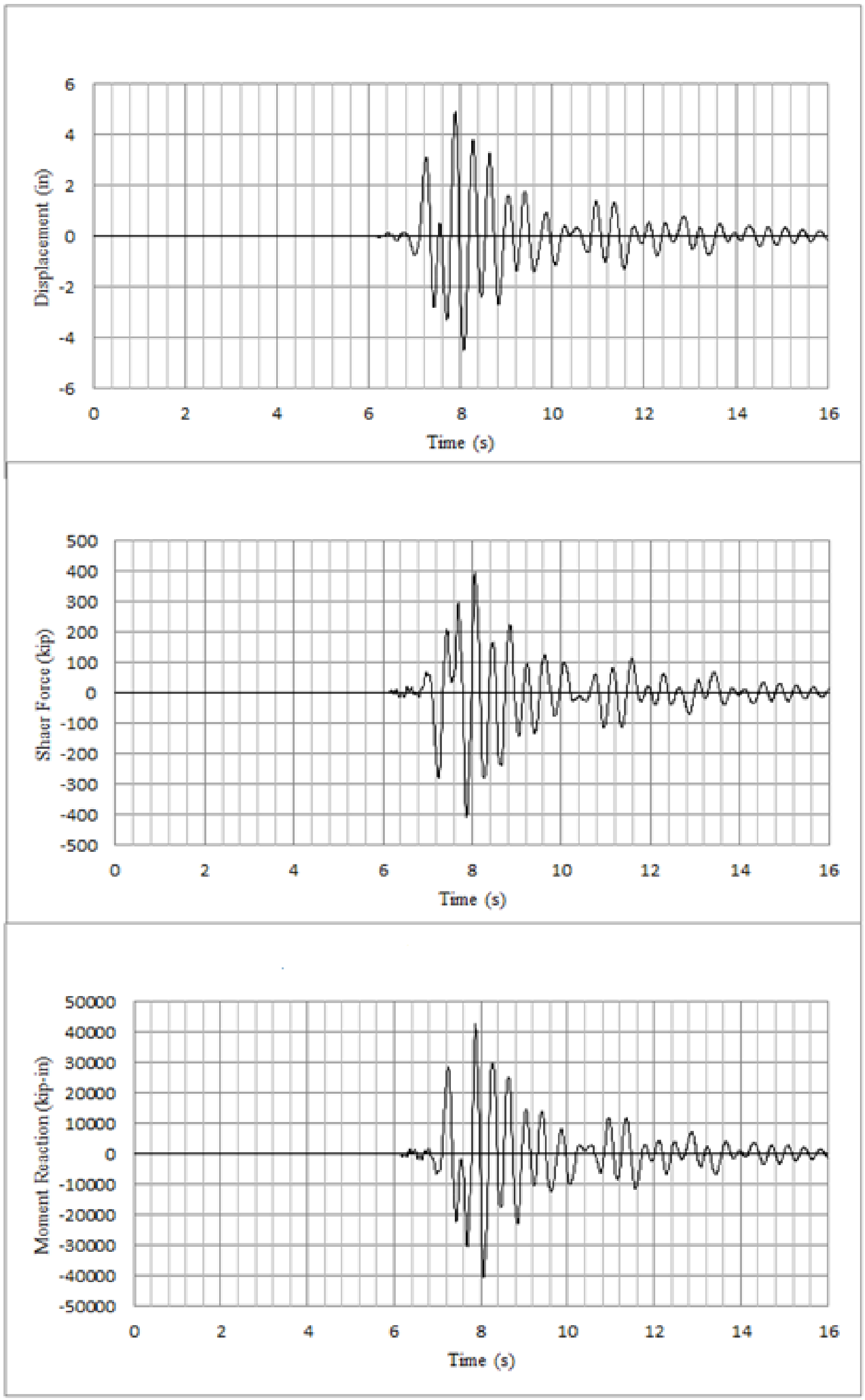

Figure 4.19 *Time history final results of short-band 2x linear analysis*
a) Roof displacement, b) Base column shear force, and c) Base column moment reaction.

As it was done for the broad-band earthquake, additional peak responses were retrieved from the last equivalent linear analysis. They are shown in in Table 4.26 and they will be used for further comparison in the following chapter. Figure 4.20 shows the time variation of the stresses and strains at a selected beam and column of the first floor. The times series are displayed in absolute values and for the first fourteen seconds of the earthquake (where the maximum values occur).

Table 4.26 *Stress-strain results of short-band 2x analysis*

Measure	***Maximum***	
Beam Stress	19.477	ksi
Beam Strain	0.0062604	in/in
Column Stress	10.356	ksi
Column Strain	0.0032936	in/in

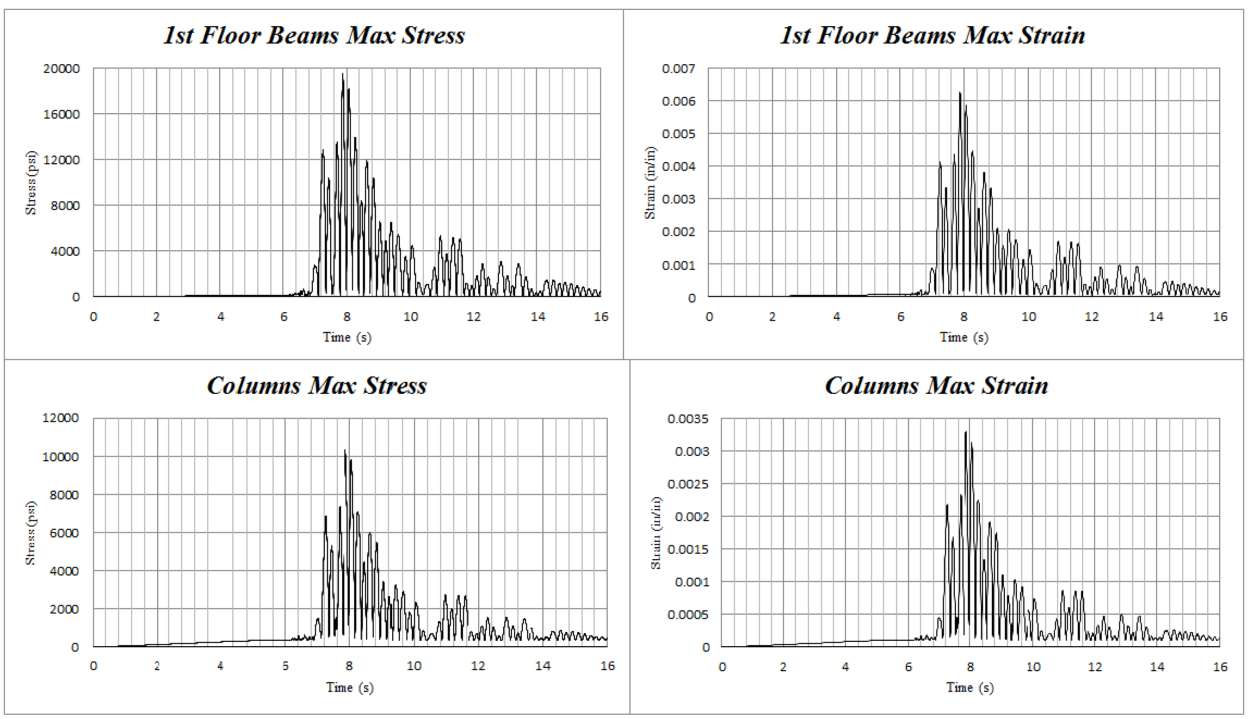

Figure 4.20 *Time history stress and strain data of short-band 2x analysis*

Because one of the objectives of the thesis is to calculate the floor response spectra with the equivalent linear method, the acceleration time histories obtained at each of the floors in the horizontal X direction were retrieved for the analysis and are shown in Figure 4.21.

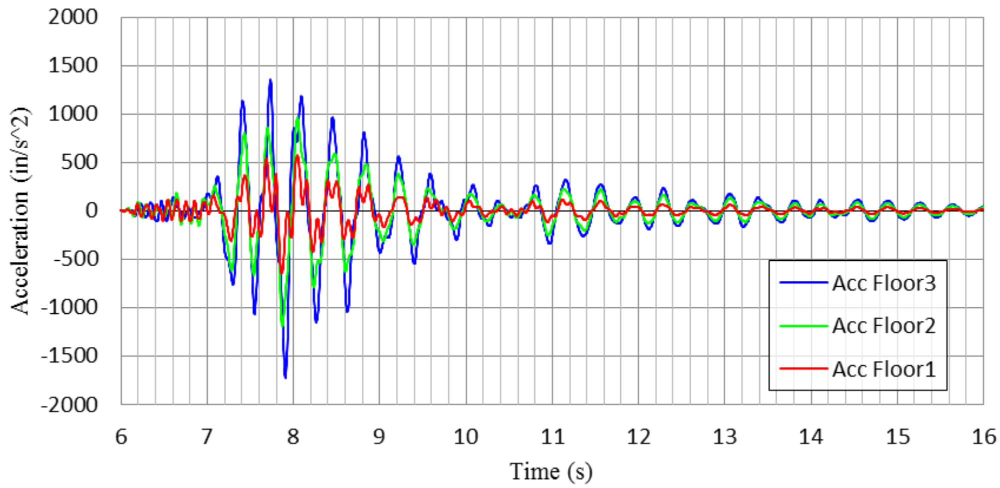

Figure 4.21 *Individual floor acceleration of short-band 2x linear analysis*

4.4 Chapter summary and conclusions

The main objective of this chapter was to put into practice the equivalent linear method to calculate the approximate response of a RC multi-story building that experiences high-intensity seismic events. This method can be implemented in any linear structural analysis software and will result in a significant reduction in computational processing time. A brief description of the methodology of the equivalent linear method is presented. The specific degradation curves to be used for the beam and column elements were presented.

To have a baseline to be used for comparison with later data, a linear analysis was carried out. The study is repeated for two seismic records with different frequency contents: a broad-band event, the 1940 Imperial Valley earthquake and short-band record, the 1986 San Salvador earthquake. It was decided to focus the attention on four response quantities. Two of them are relative to the motion of the structure: the relative displacement with respect the base and the absolute acceleration, both calculated at the top of the building. The other two are internal forces and moments: the shear force and the bending moment both at a critical column at the base of the building. On the other hand, it can be seen that the method converged rapidly with only 3 to 4 iteration were needed in order to achieve the selected level of tolerance. This is an important factor since it reduces the time needed to obtain results using the equivalent linear method.

After the linear analysis, two attempts to apply the equivalent linear method were undertaken. In the first case, the maximum normal strain at the most critical beam and column was used to calculate the secant modulus and the equivalent damping ratio. Next, the analysis was repeated using effective strains equal to the maximum strains reduced at 65% of their value. The 0.65 factor is commonly recommended when the equivalent linear method is applied to calculate the seismic response of soil deposits. Neither of these two cases produced acceptable results and thus an optimal reduction factor was obtained by varying it form 0 to 1 and calculating the response. There is no common reduction factor for the four selected responses and therefore a weighted average value was calculated emphasizing the minimization of the errors for the shear force and bending moment. Once this reduction factor was determined the seismic response of the structure was one more time analyzed with the equivalent linear method. The agreement with the full non-linear response was very good for the broad and short-band ground motions. More response quantities were calculated at this final stage, in particular the time series of the absolute accelerations of the three floors which will be used to compute floor response spectra in the following chapter.

CHAPTER V

PROPOSED REDUCTION FACTOR AND FINAL VALIDATION

5.1 Introduction

It was found and reported in Chapter 4 that the success of the equivalent linear method, when it is applied to calculate the approximate inelastic response of an RC building subjected to an earthquake, depends on the reduction factor. This is a factor that accounts for the fact that the deformation response is not perfectly cyclic, i.e. the peaks do not repeat over time. Obviously, this will always happen when the structure is subjected to a nonstationary load like an earthquake ground motion. In this case, an effective strain is calculated by reducing the maximum strain through a reduction factor. When the equivalent linear method is used for its original intended application, namely Soil Dynamics, the reduction factor is 0.65. It was shown in Chapter 4 that this value is not applicable for RC buildings, and thus an optimal reduction factor was found by a trial and error process. Two factors were obtained: one for an earthquake ground motion with a broad-band frequency content and another for a record with frequencies in a short-band range. The four response quantities that were checked to verify the accuracy of the proposed method with these factors compared very well with those obtained from a fully non-linear analysis. However, it is not evident that the factors obtained in Chapter 4 will be applicable for other earthquake records or even for the same accelerograms used but with different intensities. To extend the study to obtain a proper reduction factor, the seismic demand imposed on the building by the earthquake must be taken into account.

5.2 Linear equivalent method validation

There are many factors that affect the seismic response of a building, such as the intensity of the earthquake record, its duration and its frequency content. Each of these factors can be described by a parameter or index. A summary of these parameters is presented in a thesis by Miranda (2016) where the geographical distribution for the Island of Puerto Rico for three low intensity seismic motions. A few of these parameters that account for the main factors that affect the seismic demand imposed on buildings by an earthquake were selected; they are described in the next section. These indices will be computed for a number of historic ground motions with different characteristics and a reduction factor will be defined as a linear combination of them. The coefficients of the linear combination will be selected by a minimizing the difference between the exact non-linear response and the approximate response calculated with the equivalent linear method.

5.2.1. The peak ground acceleration

There are several factors associated with an earthquake record that has a marked influence on the response of a structure. When these factors are measured by a quantifiable parameter they are usually referred to as "earthquake intensity indices". The most common parameter used to measure the intensity of an earthquake ground motion is the "Peak Ground Acceleration" (PGA). The PGA of a given seismic event is simply the maximum absolute value of the acceleration obtained from an accelerogram. For historical reasons and due to its simplicity the PGA was (and still is) widely used as an intensity index.

It is intuitive to assume that an earthquake with a higher PGA will cause a higher level of damage than another one with a smaller PGA. However, it is well known (e.g., Park et al., 1985) that reinforced concrete structures are generally damaged not only by high stress excursions but also by a combination of repeated stress reversals. Since the PGA occurs at a specific instant of time, it may not be a proper measure of damage potential except for low-rise, short period buildings. Nevertheless, as it was mentioned the PGA is the most popular and extensively used intensity index and thus it is selected as the first parameter to be later applied to define the optimal reduction factor.

5.2.2. The peak ground velocity

The "Peak Ground Velocity" (PGV) is another parameter commonly used to characterize the amplitude of a strong earthquake. The PGV is defined in a similar way as the PGA, but with the absolute value of the velocity. Usually, the velocity records show substantially less high frequencies than the acceleration. This is because the velocity is obtained by integration of the acceleration and this effectively results in a filtering of high frequencies. Due to the fact that the velocity is less sensitive to the high frequencies of strong motions, the PGV can better characterize the amplitude of strong motions at the intermediate frequencies. Moreover, several studies have found that the PGV correlates well with observed structural damage, especially in those structures with intermediate natural periods (Akkar and Bommer, 2007).

5.2.3. The characteristic intensity

The concept of "Characteristic Intensity" (Ic) emerged from the study of the seismic damage to reinforced concrete structures by Park et al. (1985). The rate of structural damage was defined as a linear combination of the damage caused by excessive deformation and the contribution of repeated load cycles. Their experiments consisted of analyzing two columns as a linear elastic structure with one degree of freedom, with one column being more ductile than other. With this, Park et al. (1985) determined the rate of damage for both columns, which they determined to approximated with equation (5.1). The authors concluded that this would be viable representation for the destructive potential of a seismic event.

$$Ic = {A_{rms}}^{1.5}\, tf^{0.5} \tag{5.1}$$

where A_{rms} is the quadratic mean of the seismic acceleration and tf is the total duration of the seismic event in seconds.

5.2.4. The arias intensity

The "Arias Intensity" (AI) is a quantitative measure of the intensity of an earthquake based on instrumentation, and it can be regarded as the measurement of the total seismic energy absorbed by the soil. It correlates well with several commonly used demand measures of structural performance, liquefaction, and seismic slope stability (Travasarou et al., 2003). It is defined as:

$$AI = \frac{\pi}{2g} \int_0^{t_f} \left[\ddot{x}_g(t) \right]^2 dt \tag{5.2}$$

where $\ddot{x}_g(t)$ is the earthquake time history of acceleration, t_f is the total duration of the seismic event and g is the acceleration of gravity. It can be shown (using the Parseval's theorem) that the AI has a close relationship with the area under the squared amplitude of the Fourier spectrum calculated from the time history of acceleration.

5.2.5. The cumulative absolute velocity

The "Cumulative Absolute Velocity" (CAV) is another parameter proposed as an index to quantify the potential earthquake damage to structures. One of its interesting characteristics is that it is proportional to load cycles causing low-cycle fatigue type damage (Katona, 2011). The CAV is defined as the area under the curve of the absolute value of the accelerogram. In mathematical terms, it is the integral of the absolute value of the acceleration time history over the duration of the earthquake. It is defined by equation (5.3) (EPRI, 1991):

$$CAV = \int_0^{t_f} \left| \ddot{x}_g(t) \right| dt \tag{5.3}$$

where $\ddot{x}_g(t)$ is the time history of the acceleration and t_f is the total duration of the seismic event.

5.2.6. The effective design acceleration

The idea of "Effective Design Acceleration" (EDA) was proposed by Benjamin and Associates (1988). They argued that the high frequency components of ground motions do not have a significant effect on the seismic responses of structures. However their influence on the peak ground acceleration is important and therefore, they proposed a scaling parameter using the peak acceleration value. The approach consisted of only filtering out the peak accelerations that are above 8 - 9 Hz and using remaining values as the EDA.

5.2.7. Proposed optimal reduction factor

It is proposed to define the optimal reduction factor *RD* as a linear combination of the six seismic demand indices described in the previous section, i.e. as:

$$RD = \alpha_1 + \alpha_2 PGA + \alpha_3 PGV + \alpha_4 Ic + \alpha_5 AI + \alpha_6 CAV + \alpha_7 EDA \tag{5.4}$$

A linear regression was implemented to find the seven coefficients α_i in equation (5.4). The process was the following. The seismic response of the three story RC building was calculated with the program ANSYS in two ways: by means of a full non-linear analysis, as described in Chapter 3, and with the equivalent linear method presented in Chapter 4. The errors in the response calculated with the latter method were computed for four response quantities: relative displacement and absolute acceleration at the top level and bending moment and shear force at a critical column in the first floor. The average weighted error was obtained next, assigning more weight to the internal forces. Five of the earthquake records described in Chapter 3 were used to calculate the seismic response of the building: the 1940 Imperial Valley, the 1994 Northridge Sylmar, the 1966 Parkfield, the 1999 Hector Mine and the 1989 Loma Prieta ground motions. Next, the six seismic parameters for the each of the five earthquakes were calculated. The five weighted average errors along with the six indices for each of the seismic records were input into the program Microsoft Excel. Using the internal tools of this program a linear regression was performed that provided the constants that multiply each seismic parameter in the linear combination.

The final formula to calculate the optimal reduction factor *RD* is provided in equation (5.5) for the fps system and in equation (5.6) for the SI system.

Using units of feet and seconds:

$$\begin{aligned} RD = & -0.0395092 + 0.00209\,AI + 0.0001658\,CAV + 0.0234755\,EDA - 0.0048305\,Ic \\ & - 0.0159971\,PGA + 0.0332201\,PGV \end{aligned} \tag{5.5}$$

Using units of meters and seconds:

$$\begin{aligned} RD = & -0.0395092 + 0.006857\,AI + 0.000544\,CAV + 0.077019\,EDA - 0.0287059\,Ic \\ & - 0.0524837\,PGA + 0.10899\,PGV \end{aligned} \tag{5.6}$$

5.2.8. Validation of the results

In order to validate the proposed reduction factor, it was used to apply the equivalent linear method to calculate the response of the RC building model to eight seismic records. The objective was to determine the error in the non-linear seismic response calculated with the approximate method for different earthquakes. The earthquake database used consisted of four broad-band and four short-band events that were selected to represent diverse seismic loadings that can be expected in a real case scenario. The seismic records were scaled up so that they cause a non-linear behavior of the building. However, it is recalled that the equivalent linear method usually is not applicable to structures undergoing a highly non-linear response and thus the scaling has its limits. The results obtained for each of the eight seismic records is presented in Table 5.1. The table displays the seismic record applied, the scaling factor, the earthquake type in terms of frequency content, the reduction factor calculated with equation (5.5), the relative errors in the relative displacement of the top floor, the shear force and bending moment in a first floor column, the absolute acceleration of the top floor and the average error.

As it can be seen, the maximum overall average error for all of the earthquake records is 9.7% and smaller for the other seven cases (around 3%).

__Table 5.1__ Accuracy of the response predicted by the equivalent linear method with the proposed reduction factor for a collection of seismic records.

Earthquake	Scale Factor	Class	Factor	Error Disp	Error Shear	Error Mom	Error Acc	Average Error
Salvador	x2	Short	0.1278	7.1%	0.2%	0.3%	3.1%	2.7%
Imperial	x3.5	Broad	0.1071	6.6%	0.5%	0.2%	5.0%	3.1%
Loma Prieta	x2	Short	0.1804	12.8%	12.0%	12.3%	1.6%	9.7%
Northridge	x1	Short	0.1737	2.9%	0.1%	1.5%	1.0%	1.4%
Borrego	x80	Broad	0.0851	0.8%	4.0%	3.7%	3.4%	3.0%
Hector	x18	Broad	0.0637	4.2%	0.0%	1.9%	5.8%	3.0%
Managua	x 2	Broad	0.0461	5.8%	0.8%	0.5%	6.0%	3.3%
Parkfield	x 6	Short	0.1222	1.2%	0.6%	0.4%	3.4%	1.4%

5.3 Floor Response Spectrum Results

The nonstructural elements housed in a building consist of architectural components and other elements that do not contribute to the strength of the structure and mechanical and electrical equipment. Especially in the nuclear industry, these are called secondary systems. When the building is subjected to a seismic ground motion, the components rigidly attached to a slab will experience the same acceleration of the floor. Most seismic codes provide formulas to estimate the forces acting on the component which has acceptable accuracy for non-critical and rigid systems. When the equipment itself is flexible or is not rigidly attached, the concept of floor response spectra is issued to calculate the seismic forces. This tool is widely used for equipment located in nuclear power plants and other important industrial facilities. It is basically a seismic response spectrum calculated using the absolute acceleration of a floor but for linear elastic structures, it can also be computed with closed form equations (Suárez and Singh, 1989).

5.3.1. Floor spectra for the broad-band earthquake

The time history of the absolute accelerations of the three floors was obtained for the exact non-linear case and for the equivalent linear system. The building was subjected to the typical seismic record with a broad-band frequency content, namely the 1940 Imperial Valley earthquake. The damping ratio to calculate the floor response spectra was selected as 5%. Figure 5.1 display the floor response spectra for the three floors of the building obtained with the two approaches considered. The results show that for the second and third floor the equivalent linear model was able to predict almost the exact response for the full range of periods considered. In the case of the first floor, for periods close to 0.1 sec (the 5th linear natural period of the building) the equivalent linear method underestimated the peak in the spectrum, but for the rest of the periods, it can be considered to yield a good approximation.

5.3.2. Floor spectra for the short-band earthquake

The process was repeated now subjecting the building to the typical seismic event with a short-band frequency content. It is recalled that this is the 1986 San Salvador earthquake recorded at the CIG station. The acceleration of each floor obtained with the non-linear model and the equivalent linear method were retrieved and used to calculate the response spectra. The results are displayed in Figure 5.2. Examining the three graphs one can conclude that the equivalent linear method slightly underestimated the results. The differences are more pronounced at the first natural period of the building. However, in general, the equivalent linear method delivered a good approximation to the results of the full non-linear analysis for the short-band event.

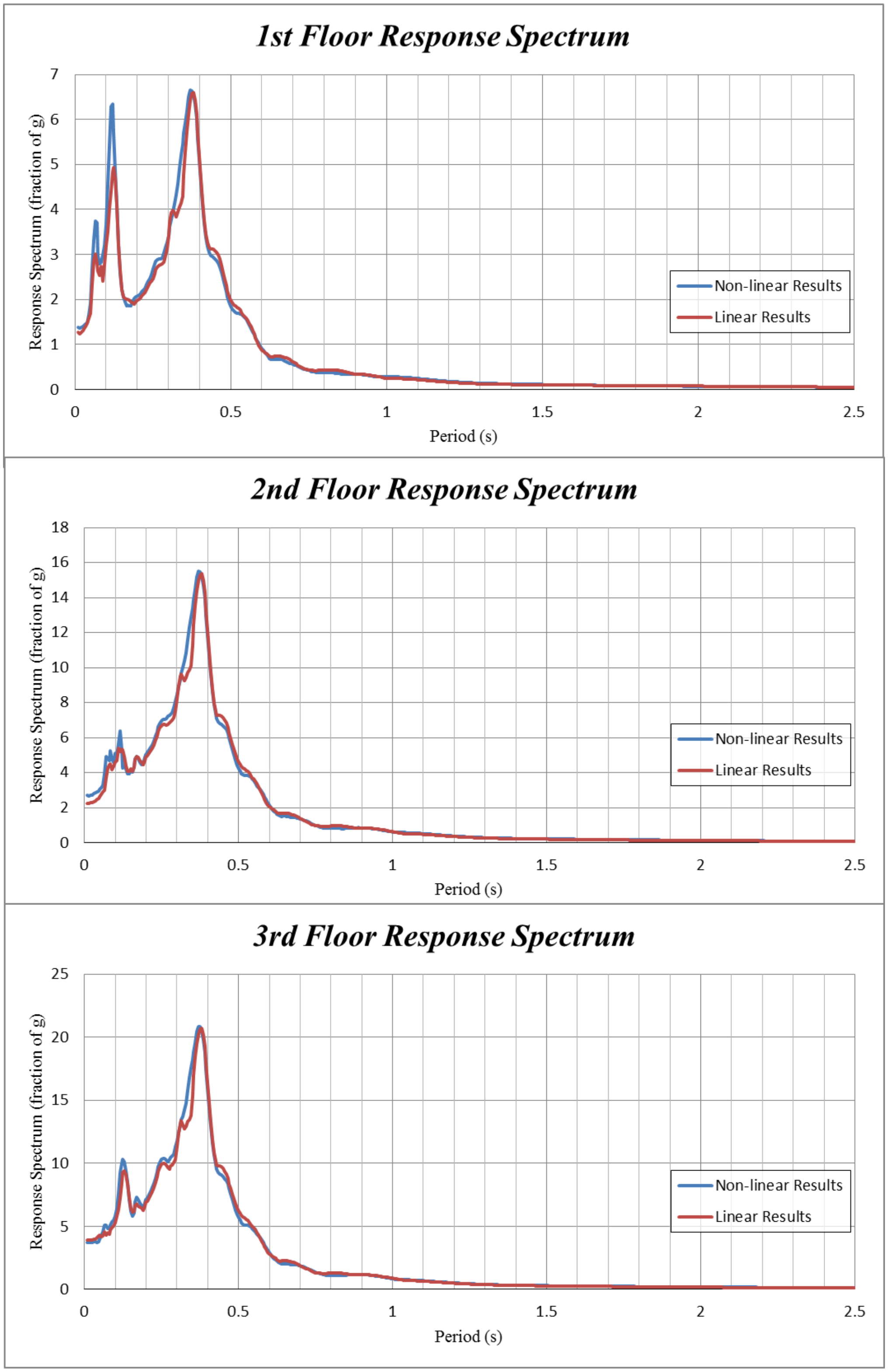

Figure 5.1 *Broad-Band event floor response spectra*

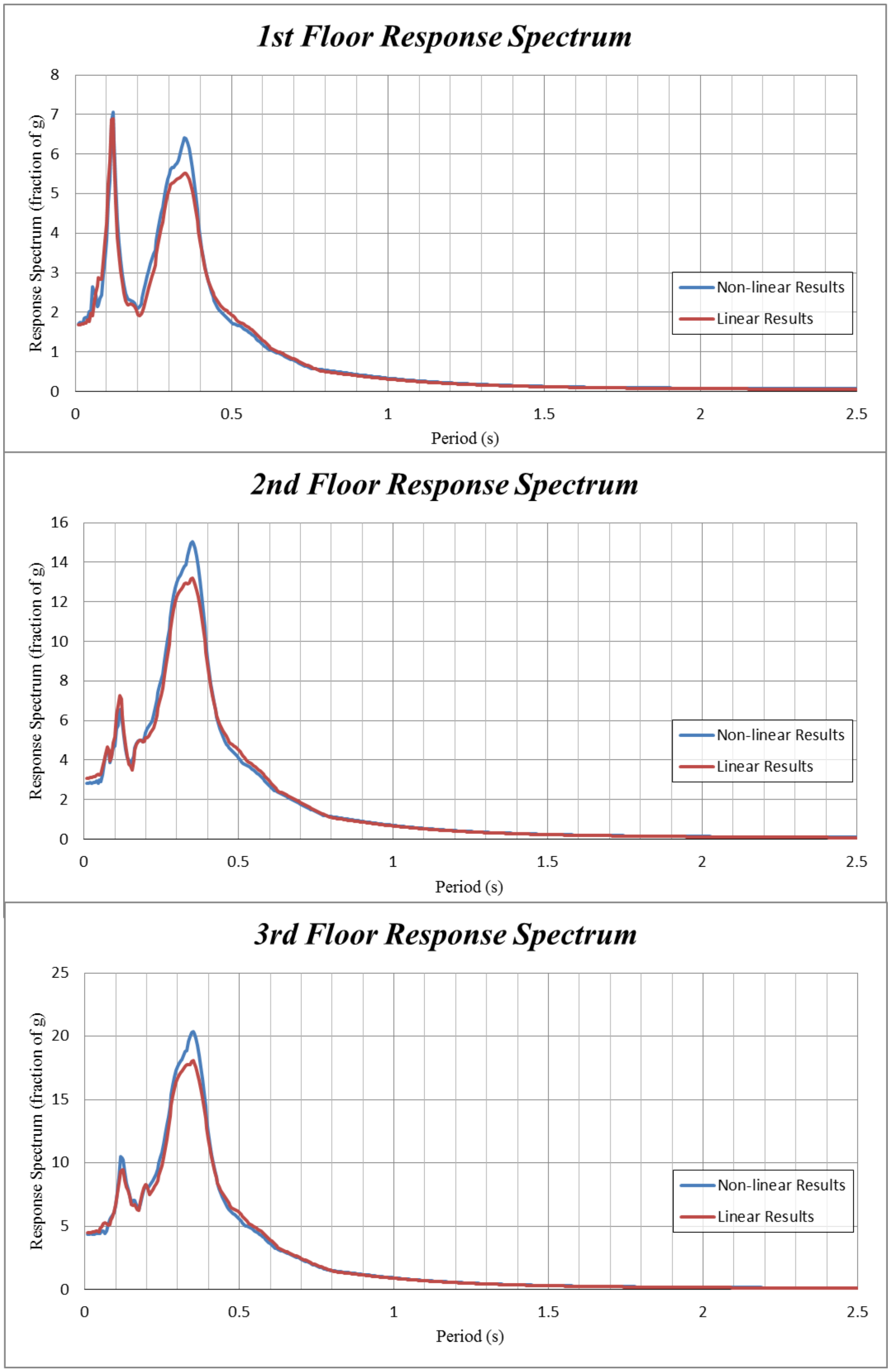

Figure 5.2 *Short-Band event floor response spectra*

5.4 Chapter Summary and Conclusions

The main objective of this chapter was to show the linear validation formulation used for the reduction factor recommended in the implementation of the equivalent linear method. In order to obtain this factor, several parameters were selected and a linear regression was the introduced to calculate each parameter coefficient. Every parameter will change in accordance with the properties of the seismic event and are not dependent on the dimensions or characteristics of the structure. Mostly all of parameters mention above can also be obtain from the accelerometers that measure seismic events.

The final validation results show a maximum overall average error for all of the earthquake records of 9.7% and a minimum of 1.4%. This error represents the difference in percentage between the results obtain from a non-linear model and the linear equivalent method develop.

Another parameter measure was the acceleration time history for each floor. Using this parameter the response spectrum was calculated for both methods. It can be seen that the equivalent linear model will result in a close approximation to the results from the non-linear models, with a slight under-estimate of the maximum value of acceleration at a particular point in time.

As a final conclusion, it can be mention that the approximations obtain from the linear equivalent method in general yields good results. This in terms also means that is a good floor response spectrum approximation that can be then implemented in the design of non-structural components.

CHAPTER VI

CONCLUSIONS AND RECOMMENDATIONS

6.1 Summary

This thesis presented the development and verification of an equivalent linear method to calculate the seismic response of reinforced concrete structures that is able to approximate as close as possible the results of a full non-linear analysis. The method was implemented and tested in a three-story building consisting of a reinforced concrete 3-D moment resistant frame. A detailed finite element model was created in the computer program ANSYS. Because in this model the plasticity is assumed to be distributed across the cross section and along the element length, the non-linear constitutive equations were defined by stress-strain curves. These were calculated using a special-purpose computer program and then input into ANSYS.

The two non-linear stress-strain curves for the beams and columns were approximated with polynomials using a non-linear regression. The resulting analytical expressions were used to calculate an effective (secant) modulus of elasticity. In addition, as required by the equivalent linear method, an equivalent damping ratio was calculated in closed form by applying the Masing's rule to form the complete hysteresis cycle. These two parameters were used to define a linear model of the structure and the seismic response was calculated. Form the response time history the peak normal strains were retrieved and reduced by a factor. New equivalent elastic moduli and damping ratios were calculated for the beams and columns and the process was repeated until the difference in the new and old E and ξ were within a preselected tolerance. It was found that the key parameter that governed the accuracy of the proposed methodology is the reduction factor used to define an effective strain from the peak strain.

To investigate whether the proposed method was a viable one, two earthquake ground accelerations were selected. They represent events with different frequency content: one was identified as the broad-band event and the other as the short-band event. They were used to conduct a preliminary evaluation of the equivalent linear method. Once it was verified that the proposed methodology yielded reasonable results, the method was further refined by using six additional earthquake records. After an equivalent linear model of the building was obtained, the accelerations at the floors were used to calculate the floor response spectra. The spectra were compared with those obtained employing the acceleration time histories resulting from the full non-linear dynamic analysis.

6.2 Limitations of the equivalent linear method and the study

The equivalent linear method has an inherent limitation, namely that the level of non-linear deformations of the structure or soil system under study cannot be very significant. Evidently, the method is not able to predict the response of a structure near collapse and this is a shortcoming that cannot be overcome. There are, however, some limitations of the present study that can be resolved. The project focused on the seismic response of a single structure, the three-story reinforced concrete building. The method should be tested in buildings with higher and lower number of floors which have, respectively, lower and higher natural periods. In addition, the lateral force resisting system chosen for the building was a special moment resistant frame. It is not clear how the method will perform in a structure with structural walls or with bracings. The performance with steel structures is also an issue that needs to be addressed.

It could be argued that the non-linear dynamic analysis carried out with ANSYS was not independently verified with another source, e.g. by comparing it with results of actual experimental tests. However, this is not deemed to be a major shortcoming for the purposes of the present study. In general, the independent verification of the results is an important issue if the objective of a project is the study of the seismic non-linear response of a structure per se. However, here the results of the equivalent linear method were compared with the non-linear analysis using the same program and methodology, and just allowing the structure to behave in a linear fashion. In this sense there is an inner consistency that should justify the results.

6.3 Conclusions

Based on the work presented in the preceding chapters, it can be concluded that the equivalent linear method, originally proposed for Geotechnical Earthquake Engineering applications, is a viable and practical approach to calculate the moderate non-linear response of reinforced concrete buildings. Of course, as pointed out in the previous section, further validations are needed but the proof-of-concept work undertaken in this thesis confirms that is worthwhile to carry out further studies.

As reported earlier, it was found that the critical parameter that governs the accuracy of the results obtained with the equivalent linear method is the reduction factor used to define an effective strain from its peak value. The definition of an effective strain is required because when the equivalent linear properties (E and ξ) are calculated, it is assumed that the response is cyclical but with the same maximum values on each cycle. Obviously, the true seismic response does not follow that pattern because the earthquake ground motions are nonstationary in nature. Therefore, it is not reasonable to use the maximum strain to define the equivalent Young's modulus and damping ratio. In Soil Dynamics application it is recommended to use a reduction factor equal to 0.65 but for the present application this value did not yield good results at all. Therefore, a particularly important contribution of this thesis is a procedure to define an optional reduction factor for each earthquake using several intensity parameters (such as the PGA, PGV, Arias Intensity, etc.)

The four response quantities used to evaluate the accuracy of the equivalent linear method were the relative displacements at the top of the building, the shear force and the bending moment at a critical column of the first floor and absolute accelerations at each of the floors. The resulting average error between the approximate and exact response was always less than 10% for the most unfavorable case.

The comparison between the floor response spectra obtained with the equivalent linear model and the full non-linear analysis was also very successful. There was a slight underestimation of the maximum accelerations at some range of periods, but it is not deemed important, given the inherent uncertainties in the seismic input. In practice, the seismic input is defined by a code prescribed design spectrum, and a number of spectrum compatible accelerograms are generated and input to the structure model. However, there is always an uncertainty involved in the design spectrum and in the compatible acceleration time history.

6.4 Recommendations for future work

Some of the limitations of the present study reported in a previous section can be removed by extending the study to other models and widen the number and type of seismic inputs. Therefore, several areas for further research are presented next.

The first suggested task is to consider building models with different numbers of floors. They could be studied using a similar finite element model, but this could be a problem for tall buildings due to the larger number of degrees of freedom. In this case it may be convenient to employ simpler frame models, as recommended below.

Another topic for further investigations is to select structures with other lateral force resisting systems to test the method. They can include structures with shear walls, with lateral bracings, or dual systems. In addition, the study can be expanded to include steel structures with different configurations.

It is also interesting to evaluate the proposed methodology in structures with irregular configurations, either in plant or in elevation. They can include structures with torsional behavior (where the stiffness and mass centers do not coincide), or buildings with setbacks, etc.

Another recommendation for further studies is to expand the number and type of seismic ground motions used to test the method. In this thesis eight accelerograms with different characteristics were used. Another possibility, instead of selecting unmodified records of historic earthquakes, is to employ accelerograms that are compatible with a prescribed design spectrum.

The model of the building developed in ANSYS to validate the equivalent linear method was a very detailed finite element model in which 3-D solid elements were used for the beams, columns and floor slabs. In the structural engineering practice, less sophisticated models are used in which the beams and columns are modeled with frame elements. For instance, this is the usual approach followed when a program like SAP2000 or ETABS are used. In this case the non-linear behavior of the elements is accounted for by means of local plasticity models; usually a moment-rotation or moment curvature is used to define the behavior of localized inelastic springs or plastic hinges at the ends of the elements. It is recommended to implement and corroborate the equivalent linear method in these types of models and programs.

The fact that an equivalent linear model of the structure is available once the method has converged, means that the so called “direct methods” can be applied to calculate the floor response spectra. These methods are attractive because they used as input the design spectrum prescribed for the main structure, as well as its dynamic properties (modes and frequencies). The floor spectra are generated using relatively simple closed form equations. However, they can only be applied in structural systems with linear elastic behavior. This topic was not pursued in this thesis, but it is a useful application of the methodology herein presented.

REFERENCES

ACI (2011) "Building code requirements for structural concrete", ACI 318-11, American Concrete Institute, Farmington Hills, MI.

Akkar, S. and Bommer, J. (2007) "Empirical prediction equations for peak ground velocity derived from strong-motion records from Europe and the Middle East", *Bulletin of the Seismological Society of America*, Vol. 97, No. 2, pp. 511-530.

ANSYS (2015) ANSYS, Inc. Version 16.0, Computer software, Canonsburg, PA.

ASCE (2006) "Minimum design loads for buildings and other structures: ASCE 7-05", American Society of Civil Engineers, Reston, VA.

Barbosa, A. and Ribeiro, G. (1998) "Analysis of reinforced concrete structures using Ansys nonlinear concrete model", *Computational Mechanics*. pp. 1-7.

Benjamin, J. & Associates (1988) "A criterion for determining exceedance of the operating basis earthquake", *EPRI Report NP 5930*, Electric Power Research Institute, Palo Alto, CA.

Bommer, J. and Acevedo, A. (2004) "The use of real earthquake accelerograms as input to dynamic analysis", *Journal of Earthquake Engineering*, Vol. 8, No. 1, pp. 43-91.

Combescure, D. (2002) "CAMUS 2000 Benchmark - Experimental results and specifications to the participants", SEMT/EMS/RT/02-067/A.

Deierlein, G., Reinhorn, A. and Willford, M. (2010) "Nonlinear structural analysis for seismic design", *NEHRP Seismic Design Technical Brief No. 4*, National Institute of Standards and Technology (NIST), Washington, DC.

EPRI (1991) "Standardization of the cumulative absolute velocity", Electrical Power Research Institute, Report EPRI TR-100082-T2, Palo Alto, CA.

FEMA (2009) "FEMA P695 - Quantification of building seismic performance factors", Federal Emergency Management Agency, Washington, DC.

Fragiadakis, M., Vamvatsikos, D. and Aschheim, M. (2014) “Application of nonlinear static procedures for the seismic assessment of regular RC moment frame building”, *Earthquake Spectra*. Vol. 30, No. 2, pp. 767-794.

Hognested, E. (1951) “A study of combined bending and axial load in reinforced concrete members”. In: *Bulletin No.399*, University of Illinois Engineering Experiment Station, Urbana, IL.

Hudson, M., Idriss, I. and Beijae, M. (1992) “User’s Manual for QUAD4M - A computer program to evaluate the seismic response of soil structures using finite element procedures incorporating a compliant base”. In: *Technical Report (rev. 2003)*, Department of Civil & Environmental Engineering, University of California, Davis, CA.

Huei-Huang, L. (2015) “Basics of nonlinear simulation”. In: *Finite Element Simulations with Ansys Workbench 16*, Chapter 13.1, pp. 466-477, SDC Publications, KS.

IBC (2006) “International Building Code”, International Code Council, Falls Church, VA.

IBC (2015) “International Building Code”, International Code Council, Falls Church, VA.

Jiang, W., Li, B., Xie, W. and Pandey, M. (2015) “Generate floor response spectra: Part 1. Direct spectra-to-spectra method”. In: Nuclear Engineering and Design, Vol. 293, pp. 525-546.

Katona, T. (2011) “Interpretation of the physical meaning of cumulative absolute velocity”. In: *Pollack Periodica: An International Journal for Engineering and Information Science,* Vol. 6, No. 1, pp. 1-8.

Lepage, A., Shoemaker, J. and Memari, A. (2012) “Accelerations of nonstructural components during nonlinear seismic response of multistory structures, *Journal of Architectural Engineering*. Vol. 18, No. 4, pp. 285-297.

Mander, J., Priestly, M. and Park, R. (1988) “Theoretical Stress-Strain model for confined concrete”. In: *Journal of Structural Engineering.* Vol. 114, No. 9, pp. 1804-1826.

Mathematica (2014). Wolfram Research, Inc. Version 10.0, computer software, Champaign, IL.

Miranda, V. (2016) “Seismic parameters of earthquakes measured records in Puerto Rico and its distribution” (in Spanish), *Master of Science Thesis,*University of Puerto Rico, Mayagüez, PR.

Moehle, J. (1992) "Displacement-based design of RC structures subjected to earthquakes", *Earthquake Spectra*. Vol 8, No. 3, pp. 403-425.

Musmar, M. (2013) "Analysis of shear walls with openings using solid 65 elements", *Jordan Journal of Civil Engineering.* Vol. 7, No. 2, pp. 164-173.

Nuclear Regulatory Commission (2016a). "10CFR21: NRC Regulations Title 10, PART 21 - Reporting of Defects and Noncompliance", Washington, DC.

Nuclear Regulatory Commission (2016b). "10CFR50 Appendix B - Quality Assurance Criteria for Nuclear Power Plants and Fuel Reprocessing Plants", Washington, DC.

Park, Y., Ang, A., and Wen, Y. (1985) "Seismic damage analysis of reinforced concrete buildings", *Journal of Structural Engineering*. Vol. 111, No. 4, pp. 740-757.

PEER (2010) OpenSees, Version 2.4.6, computer software, Berkeley, CA.

PEER (2016) "Ground Motion Database", Pacific Earthquake Engineering Research Center, University of California at Berkeley, website: http://ngawest2.berkeley.edu/.

Pfrang, E., Siess, C. and Sozen, M. (1964) "Load moment curvature characteristics of reinforced concrete cross sections", *ACI Journal*, Vol 61, No. 7, pp. 763-778.

Richard, B., Martinelli, P., Voldoire, F., Corus, M., Chaudat, T., Abouri, S. and Bonfils, N. (2015) "SMART 2008: Shaking table test on an asymmetrical reinforced concrete structure and seismic margins assessment", Engineering *Structures*, Vol. 105, pp. 48-61.

Richard, B., Cherubini, S., Voldoire, F., Charbonnel, P., Chaudat, T., Abouri, S. and Bonfils, N. (2016) "SMART 2013: Experimental and numerical assessment of dynamic behavior by shaking table test of an asymmetrical reinforced concrete structure subjected to high intensity ground motions", *Engineering Structures*, Vol. 109, pp. 99-116.

Schnabel, P., Lysmer, J. and Seed H. (1972) "SHAKE: A computer program for earthquake response analysis of horizontal layered sites", Earthquake Engineering Research Center, Report No. UCB/EERC-72/12, University of California, Berkeley, CA.

Seed, H. and Idriss, I. (1970) "Soil moduli and damping factors for dynamic response analysis", Earthquake Engineering Research Center, Report EERC 70-10, University of California, Berkeley, CA.

Simos, N. and Hofmayer, C. (2013) “Experimental studies of reinforced concrete structures under multi-directional earthquakes and design implications”, *U.S. Nuclear Regulatory Commision*, NUREG/CR-7119, Washington, DC.

Singh, M. (1975) “Generation of seismic floor spectra”, *Journal of the Engineering Mechanics Division, ASCE,* Vol. 101, No. EM5, pp-593-607.

Singh, M., Moreschi, L., Suárez, L. and Matheu, E. (2006a) "Seismic design forces: I - Rigid nonstructural components”, *Journal of Structural Engineering*, Vol. 132, No. 10, pp. 1524-1532.

Singh, M., Moreschi, L., Suárez, L. and Matheu, E. (2006b) "Seismic design forces: II - Flexible nonstructural components”, *Journal of Structural Engineering*, Vol. 132, No. 10, pp. 1533-1542.

Structure Express (2015) *SE::MC - Moment Curvature Analysis*, computer software, Kirkland, WA.

Suárez, L. and Singh, M. (1989) “Floor spectra with equipment-structure equipment interaction effects”, *Journal of Engineering Mechanics,* Vol. 115, No. 2, pp. 247-264.

Suárez, L. (2008) “Non-linear dynamic analysis of soils”, *Dynamics of Soils and Foundations*, Chapter 7, pp. 1-8, University of Puerto Rico, Mayaguez, PR.

Travasarou, T., Bray, J. and Abrahamson, N. (2003). “Empirical attenuation relationship for Arias Intensity”, *Earthquake Engineering and Structural Dynamics*, Vol. 32, pp. 1133–1155.

Villaverde, R. (2004). “Seismic analysis and design of nonstructural elements”, Chapter 19, pp. 19.1-19.42, in *Earthquake Engineering: from Engineering Seismology to Performance-Based Engineering*, Bozorgnia, Y. and Bertero, V., Editors, CRC Press, Boca Raton, FL.

Wieser, J., Pekcan, G., Zaghi, A., Itani, A. and Maragakis, J. (2013). “Floor accelerations in yielding special moment resisting frame structures”, *Earthquake Spectra,* Vol. 9, No. 3, pp. 987-1002.

APPENDIX A

MATLAB PARAMETERS SOURCE CODE ALGORITHM

This appendix shows the source code that was used in order to generate each parameter of the proposed optimal reduction factor. The algorithm code is written in the computer base language compatible with the software “Matlab”. The code was developed and explained in detail in Miranda (2016), Masters in science thesis, from the University of Puerto Rico at Mayagüez campus. Some modifications were done to the algorithm in order to implement it for this thesis objectives.

A.1 Main Matlab source code algorithm

The algorithm is using as an example the seismic event of “Parkfield 1966”. The only parameters needed to be adjusted are the “Input Data” section of the code in order to analyze other cases.

Code:

```
clc; clear all; close all; format short g

% ----------------------- Input Data -----------------------------

g    = 32.185 ;           % acceleration
nom  = 'Parkfield1966';   % name on file txt
dt   = 0.01;              % time step [seg]
PRA  = 0;                 % pic rock accel. fracc. of g
npt  = 1;                 % fraction (0-1) of points to be ploted
Dt   = 6;                 % offset of the initial displacement [seg]
X    = 6;                 % scale factor
```

```
% ------- Reading and scaling of original accelerogram -------------

terr = load ([nom,'.txt']);      % reading of the seismic record
[nr,nc]  = size(terr);           % rows and columns of the file
nt       = nr*nc;                % number of points in the accelerogram
xg(1:nt) = terr'*X;              % vector with data from the file
Xm  = max( abs(xg) );            % original maximum from accelerogram
if PRA ~= 0
   xg  = PRA/Xm * xg;         % scale the accelerogram to the given PRA
   PRA = Xm;                     % only if PARA is zero
end
tf  = (nt-1) * dt;               % final time of the record
t   = 0: dt: tf;                 % vector of times
ng  = round(npt*nt);             % number of points to plot

% ---------------- Calculation of accel and vel ---------------------

%Acceleration
xg1=xg'*g;

%Velocity
vel1=cumtrapz(t, xg1);

% ------------------ Parameters Calculation -------------------------

[PGA1,pPGA1]=max(abs(xg1));                         % PGA

[PGV1,pPGV1]=max(abs(vel1));                        % PGV

Arms1=sqrt((1/t(end))*trapz(xg1.^2)*dt);
Ic1=(Arms1).^(3/2)*sqrt(t(end));                    % IC

AI1=(pi/(2*g)).*(cumtrapz(t,(xg1).^2));             % AI
AI1=AI1(end);

CAV1=cumtrapz(t,abs(xg1));                          % CAV
CAV1=CAV1(end);

[EDA1B]=fEDA_vma(dt,xg1);                           % EDA

%------------------------ Display the values ----------------------

disp(' **************** Each Parameter *************');
disp(' ')
disp(['=> PGA: ',num2str(PGA1)]);
disp(['=> PGV: ',num2str(PGV1)]);
disp(['=> Ic: ',num2str(Ic1)]);
disp(['=> AI: ',num2str(AI1)]);
disp(['=> CAV: ',num2str(CAV1)]);
disp(['=> EDA: ',num2str(EDA1B)]);
```

A.2 EDA Matlab separate function

This function must be defined separately in order to calculate parameter "EDA". This step must be performed before or simultaneously with the main code in order to function correctly.

Code:

```
function [EDA]=fEDA_vma(dt,xg)
xg = reshape(xg,[],1);
np=length(xg);
fs=1/dt;
Fn=fft(xg);
fres=fs/np;
m=0:ceil(np/2);
freqs = m*fres;

%Signal filtration ( Low Pass frequency = 9 Hz )
fcorte1=0;
fcorte2=9;
j=find(freqs>=fcorte1 & freqs<=fcorte2 )';
%Fn(1:j(1))=0;
%Fn(end-j(1)+1:end)=0;
Fn(j(end):end-(j(end)-1))=0;


% Signal Gathering
sn = ifft(Fn);
EDA=max(abs(sn));
```

APPENDIX B

EQUIVALENT LINEAR METHOD FORMULATION

This appendix shows the source code that was developed to calculate the secant modulus of elasticity (E) and damping ratio (ξ) used in the equivalent linear method. The algorithm code is written in language compatible with the software "Mathematica". Below is shown in detail the step by step process of the formulation that produced the final results. The results of each step are also plotted in order to have a better understanding and to help to verify the formulation of the method.

B.1 Mathematica beam equation formulation

```
ClearAll["Global`*"]
```

Linear equivelant method development

Beam section:

Polynomial representation of the non-linear (stress vs strain) curve

```
f[ε_] = -1.43894*^12 ε^4 + 5.05688*^10 ε^3 - 6.31157*^08 ε^2 + 3.41652*^6 ε;
f2[ε_] = 1.43894*^12 ε^4 + 5.05688*^10 ε^3 + 6.31157*^08 ε^2 + 3.41652*^6 ε;
```

The maximum value of strain (in/in)

```
εa = 0.007;
```

The maximum value of stress (psi)

```
σa = f[εa]
6879.15
```

Grafical representation of the polynomial approximation of the backbone curve

```
Plot0a = Plot[f[ε], {ε, 0, εa}];
Plot0b = Plot[f2[ε], {ε, -εa, 0}];
Show[{Plot0a, Plot0b}, PlotRange -> All]
```

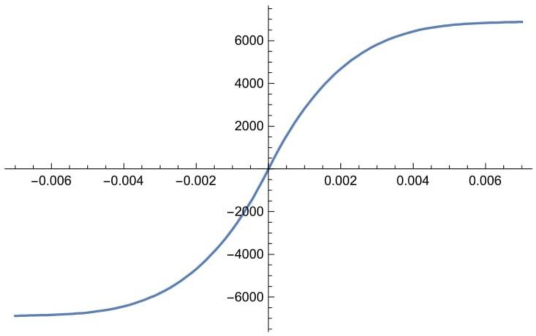

Cyclical approximation function

-Positive :

Fp = 2 * f[$\frac{\varepsilon + \varepsilon a}{2}$] - σa

$$-6879.15 + 2 \left(1.70826\times 10^{6} (0.007+\varepsilon) - 1.57789\times 10^{8} (0.007+\varepsilon)^2 + 6.3211\times 10^{9} (0.007+\varepsilon)^3 - 8.99338\times 10^{10} (0.007+\varepsilon)^4\right)$$

Grafical representation of the positive side

Plot1 = Plot[Fp, {ε, -εa, εa}]

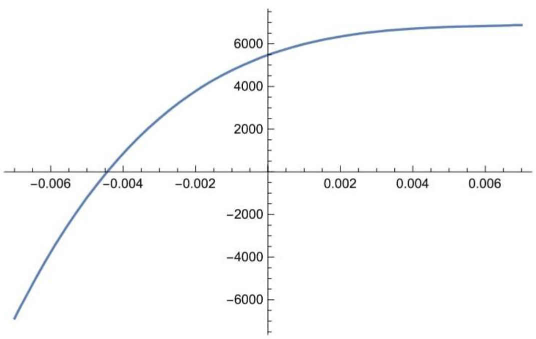

-Negative :

Fn2 = σa + 2 * f2[$\frac{\varepsilon - \varepsilon a}{2}$]

$$6879.15 + 2 \left(1.70826\times 10^{6} (-0.007+\varepsilon) + 1.57789\times 10^{8} (-0.007+\varepsilon)^2 + 6.3211\times 10^{9} (-0.007+\varepsilon)^3 + 8.99338\times 10^{10} (-0.007+\varepsilon)^4\right)$$

Grafical representation of the negative side

Plot2 = Plot[Fn2, {ε, -εa, εa}]

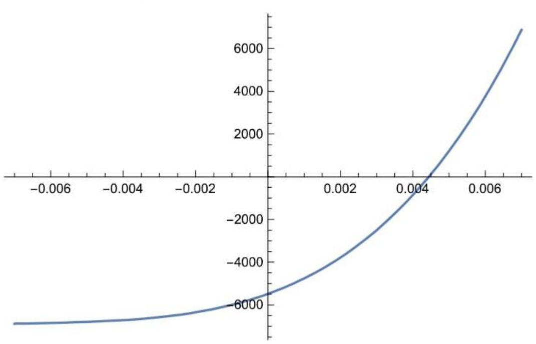

Full cyclical form and Backbone

```
Show[{Plot0a, Plot0b, Plot1, Plot2}, PlotRange → All]
```

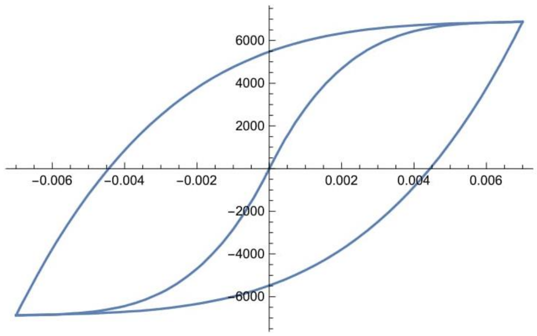

Final Calculations for the linear method:

```
Clear[εa]
```

Final formulation for Modulos (E):

$$Esec = \frac{f[\varepsilon a]}{\varepsilon a};$$

```
Simplify[Esec]
```

$3.41652\times 10^{6} - 6.31157\times 10^{8}\,\varepsilon a + 5.05688\times 10^{10}\,\varepsilon a^{2} - 1.43894\times 10^{12}\,\varepsilon a^{3}$

Grafical representation of the Modulos

```
Plot[Esec, {εa, 0, 0.007}]
```

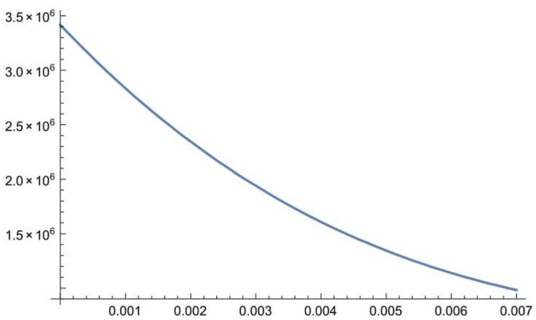

Final damping formulation (ξ):

$$\xi = \frac{2}{\pi}\left(\frac{2\int_0^{\varepsilon a} f[\varepsilon]\,d\varepsilon}{\varepsilon a * f[\varepsilon a]} - 1\right);$$

```
Simplify[ξ]
```

$\left(\varepsilon a\left(1.33936\times 10^{8} - 1.60965\times 10^{10}\,\varepsilon a + 5.49635\times 10^{11}\,\varepsilon a^{2}\right)\right) /$
$\left(3.41652\times 10^{6} - 6.31157\times 10^{8}\,\varepsilon a + 5.05688\times 10^{10}\,\varepsilon a^{2} - 1.43894\times 10^{12}\,\varepsilon a^{3}\right)$

Grafical representation of the Damping

```
Plot[ξ, {εa, 0, 0.007}, PlotRange → Full]
```

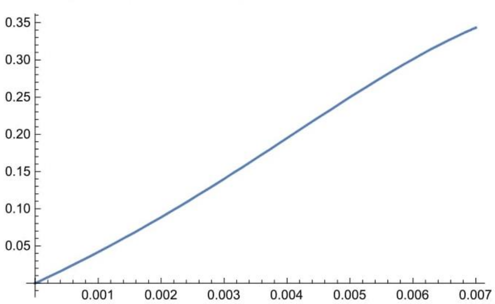

B.2 Mathematica column equation formulation

Column section:

Polynomial representation of the non-linear (stress vs strain) curve

```
f[ε_] = -3.68860*^11 ε^4 + 2.41744*^10 ε^3 - 4.40088*^8 ε^2 + 3.12431*^6 ε;

f2[ε_] = 3.68860*^11 ε^4 + 2.41744*^10 ε^3 + 4.40088*^8 ε^2 + 3.12431*^6 ε;
```

The maximum value of strain (in/in)

```
εa = 0.007;
```

The maximum value of stress (psi)

```
σa = f[εa]
```

7712.04

Grafical representation of the polynomial approximation of the backbone curve

```
Plot0a = Plot[f[ε], {ε, 0, εa}];

Plot0b = Plot[f2[ε], {ε, -εa, 0}];

Show[{Plot0a, Plot0b}, PlotRange -> All]
```

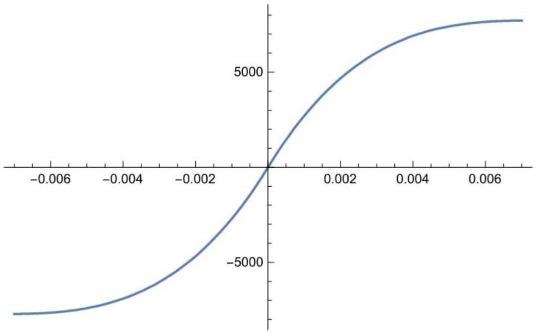

Cyclical approximation function

-Positive :

$$Fp = 2 * f\left[\frac{\varepsilon + \varepsilon a}{2}\right] - \sigma a$$

$$-7712.04 + 2\left(1.56216\times10^{6}\,(0.007+\varepsilon) - 1.10022\times10^{8}\,(0.007+\varepsilon)^{2} + 3.0218\times10^{9}\,(0.007+\varepsilon)^{3} - 2.30538\times10^{10}\,(0.007+\varepsilon)^{4}\right)$$

Grafical representation of the positive side

```
Plot1 = Plot[Fp, {ε, -εa, εa}]
```

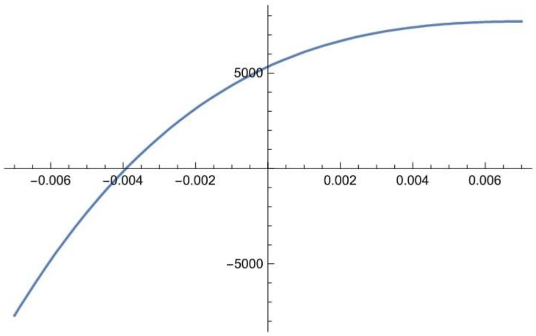

-Negative :

```
Fn2 = σa + 2 * f2[(ε - εa)/2]
```

7712.04 + 2 $\left(1.56216\times10^{6}\ (-0.007+\varepsilon) + 1.10022\times10^{8}\ (-0.007+\varepsilon)^{2} + 3.0218\times10^{9}\ (-0.007+\varepsilon)^{3} + 2.30538\times10^{10}\ (-0.007+\varepsilon)^{4}\right)$

Grafical representation of the negative side

```
Plot2 = Plot[Fn2, {ε, -εa, εa}]
```

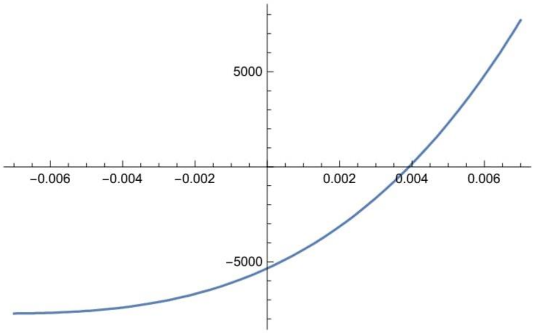

Full cyclical form and Backbone

```
Show[{Plot0a, Plot0b, Plot1, Plot2}, PlotRange → All]
```

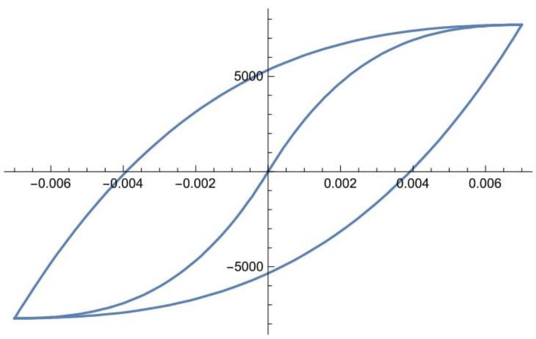

Final Calculations for the linear method:

```
Clear[εa]
```

Final formulation for Modulos (E):

```
Esec = f[εa]/εa;
Simplify[Esec]
```

$3.12431\times10^{6} - 4.40088\times10^{8}\ \varepsilon a + 2.41744\times10^{10}\ \varepsilon a^{2} - 3.6886\times10^{11}\ \varepsilon a^{3}$

Grafical representation of the Modulos

```
Plot[Esec, {εa, 0, 0.007}]
```

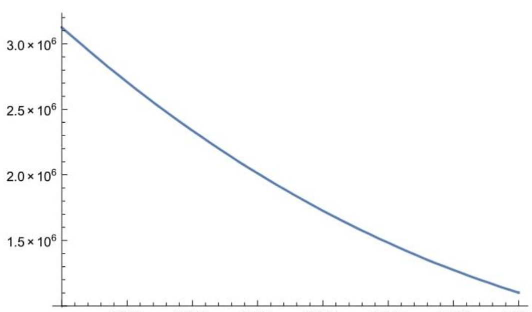

Final damping formulation (ξ):

$$\xi = \frac{2}{\pi}\left(\frac{2\int_0^{\varepsilon a} f[\varepsilon]\, d\varepsilon}{\varepsilon a * f[\varepsilon a]} - 1\right);$$

Simplify[ξ]

$$(\varepsilon a\ (-0.000253184 + 0.0208614\ \varepsilon a - 0.381972\ \varepsilon a^2)) / (-8.47018 \times 10^{-6} + 0.0011931\ \varepsilon a - 0.0655381\ \varepsilon a^2 + 1.\ \varepsilon a^3)$$

Grafical representation of the Damping

Plot[ξ, {εa, 0, 0.007}, PlotRange → Full]